CHAPTER 5. PROPERTIES OF CONFIGURATIONS.

5.0 OVERVIEW

This chapter differs in character from the preceding ones. While each of them deals with particular kinds of configurations — most concerning their existence and constructions — here we consider certain properties of configurations that have attracted the interest of researchers at various times.

We begin by presenting in Section 5.1 the information available concerning the connectivity properties of configurations. While some of the first papers ignored the issue, it quickly became apparent that restricting the discussion to connected configurations leads to considerable simplification in formulation of results. However, the importance of the degree of connectedness has been slow to emerge. Even today, it is not clear to what extent various properties depend on whether the configuration is 2-connected or has higher degree of connectivity.

Section 5.2 deals with Hamiltonian multilaterals — the analogs of Hamiltonian circuits in graphs. The recent result that there exist 3-connected 3-configurations with Hamiltonian multilaterals is presented; this solve negatively a long standing conjecture that 3-connectedness is sufficient for Hamiltonicity.

The next section deals with the related concept of multilateral decomposition of a configuration. By this is meant a family of multilaterals that include all lines and all points of the configuration, each just once. The topic goes back to the "prehistory" of configurations, and leads to many still open questions.

Section 5.4 is devoted to the presentation of the known facts about configurations that have no trilaterals, or, more generally, no k-laterals for $k = 3, 4, \dots, h$. This is an old topic that has recently been revived, and has turned pout to be related to interesting question about graphs.

In Section 5.5 we consider the configurations for which every points is incident with the same number of trilaterals – another old topic in configurations theory.

Section 5.6 is concerned with the recently proposed question what is the largest dimension that a configuration isomorphic to a given one can span. The few results are supplemented by many open questions.

Section 5.7 deals with a topic that has attracted attention only recently — configurations that can be continuously modified while keeping their combinatorial structure and keeping a sizable part of the configuration unchanged. The latest available results are presented, but there is a wide array of open questions o occupy geometers in the future.

Duality and selfduality, and the special cases of polarity and selfpolarity are considered in Section 5.8. The material available shows only too clearly how much is still to be discovered.

The final section, Section 5.9, is devoted to a list of open problems. These are only a few specific questions, meant to illustrate the topics considered. By no means is the list supposed to be exhaustive.

5.1 CONNECTIVITY OF CONFIGURATIONS

We start by recalling from Section 1.4 the concept of Levi graph L(C) of a configuration C. This is a bipartite graph (that is, there are two sets of nodes — black and white) with no edge connecting vertices of the same color. Usually the black nodes of L(C) correspond to the vertices of C, while the white ones correspond to the lines of C. A black node is connected to a white node by an edge of L(C) if and only if the corresponding vertex of C is incident with the corresponding line. The advantage of L(C) is that the graph L(C) represents the configuration *faithfully* — that is, knowing the Levi graph of a configuration enables one to determine the (combinatorial) configuration uniquely. An example of the Levi graph of a (12_3) configuration is presented in Figure 5.1.1.

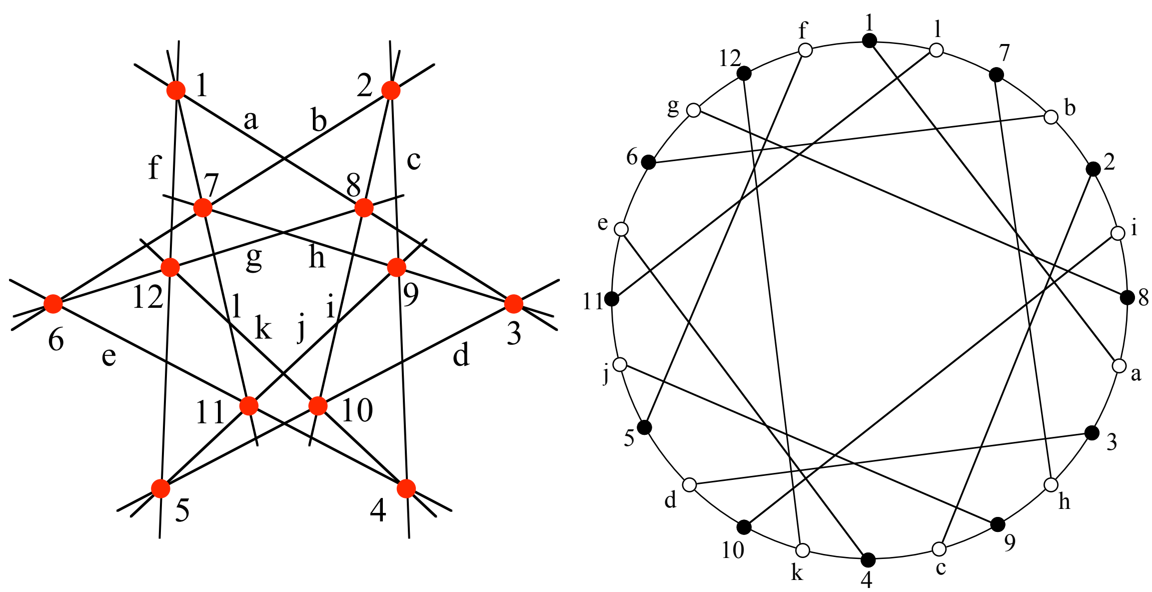

Figure 5.1.1. A configuration (12_3) and its Levi graph. Since the graph admits an incidence-preserving color reversal, which yields a graph isomorphic to the original (by reflection in the line bisecting the segments 7 h and 12 k, for example), the configuration is self-dual.

For a given configuration C, the Levi graph L(C) is uniquely determined. However, L(C) may admit various presentations, with different properties. For ex ample, in Figure 5.1.2 is shown another rendition of the Levi graph of the configuration (12_3) in Figure 5.1.1; it can be understood as an imbedding of the Levi graph in the torus. This presentation shows that all vertices of this configuration form one orbit under automorphisms of the configuration, and that all lines form one orbit as well. This is not easily visible from either the drawing of the configuration or its Levi graph in Figure 5.1.1.

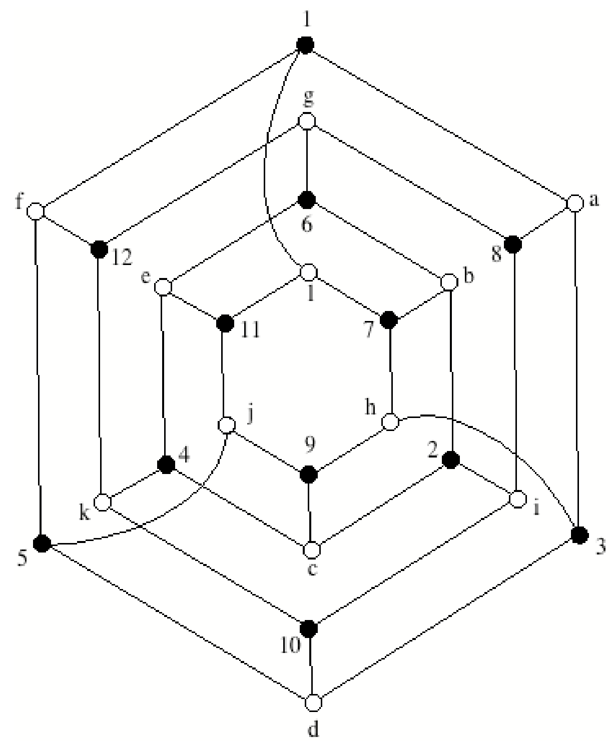

Figure 5.1.2. Another rendition of the Levi graph of the configuration (12_3) in Figure 5.1.1. It is easy to visualize this graph embedded in a torus in such a way that the combinatorial equivalence of all vertices of the configuration is obvious.

The main utility of Levi graphs comes from the fact that the graph-theoretic properties of L(C) may be used to define or determine properties of the configurations involved. We shall return to this topic in the next section, in the context of multilaterals.

Levi graphs are particularly useful in connection with questions about the connectivity of configurations. Concepts such as "connected", "k-connected", etc. for a configuration are defined by asking whether its Levi graph has the property in question. It is clear that these concepts can be defined directly in the configurations, but the formulations, distinctions, relevance, and familiarity are in many cases more easily perceived on the Levi graphs.

Theorem 5.1.1. Every connected combinatorial or geometric k-configuration C is 2-connected.

Proof. Note that a configuration is connected but not 2-connected (that is, the deletion of a single point from the Levi graph of C disconnects the graph) if and only if the dual configuration has the same property. Hence for a proof of the theorem by contradiction we may assume that there is a line L whose removal disconnects the configuration. At least one of the connected components resulting from the removal of L has at most h points incident with L, where $1 \leq h \leq k/2$. Then the number of incidences of the m lines of this component with the p points of the component is, on the one hand, equal to km, but on the other hand equal to $k(p - 1) + h$, since L was incident with h points. These numbers should be equal, but as one of them is divisible by k and the other is not, a contradiction was reached. ¨

Theorem 5.1.1 is due to Steinitz [S1], as is the idea of its proof. We have seen earlier (Corolary 2.5.3) a different proof of this result. But that proof relied on the construction of an orderly configuration table, which was a rather deep result. The approach here provides a good example of the utility of introducing graph-theoretic concepts (in particular, the Levi graph), in considerations of configurations. Steinitz did not have such tools, and as a consequence he needed more than a page of densely printed (and clumsily formulated) arguments to state and prove Theorem 5.1.1.

As a strengthening of Theorem 5.1.1 one might conjecture that each connected k-configuration, $k \geq 3$, is 3-connected. However, this is not the case. A counterexample is shown in Figure 5.1.3. It is known that all combinatorial configurations (n_3)

with $n \le 13$ are connected and, moreover, are 3-connected. This is best possible since for $n = 14$ there are counterexamples to both parts. The combinatorial configuration consisting of two disjoint copies of the Fano configuration is disconnected, while the configuration in Figure 5.1.3 is connected but not 3-connected. Any disconnected geometric (or topological) configuration (n_3) must have $n \ge 18$.

For 4-configurations the corresponding numbers are:

- There are disconnected combinatorial configurations (n_4) if and only if $n \ge 26$.
- There are disconnected topological configurations (n_4) if and only if $n \ge 34$.
- There are disconnected geometric configurations (n_4) if and only if $n \ge 36$.

The example in Figure 5.1.3 shows that there are 2-connected 2-configurations that are not 3-connected. This leads to the following problem:

If $k \ge 4$ and $2 \le j < k$, do there exist j-connected k-configurations that are not (j+1)-connected?

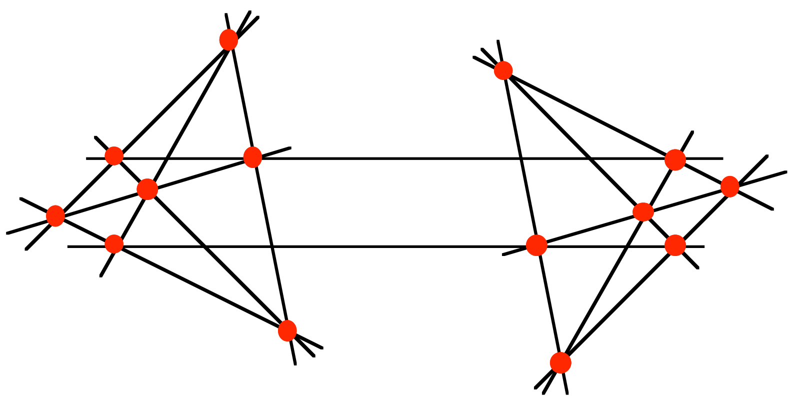

Figure 5.1.3. A connected configuration (14_3) which is not 3-connected.

An affirmative answer is given by the construction described in the proof of the following theorem:

Theorem 5.1.2. For each $k \ge 4$ and each j with $2 \le j < k$ there exist geometric k-configurations that are j-connected but not (j+1)-connected.

Proof. We consider first the case $j = 2$. The text deals with arbitrary k, and the illustration in Figure 5.1.4 presents in parallel the case $k = 4$. We start with copies of configurations $LC(k)$ described in Section 1.1 (see also [P9]), with a slight modification. As described in Section 1.1, LC(k) consists of an array of k^k points of the integer lattice in the Euclidean k-space E^k, with all coordinates in range [0, k-1], together with the lines parallel to the coordinate axes through these points. The modification we need here is that in one of the directions the coordinate k–1 is replaces by a convenient other integer. Our attention focuses on one of the lines in that direction, and the k points on it. (If desired, we way think of these configurations as projected into the plane.) In Figure 5.1.4 this situation is schematically indicated; one of the gray rectangles represents the modified configuration LC(k), the dashed line within the rectangle represents the chosen line, and the four dots represent the four points of LC(k) on that line. We need 2k configurations of this type, indicated by the gray rectangles, and positioned in such a way that two of the solid lines connect the k configurations at left with the k configurations at right, while each of the other 2k–2 solid lines connects the k copies in each half among themselves. Note that in each half, a single configuration is placed differently than the other k–1. Finally, we delete the dotted lines, thus creating a k-configuration. It is obvious that the resulting configuration is 2-connected, but the deletion of the two lines running between the two halves disconnects it; hence the configuration is not 3-connected.

For j > 2 we proceed analogously, but with an additional step. The construction is illustrated in Figure 5.1.5.

The first modification of the above construction is that the left half now has j–1 dots "above" the rest, and the right half has k–j+1 such points. Naturally, the corresponding numbers are the "bottom" are k–j+1 and j–1. Also, we do not insert the bottom connecting line between the two halves. Instead, we take a stack of k copies of what we constructed so far (it is best to imagine these copies to be in parallel planes, stacked above each other), and connected the corresponding points that were originally connected by the omitted bottom line. This is the desired configuration. It is clearly j-connected,

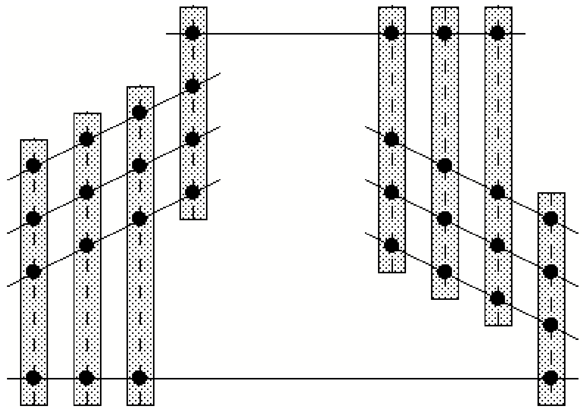

Figure 5.1.4. The construction of a geometric 4-configuration that is 2-connected but not 3-connected.

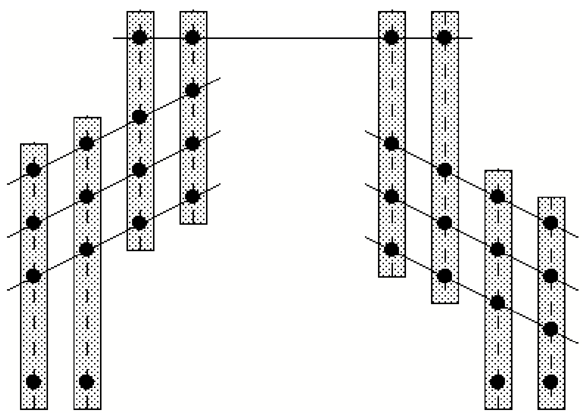

Figure 5.1.5. The construction of a geometric 4-configuration that is 3-connected but not 4-connected.

but the right part at each level can be disconnected from the rest by the omission of the j–1 lines connecting it to the other levels, and the line connecting it to the other half at its own level. ¨

It is clear that these constructions lead to very large configurations even in the smallest cases: (2048_4) in Figure 5.1.4, and (8192_4) in Figure 5.1.5. There probably exist much smaller configurations with the same properties — but justifying the existence of the appropriate projective images to yield the alignments necessary may be more involved. Rather obviously, much smaller combinatorial configurations with the properties discussed in Theorem 5.1.2 may exist, but this seems of rather marginal interest. On the other hand, even though one may expect to find combinatorial configurations of this type that are smaller than the corresponding geometric ones, no actual examples seem to be available.

*   *   *   *   *

In course on configurations I gave in the 1990 I made several conjectures that aimed at extending the result of Theorem 5.1.5 above to unbalanced [q,k]-configurations with $3 \le q \ne k \ge 3$. Xin Chen, a student in that course, produced various counterexamples; among them one proving that there exist [4,3]-configurations which are 1-connected but not 2-connected.

A small modification of Chen's procedure leads to:

Theorem 5.1.3. Combinatorial [q,k]-configurations that are 1-connected but not 2-connected exist if and only if $q \ne k$.

Proof. As we have seen in Theorem 5.1.5, every connected k-configuration 2-connected. For the other direction, due to duality, if $q \ne k$ it is enough to consider the case $q > k$. We start by forming a [q,k]-configuration, **cyclic** as far as possible. By this is meant that one uses as many cyclic sequences as necessary -- in the illustration below we need two such cycles. These configurations are generalization of the cyclic configurations $\mathbf{C}_3(n)$ we introduced on In Section 2.1. (The use of "cyclic" configurations comes only to simplify the checking that the tables which will be constructed are actually configuration tables.) Then we use a Martinetti-type construction (see Section 2.4): we select some $k-1$ lines with a property specified below, add one more point, and form a fragment in which all points except the new one are incident with q lines, and the new point is incident with k lines. The selected lines (which are then omitted) should be such that their points can be grouped in a way that no pair occurs in any other line; the new point is "cross-connected" to the points in these lines. As an illustration, the case $q = 4$, $k = 3$ is explicitly presented in detail . Here we take $n = 12$, the chosen lines are 1 2 4 and 7 8 10, and the additional point is 0. This way the configuration

1	2	3	4	5	6	**7**	8	9	10	11	12	1	2	3	4
2	3	4	5	6	7	**8**	9	10	11	12	1	5	6	7	8
4	5	6	7	8	9	**10**	11	12	1	2	3	9	10	11	12

yields the subfiguration

0	**0**	**0**	2	3	4	5	6	8	9	10	11	12	1	2	3	4
1	**2**	**4**	3	4	5	6	7	9	10	11	12	1	5	6	7	8
7	**8**	**10**	5	6	7	8	9	11	12	1	2	3	9	10	11	12

If three copies of this fragment are taken, distinguished by the number of dashes, and a line 0 0' 0" is added, we get a combinatorial $(39_4, 52_3)$ configuration which is connected but not 2-connected.

In the general case, the additional point 0 of the fragment will be on k lines only, thus having a deficit of q–k lines. To supply these we find a connected [q–k, k]-configuration C. Then we take as many copies of the fragment as there are points in C, and identify the point 0 of one copy of the fragment with each point of the configuration C. (In the above example, C is the [1, 3]-configuration which consists of just three points and one line.) This clearly yields a [q,k]-configuration of type which is connected but not 2-connected since each copy of the point 0 disconnects the configuration. ¨

It is not known whether the $(39_4, 52_3)$ configuration is the smallest of this type.

Theorem 5.1.3 deals with combinatorial configurations, and the question arises whether there exist connected geometric [q,k]-configurations, with $q \neq k$, that are not 2-connected.

A partial affirmative answer is given by the following result.

Theorem 5.1.4. For every q and k, with $\min\{q,k\} \geq 3$ and $q \neq k$, there exist geometric [q,k]-configurations that are connected but not 2-connected.

Proof. We first consider the case [4,3]-configurations. We start with a tricyclic 3-configuration C_1 shown in Figure 5.1.6. (This particular configuration is (54_3), but it is likely that smaller configurations of the same general type could be used in the construction.) The significance of the two heavily drawn lines will be explained soon. As in some of the other constructions, the next step is best explained by thinking of the configuration C_1 as contained in a plane of the 3-dimensional space. By adding two congruent copies, situated perpendicularly above and below C_1, and adding vertical lines through all points of C_1, we obtain a configuration $(162_4, 216_3)$, which we designate

C_2. Now we delete the two heavily drawn lines from the configuration C_1 — but not from the two copies of it, which we used in C_2. Instead of these two lines we introduce three new lines, as shown in Figure 5.1.7, and a new point incident with all three of these. (The existence of such a triplet of lines depends on the variability afforded to tricyclic configurations by the presence of an arbitrary parameter.) This step leads from C_2 to a prefiguration C_3. All lines in C_3 are incident with three points, and all points of C_3 except the newly introduced point are incident with four lines.

In the final step we take two additional copies of C_3 and connects the three exceptional points by a line. This results in a [4,3]-configuration which is connected but obviously is not 2-connected.

An easy modification of this construction for works for $q > 4$. All that is needed is to use copies of C_2 to construct (in 4-space, for greater comfort) a [5,3]- or [6,3]- etc. configuration, before proceeding to C_3 and to the final configuration.

Clearly, the polars of these configurations (or, more precisely, of their projections into the plane) yield the appropriate connected but not 2-connected [3,k]-configurations, with $k \geq 4$.

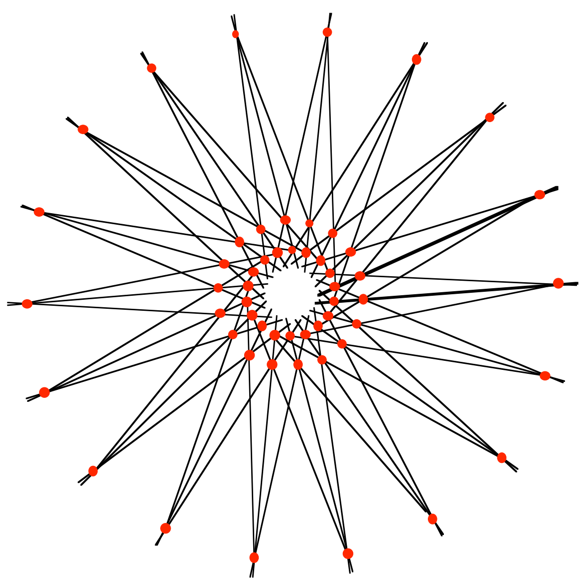

Figure 5.1.6. The tricyclic configuration C_1 used in the proof of Theorem 5.1.4.

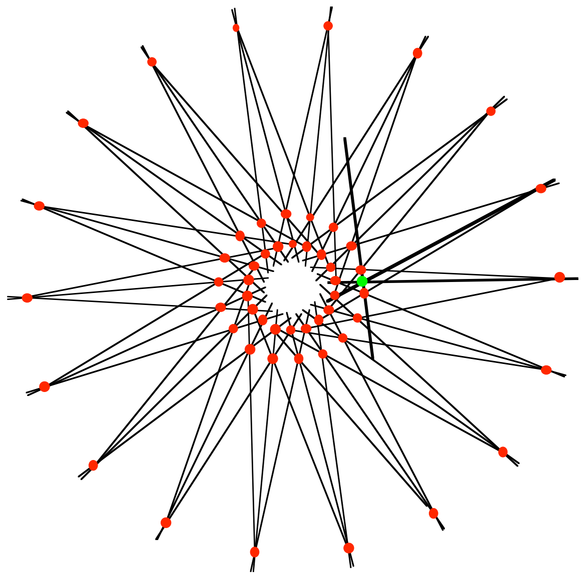

Figure 5.1.7. The prefiguration C_3 used in the proof of Theorem 5.1.4. The new point is indicated by the green dot.

Now, if min{q, k} ≥ 4, we need an additional step in the construction. We shall assume that q ≥ k, since otherwise we could construct the dual configurations. We start again with the (54_3) configuration C_1 shown in Figure 5.1.6. By repeatedly using the procedure we designated (5m) in Section 3.3, we generate from C_1 a [q,k]-configuration C*. In Section 3.3 we went only one step, from 3- to 4-configurations. But an easy modification allows the construction of a k-configuration C** that contains the original C_1 as a subconfiguration. By stacking k copies of C** and connecting them with lines through corresponding points, a [k+1,k]-configuration is obtained; repetition of this step leads to the required C*. Now we replace – as before – the two lines drawn heavily in Figure 5.1.6 by the three lines and a point as shown in Figure 5.1.7. The newly introduced point O is the only point that is on just q-1 lines. Now taking k-1 additional copies of C* and connecting the k points (O and its images in the other copies of C*) by a line gives the desired [q,k]-configuration which is connected but not 2-connected.

* * * * * *

Two elements (points or lines) of a configuration are said to be **independent** if they are:

- Two points that are on no line of the configuration;
- Two lines if they are not incident with a point of the configuration;
- A point and a line if they are not incident.

A family of elements in a configuration is called **independent** if any two of its elements are independent.

A configuration C is said to be **unsplittable**[1] if the deletion of any independent family of its elements leaves a connected configuration. In other words, if for every independent family F, any two elements that do not belong to the family F are in a multilateral that does not use any element in F. Equivalently, C is **splittable** if it can be disconnected by an independent family of elements.

For example, the (12_3) configuration in Figure 5.1.8 has several 5-element independent families but no 6-element independent families. It is easy (even if tedious) to check that the configuration is unsplittable. Similarly, for the (15_3) configuration in Figure 5.1.9, the maximal number of elements in an independent family is 6, and the configuration is unsplittable. These and other examples lead to

Conjecture 5.1.1. The maximal number of elements in an independent family in a connected configuration (n_k) is $[n/k] + 1$.

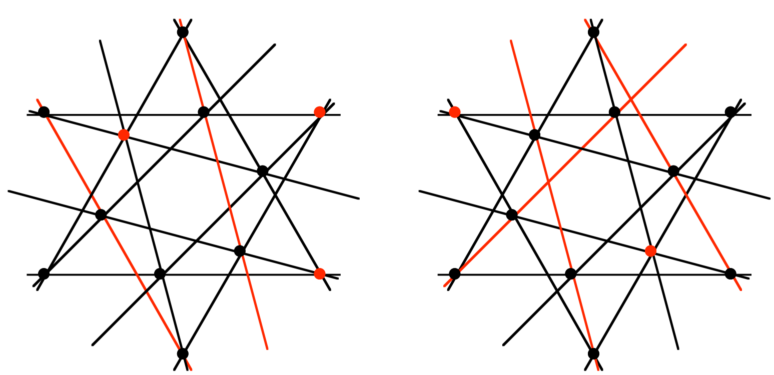

Figure 5.1.8. Two independent families of five elements each (shown in red), that do not disconnect the (12_3) configuration.

---

1 The material on independent families and unsplittable configurations is part of an ongoing collaboration with Tomaz Pisanski; it was presented in part in [P9].

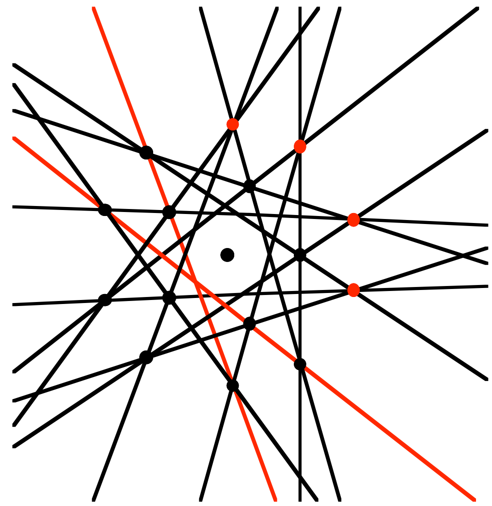

Figure 5.1.9. An independent family of six elements (red) in a (15_3) configuration.

We shall encounter unsplittable configurations in Section 5.6. Here we shall conclude with

Theorem 5.1.5. Every unsplittable 3-configuration is 3-connected.

Proof. Assume that a connected configuration C is not 3-connected; we shall show it is splittable. As a consequence of Steinitz's theorem 2.5.1 it is possible to present C in an orderly configuration table, hence it must be at least 2-connected.

If C is not 3-connected, it can be disconnected by two elements, and we have the two possibilities:

(i) Both elements are of the same kind; without loss of generality we can assume that the disconnecting set consists of two points.

(ii) The disconnecting set consists of one point and one line.

If either of these disconnecting sets were not a splitting set, the two points must be incident with a line of C, or the points and line must be incident, respectively.

In case (i), let the two points be A and B, and let L be the line incident with both. Let D be the third point of L. It is impossible that of the six lines incident with L, only two come from the same connected component. (If this were the case, either the two lines would be incident with the one of the points A, B, D — which would mean that C is not

2-connected; or else the two lines would be incident one each with A and B. Then taking two copies of this components, together with A, B, and L, and attaching three such systems at a point corresponding to D in all three, would again yield a configuration that is not 2-connected.) So each component has three lines incident with L. Since L is incident with only six lines, and A, B disconnect C, the arrangement must be like the one in Figure 5.1.11. But then the point B and line M are a splitting set.

In case (ii), the situation must again be as shown in Figure 5.1.10, with A and L the disconnecting elements, and again M and B are a splitting set. ¨

We may note that the converse of Theorem 5.1.5 does not hold. There are 3-connected configurations that are splittable. The smallest I know is the (15_3) configuration shown in Figure 5.1.11.

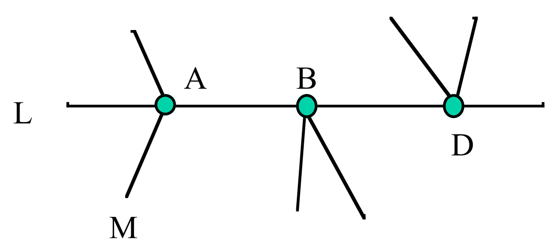

Figure 5.1.10. Schematic arrangement used in the proof of Theorem 5.1.5.

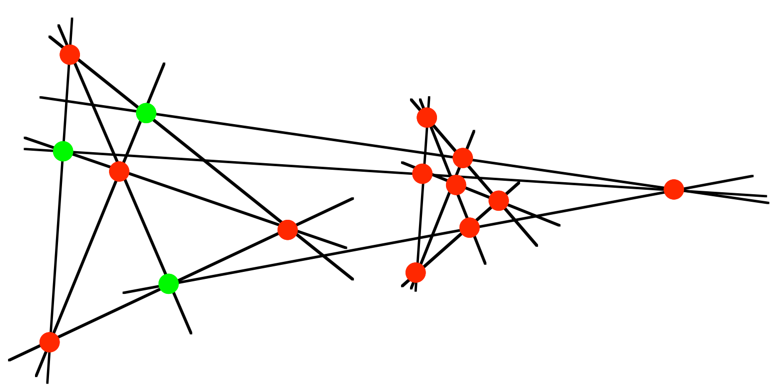

Figure 5.1.11. This 3-connected configuration (15_3) is splittable. A splitting set consists of the three green dots.

Exercises and problems 5.1

1. The geometric [q,k]-configurations constructed in the proof of Theorem 5.1.4 are quite large, even in the case of [4,3]-configurations. Find smaller examples of connected but not 2-connected geometric [4,3]-configurations.

2. Do there exist reasonably-sized 2-connected but not 3-connected geometric [4,3]-configurations? It is clear that this question can be generalized.

3. Without relying on polarity, give a detailed proof of Theorem 5.1.4 for the case of geometric [3,4]-configurations.

4. Prove that Conjecture 5.1.1 is true for k = 2, even without the connectedness assumption. Show that it is invalid for k = 3 if connectedness is not assumed.

5. Show that Conjecture 5.1.1 holds for all (10_3) configurations.

6. Show that the cyclic configuration $\mathbf{C}_3(n)$ (see Section 2.1 for the definition) is unsplittable.

7. Investigate which of the cyclic configurations $\mathbf{C}_3(n,a,b)$ (see definition in Exercise 2.1.2) are unsplittable.

8. The independent families of elements of a configuration C can be characterized as corresponding to independent (that is, unconnected) sets of vertices in the **independence graph** I(C) of C. (The independence graph of C can be defined as the (graph-theoretic) **square** of the Levi graph L(C); this is the graph in which two vertices are connected by an edge is they are connected in the original graph, or if they share a common adjacent vertex. Equivalently, I(C) is the union of L(C) with the edges of the Menger graph M(C) described in Section 1.4, and the edges of M(C*), where C* is the configuration dual to C.)

5.2 HAMILTONIAN MULTILATERALS

As another example of the utility of Levi graphs, we consider in this section and the next some of the known results on multilaterals in configurations. We start by expanding the appropriate definitions from Section 1.3.

We call **multilateral** (or, if appropriate, **r-lateral**) any sequence of points P_i and lines L_i of a configuration that can be written as $P_0, L_0, P_1, L_1, \dots, P_{r-1}, L_{r-1}, P_r = P_0$, with each L_i incident with P_i and P_{i+1} (all subscripts understood mod r). Thus, an r-lateral in a configuration C corresponds to a (2r)-circuit in the Levi graph L(C). A **multilateral path** satisfies the same conditions except the coincidence of the first and last elements. Instead of 3-lateral we shall say **trilateral**, and analogously **pentalateral**, etc.[1] A **circuit decomposition** of a graph is any family of disjoint simple circuits that together include all vertices of the graph. Clearly, not every graph has a circuit decomposition, but as we have seen in Section 2.5, the Levi graph of every connected k-configuration, $k \geq 2$, has such a decomposition. The corresponding multilaterals of the configuration are said to be a **multilateral decomposition** of the configuration. A multilateral decomposition consisting of a single multilateral is a **Hamiltonian multilateral** of the configuration. In other words, a Hamiltonian multilateral of a configuration passes through all its points and uses all its lines, each precisely once.

The Hamiltonian circuit of the Levi graph in Figure 5.1.1 corresponds to a Hamiltonian multilateral of the configuration. On the other hand, from the Levi graph of the same configuration shown in Figure 5.1.2 we easily see the possibility of a circuit decomposition of the Levi graph into four 6-circuits, hence yielding a decomposition of the configuration (12_3) in Figure 5.1.1 into four trilaterals (that form a cycle of mutually inscribed / circumscribed trilaterals). It is also easy to observe a decomposition of this configuration into three quadrilaterals, such as la8g6b71, 3d10i2c9h, 5f12k4e11j.

---

[1] The terms "trilateral", "pentalateral" and others were used by Martinetti [M1] in 1886, but in a slightly different meaning.

As another example, in Figure 5.2.1 we show a Hamiltonian multilateral of a configuration (10_3), as well as a decomposition of the same configuration into two pentalaterals.

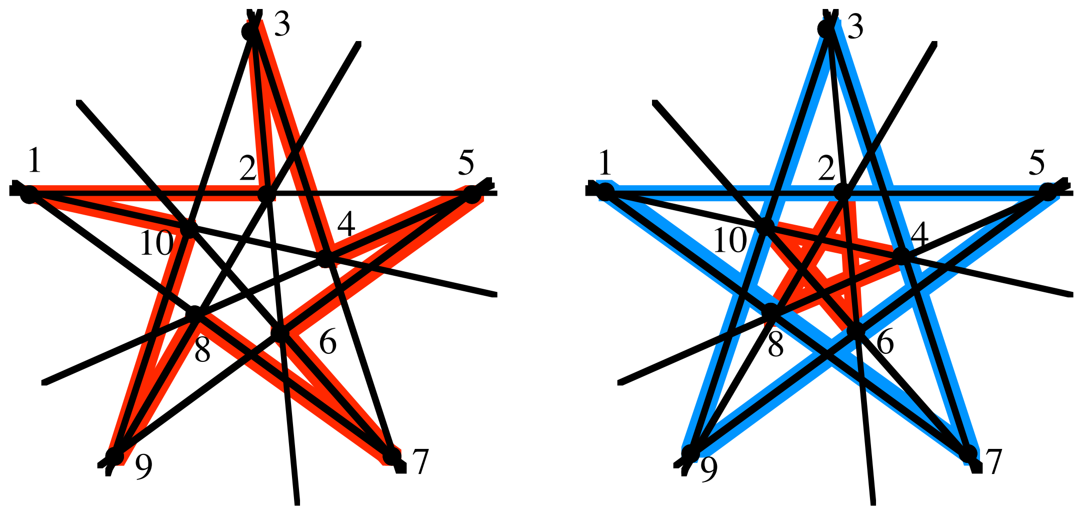

Figure 5.2.1. A configuration (10_3) with one Hamiltonian multilateral, and one decomposition into two pentalaterals that are mutually inscribed/circumscribed.

The remaining part of this section is devoted to a survey of results known about Hamiltonian multilaterals. The great majority of these results deal with 3-configurations.

To begin with, here are some historical notes; in all of these papers the *circuit* terminology has been used, but we present them in our terms. Kantor in 1881 [K4] states *as a theorem* that every (n_3) configuration has a Hamiltonian multilateral. Martinetti [M2] in 1887, Schoenflies [S2] in 1888 and Brunel [B30] in 1895 consider Hamiltonian multilaterals as self-inscribed/circumscribed polygons. Schröter in 1889 [S8] states that he confirmed the existence of Hamiltonian multilaterals in all (10_3) configurations, and Steinitz in 1897 [S18] does the same for all (11_3). Steinitz also observed that connectedness is a necessary condition, a fact not mentioned by earlier writers. He also provided a first example of a connected configuration that does not admit a Hamiltonian multilateral. The smallest configuration that would fit his description is (28_3). In 1990, Gropp [G9] announced that all connected configurations (n_3) with $n \leq 14$ have Hamiltonian multilaterals. The statement (a1) in the paper [K9, p. 128] by Kelmans, to the effect that every 3-valent, 3-connected bipartite graph with at most 30 vertices has a Hamiltonian circuit, implies that all connected (n_3) configurations with $n \leq 15$ have Hamiltonian multilaterals.

The example of Steinitz mentioned above was improved in [D10] by the construction of the configuration (22_3) shown in Figure 5.2.2. It is not known whether every connected configuration (n_3) with $16 \leq n \leq 21$ admits a Hamiltonian multilateral.

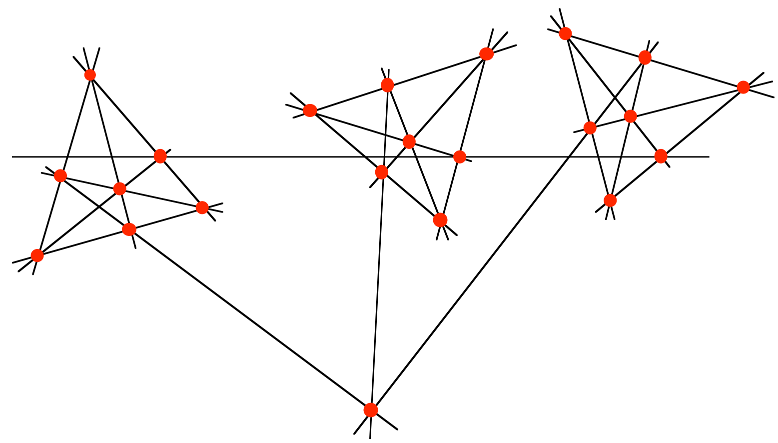

Figure 5.2.2. A (22_3) configuration that does not admit any Hamiltonian multilateral. It is obvious that such configurations (n_3) can be constructed for every $n \geq 22$.

The fact that all connected configuration (n_3) without a Hamiltonian multilateral known at the time were only 2-connected led the author to conjecture in 2002:

Conjecture 5.2.1. All 3-connected (n_3) configurations admit Hamiltonian multilaterals.

However, this conjecture was disproved in [G45]:

Theorem 5.2.1. There exists a 3-connected geometric configuration (25_3) that does not admit a Hamiltonian multilateral.

We shall prove this by a construction, fashioned after the arguments presented in [G45].

Our construction starts with the smaller graph shown in Figure 5.2.3, devised by M. N. Ellingham and J. D. Horton in [E1]. This graph has no Hamiltonian circuit that uses both heavily drawn edges. The *proof* of this assertion is simply a follow-up of a few alternatives — the non-trivial, clever part is the *discovery* of the graph. For the next step we insert two additional vertices in each of the heavily drawn edges of Figure 5.2.3, resulting in the graph shown in Figure 5.2.4. From this the graph of Figure 5.2.5 was constructed by Georges [G1]. It is a non-Hamiltonian, 3-connected, bipartite graph. Again, the proof of non-Hamiltonicity consists of the examination of several possibilities, and showing that neither leads to a Hamiltonian circuit. After the graph is constructed, this is a matter of routine checking, as are the other relevant properties. At this step, as in the earlier, it is the construction of the graph that is ingenious. The main result of the construction that is relevant to the present aim is the fact that the Georges graph has girth 6. Since it is bipartite, it follows that it is the *Levi graph* of a combinatorial configuration (25_3). This is its relevance for the present goal.

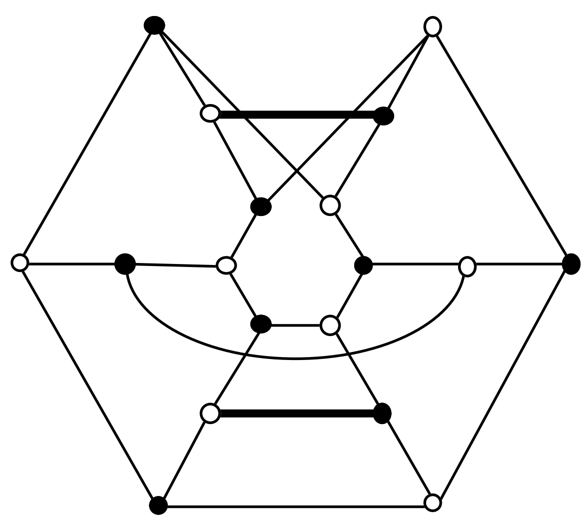

Figure 5.2.3. This bipartite graph found by Ellingham and Horton [E1] does not admit a Hamiltonian circuit that uses both heavily drawn edges.

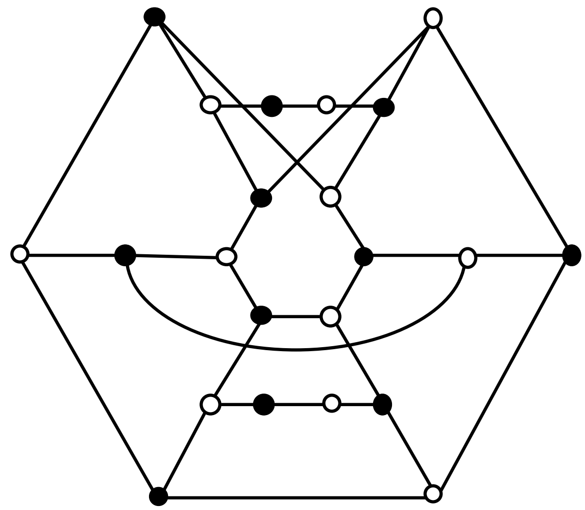

Figure 5.2.4. A modification of the graph in Figure 5.2.3.

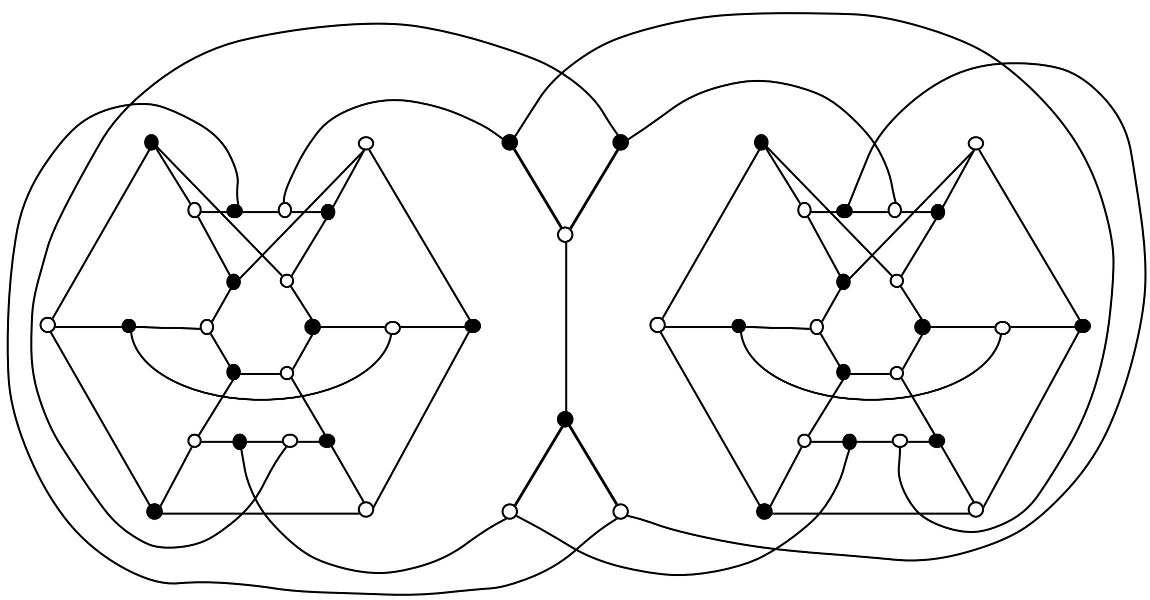

Figure 5.2.5. The Georges graph, resulting from a combination of two copies of the graph in Figure 5.2.4. The graph is bipartite, 3-connected, non-Hamiltonian, and has girth 6.

We shall now apply the method of Steinitz described in Section 2.6 to obtain first a realization of this combinatorial configuration (25_3) as a prefiguration, and then apply a continuity argument to establish the possibility of its realization by a geometric configuration. To begin with we label the Georges graph in a more-or-less random way, as in Figure 5.2.6. This labeling leads to the configuration table, shown in Table 5.2.1. This is turned into an orderly configuration table, shown in Table 5.2.2, as required for the application of Steinitz's construction. (This table was not constructed by following the rather cumbersome Steinitz algorithm, but by a straightforward "greedy" algorithm: Taking the first available choice at each step. It worked very well in the present case.)

Table 5.2.3 shows the Georges configuration with columns (that is, lines) permuted so that a decomposition of the configuration into "multilaterals" becomes obvious. This is accomplished by making the second entry in a column equal to the third entry in the preceding column, the first column being chosen arbitrarily. The exception is the last column of a multilateral, in which the last entry is the same as the second entry of the

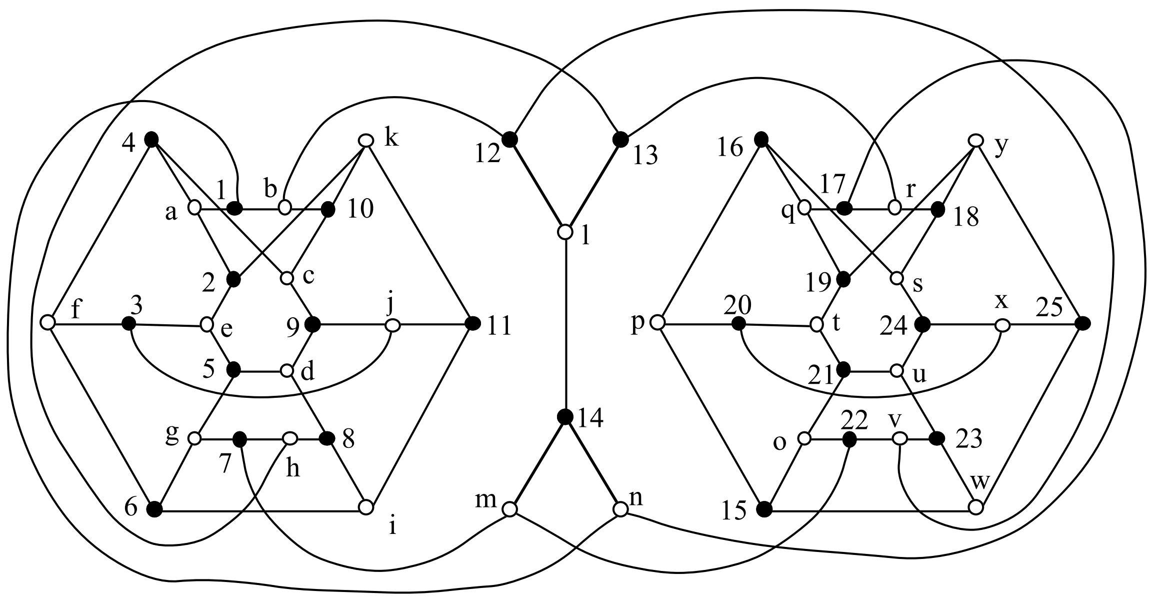

Figure 5.2.6. A labeling of the Georges graph that allows us to interpret it as the Levi graph of a combinatorial configuration. The task is simplified by the fact that there are sufficiently many characters to label all lines.

a	b	c	d	e	f	g	h	i	j	k	l	m
1	1	4	5	2	3	5	7	6	3	2	12	7
2	10	9	8	3	4	6	8	8	9	10	13	14
4	12	10	9	5	6	7	13	11	11	11	14	22

n	o	p	q	r	s	t	u	v	w	x	y
1	15	15	16	13	16	19	21	12	15	20	18
14	21	16	17	17	18	20	23	22	23	24	19
17	22	20	19	18	24	21	24	23	25	25	25

Table 5.2.1. A configuration table of the Georges configuration, as read off Figure 5.2.6.

a	b	c	d	e	f	g	h	i	j	k	l	m
1	10	4	5	2	3	6	7	8	9	11	12	14
2	12	9	8	3	4	5	13	6	11	0	14	7
4	1	10	9	5	6	7	8	11	3	2	13	22

n	o	p	q	r	s	t	u	v	w	x	y
17	15	16	19	13	18	20	21	22	23	24	25
1	22	15	17	18	16	21	24	23	25	20	19
14	21	20	16	17	24	19	23	12	15	25	18

Table 5.2.2. An orderly configuration table for the Georges configuration.

first column. In cases like the present one, where the first multilateral does not exhaust the columns, the first remaining column is used to start a new polygon. In the case of the George configuration, the first is a 22-gon, the second a triangle. Figure 5.2.7 provides an illustration of the two circuits in the Levi graph, that correspond to two multilaterals.

a	f	i	j	e	g	m	o	t	y	r	q	s
1	3	8	9	2	6	14	$\boxed{15}$	20	25	13	19	18
2	4	6	11	3	5	7	22	21	19	18	17	16
4	6	11	3	5	7	22	21	19	18	17	16	24

u	v	b	n	l	h	d	c	k	p	x	w
21	22	10	17	12	7	5	4	11	16	24	23
24	23	12	1	14	13	8	9	10	$\boxed{15}$	20	25
23	12	1	14	13	8	9	10	2	20	25	15

Table 5.2.3. A rearrangement of the columns of the Georges configuration used to show a decomposition into multilaterals. The boxed labels are explained in the text.

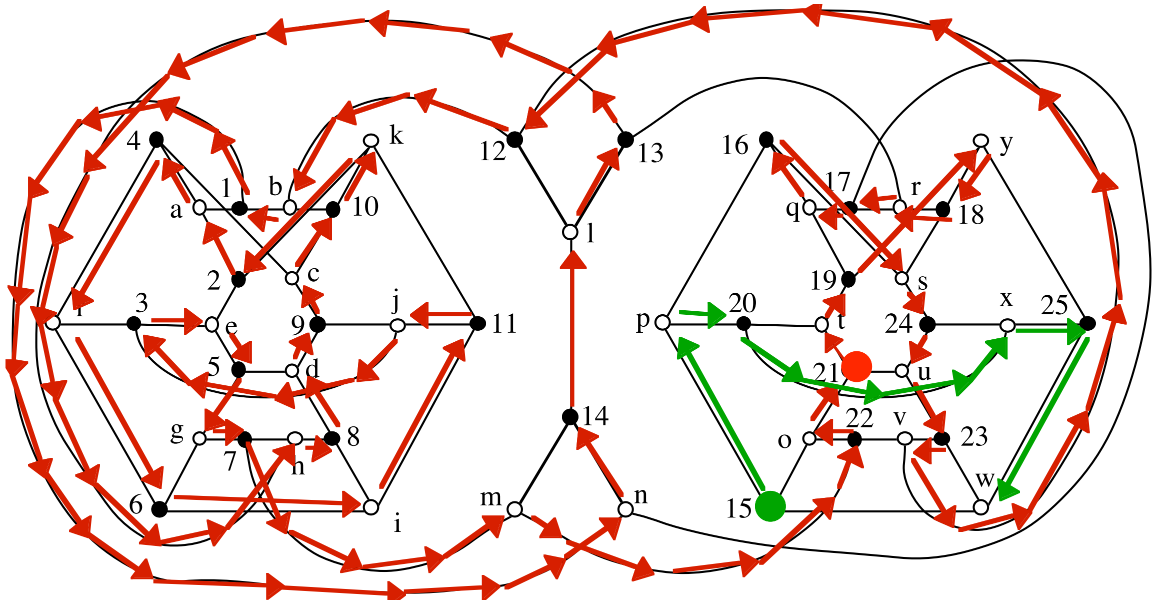

Figure 5.2.7. The two multilaterals from Table 5.2.3 that lead to a multilateral decomposition of the Georges graph.

As a last step in the Steinitz algorithm before the geometric construction, we permute the columns (lines) once more. Some vertex of a column of the last multilateral (the second in this case) must be a vertex that appeared in a previous multilateral, since otherwise the configuration would not be connected. (In the present case, we chose the vertex labeled 15.) We place that column as the first of the last multilateral, and place as the last column of the previous multilateral its column that contains the same vertex. The other columns in both multilaterals are permuted accordingly, so as to preserve the multilaterals present. The configuration table obtained in this step (resulting from the choice of 15 as the special vertex) in shown in Table 5.2.4.

The geometric realization now proceeds very simply. It can be followed in Figure 5.2.8 which was obtained using “Geometer’s Sketchpad”™ and modified by ClarisDraw™. The idea follows the explanations given in Section 2.6: Choose the vertices as arbitrary points, except when constrained to lie on one or two previously

t	y	r	q	s	u	v	b	n	l	h	d	c
20	25	13	19	18	21	22	10	17	12	7	5	4
21	19	18	17	16	24	23	12	1	14	13	8	9
19	18	17	16	24	23	12	1	14	13	8	9	10

k	a	f	i	j	e	g	m	o	p	x	w
11	1	3	8	9	2	6	14	$\boxed{15}$	16	24	23
10	2	4	6	11	3	5	7	22	$\boxed{15}$	20	25
2	4	6	11	3	5	7	22	21	20	25	15

Table 5.2.4. A rearrangement of the columns of Table 5.2.3, needed for the application of Steinitz's geometric construction.

constructed lines. In this example we start with arbitrary points 21 and 19. Points 18 and 17 are also chosen freely, but the choice of 16 has to be on the line q through the previously determined points 19 and 17, and then 24 must be on the line s through 16 and 18; similarly, the point 23 must be on the line u = [21, 24]. The points 12 and 1 can be chosen freely, but 14 must be on the line n = [1, 17], and 13 on the intersection point of the lines r = [17, 18] and l = [12, 14]. Next, points 8, 9, 10, 2 are free, but 4 must be on the line a = [1, 2]. The point 6 is free, while 11 is the intersection point of lines i = [6, 8] and k = [10, 2], and point 3 is the intersection point of the lines f = [4, 6] and j = [9, 11]. Similarly, 5 is the intersection point of d = [8, 9] and e = [2, 3], and 7 is the intersection point of h = [8, 13] and g = [5, 6], while 22 is the intersection point of lines v = [23, 12] and m = [7, 14]. This completes the construction of the first multilateral. To start with the next (the trilateral), we select 15 on the line o = [22, 21], then 20 as the intersection point of t = [21, 19] and p = [16,15]. The only remaining problem is the selection of point 25, which should be at the intersection of **three lines**, namely y = [18, 19], x = [24, 20], and w = [23, 15]. It is to be expected that three lines do not have a common point. This is quite general, and it is the final solution given by Steinitz, with the selections made: the last line may need to be taken as a circle (or a parabola).

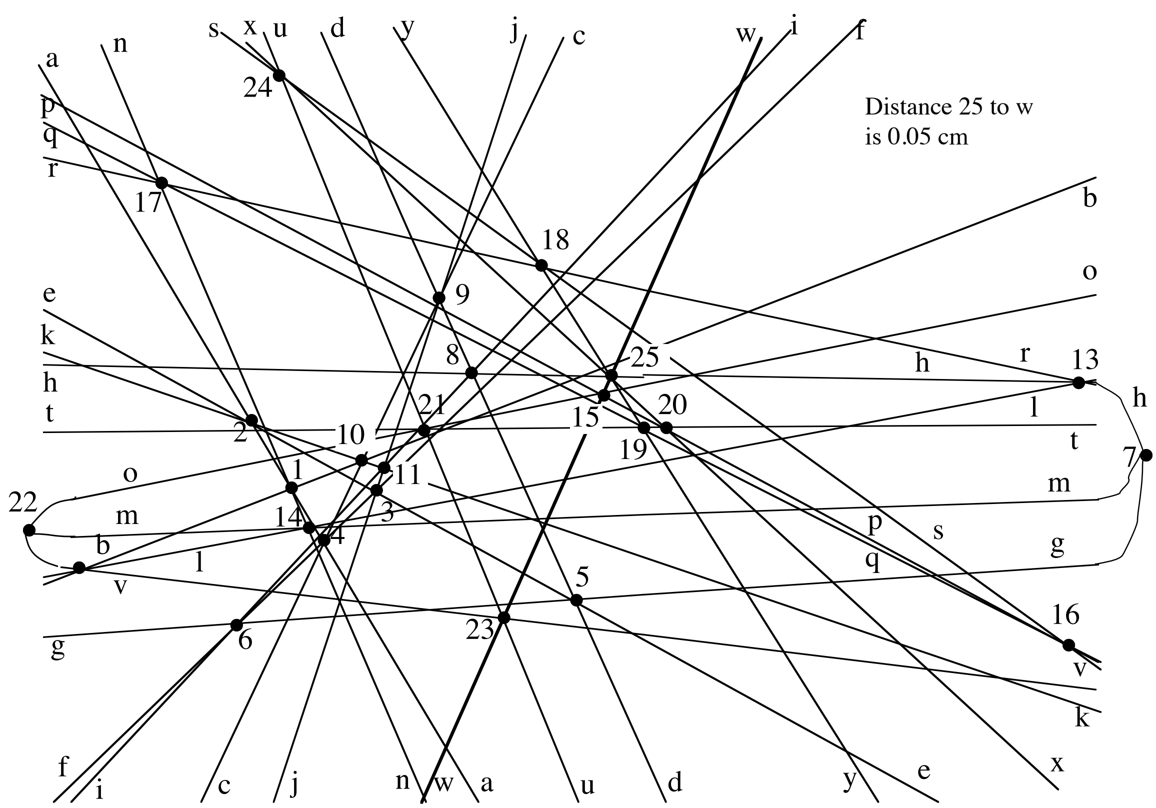

Figure 5.2.8. The construction of a 3-connected geometric configuration that does not admit a Hamiltonian multilateral. In the actual construction shown (using "Geometer's Sketchpad"™) the final incidence was missed by about 0.5 mm due to the discreteness of the underlying software. The curves at left and right are meant to indicate that the triplets of lines do meet at the points they are supposed to – but too far for inclusion in an intelligible version of the diagram.

In fact in this case — just as for many other configurations — by judicious choices of the free parameters one may find selections in which the point 25 is on a certain side of the line w, as well as selections where it is on the other side. By continuity, this implies that there is a position of incidence. The final conclusion, therefore, is that the Georges configuration can be realized geometrically, by points and straight lines. Hence it is a 3-connected non-Hamiltonian geometric configuration (25_3). ¨

The result of Theorem 5.2.1 can be extended to geometric configurations of almost all sizes:

Theorem 5.2.2. For each $n \geq 33$ there exist 3-connected geometric configurations (n_3) that do not admit Hamiltonian multilaterals.

Proof. Selecting any of the vertices of the (25_3) configuration of Theorem 5.2.1, (see Figure 5.2.9(a), where the gray oval stands for the rest of the Georges configuration (25_3), denoted here by G. We delete that vertex and replace it by the three intersection points of the lines incident with the deleted vertex and a new line L (see Figure 5.2.9(b)). We denote this truncated version of G by G'. Taking now the similarly truncated version H' of any configuration (p_3), we make its three lines incident with the three points on L (Figure 5.2.9(c)). Since both (7_3) and (8_3) have truncated versions realizable by straight lines, the above results in a configuration with $n \geq 24 + 3 + 6 = 25 + 1 + 7$ points and lines. This configuration is clearly 3-connected but it cannot be Hamiltonian.

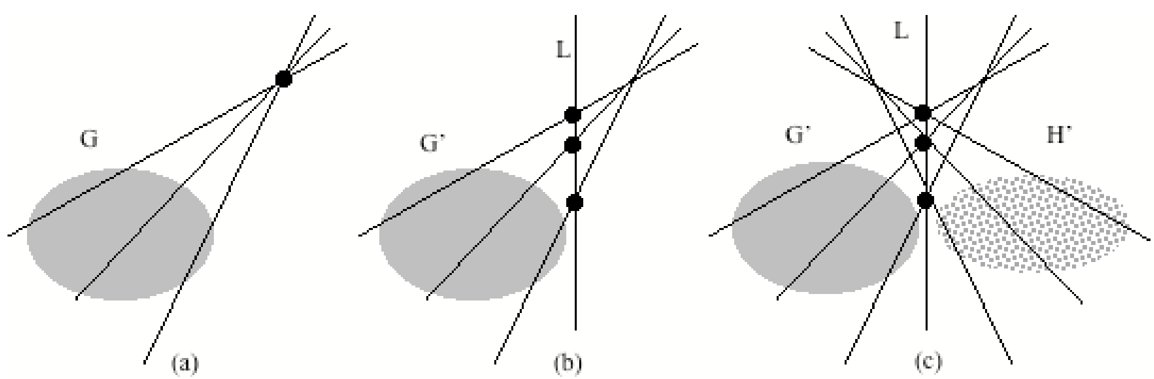

Figure 5.2.9. The construction establishing Theorem 5.2.2.

Indeed, any Hamiltonian multilateral would have to use L and two of its points, one of which must be on a line toward G', the other towards H'. The third point on L must be on one line from G' and another from H'. But then there would be a multilateral in G' using L, and therefore – by identifying the three points of G' that are on L – we would get a Hamiltonian multilateral of G. ¨

A few remarks on the background of Theorem 5.2.1. I learned of Georges' paper [G1] and his non-Hamiltonian graph from Gropp [G9]. But Gropp but makes no connection between the Georges graph and configurations, and in particular, does not observe the fact that the Georges graph has girth 6 and is therefore the Levi graph of a configuration (combinatorial at least). It should also be noted that in [G1], the rendition of the Ellingham-Horton graph, shown above in Figure 5.2.3, is missing one of the special edges.

Gropp [G9], [G19] also mentions that a result similar to Georges' has been found earlier by Kelmans [K8]. This may well be the case; however, I find the presentation in [K8] (both in the Russian original, and in the translation) too confusing to be able to decide whether the graph he constructs has girth 6. Like Georges, Kelmans does not mention girth, or configurations. The claim in [G9] that Kelmans' 50-vertex graph is the same as Georges seems quite unjustified. The expanded version of Kelman's paper (see [K9]) remains inscrutable to the present author. Moreover, there is no mention in [K9] of girth 6, of Levi graphs, or of any type of configurations

*   *   *   *   *

A natural question that can be asked in view of Theorems 5.2.1 and 5.2.2 is:
Does every geometric 4-configuration admit a Hamiltonian multilateral?

As we shall now show, there is a negative partial answer:

Theorem 5.2.3. There exist 2-connected geometric 4-configurations that do not admit any Hamiltonian multilaterals.

Proof. We provide a conceptually simple construction that, unfortunately, leads to such configurations but of relatively large sizes. We use configurations (or, more precisely, fragments of configurations) such as the halves of the configurations in Figure 5.1.5. With the same conventions, we can assume that we start with an arbitrary (n_4), for example, the C(4) used in Section 5.1. (We note that the configuration (18_4) in Figure 3.3.4 could be used, but at the cost of some detailed arguments about cross-ratios.) As indicated in Figure 5.2.10, we start with eight copies, delete from each a line and take suitable projective transforms so that the points that are on three lines each are aligned as shown in Figure 5.2.10, using an additional line L and an additional point P. Since each of L and P can be used only once in any multilateral, there is no possibility for involvement of more that two of the groups of four starting configurations. Hence this non-Hamiltonian configuration is a (4087_4); if we start with (18_4) the result is a still formidable (289_4). A somewhat smaller example can be found by replacing, in each set of four, one configuration by a single point; this would lead to a non-Hamiltonian (3077_4) if using C(4), or (221_4) if using (18_4).

It is easy to see that a similar construction can be applied to k-configurations for all k ≥ 5, starting with any single geometric configuration of that kind; for example, C(k) can be used. Obviously, the configurations obtained will be monstrously large.

An unsolved problem is the question whether there are non-Hamiltonian geometric 4-configurations that are 3- or 4-connected.

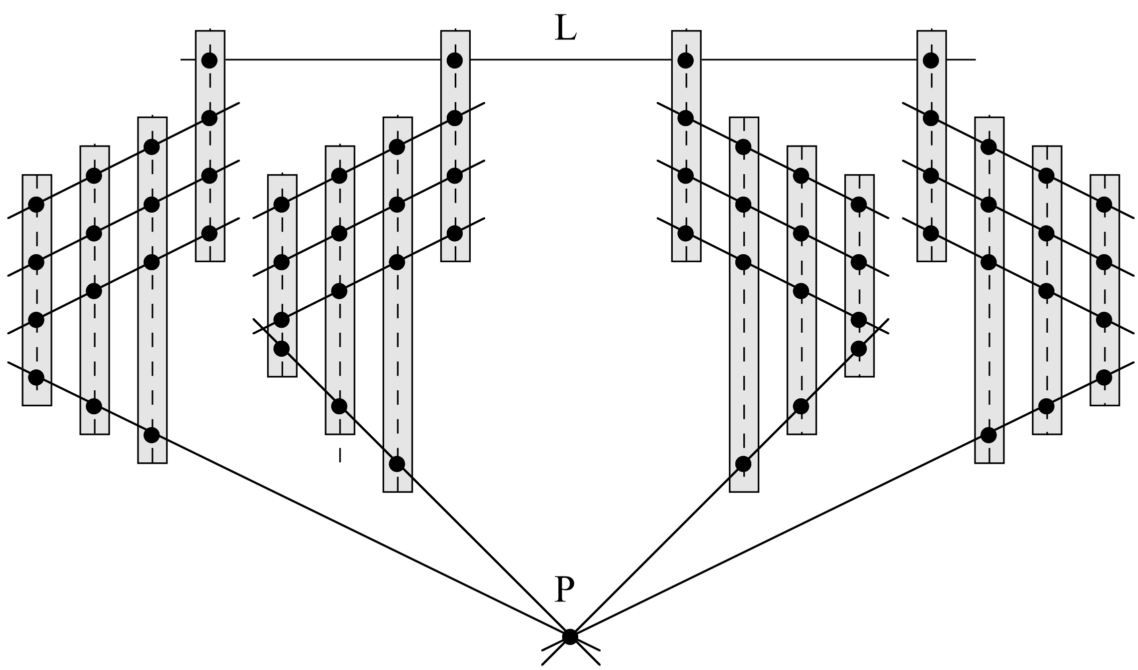

Figure 5.2.10. The scheme of the construction of a 2-connected geometric configuration (289_4) that does not admit any Hamiltonian multilaterals. Each gray rectangle represents an (18_4) configuration from which one line has been omitted.

A different direction in the study of Hamiltonian multilaterals in configurations is opened by the following generalization:

Definition. A [q,k]-configuration has a Hamiltonian multilateral if and only if it has a multilateral M such that:

(i) Every element of one of the two kinds (points or lines) is contained in the multilateral M;

(ii) Every element (of both kinds) is incident at most once with the multilateral M.

Obviously, this definition reduces to the standard one in case of balanced configurations ($q = k$).

Except for a few examples of type [3, 4] with Hamiltonian multilaterals, there seems to be no information available on this topic.

It also seems that the concept has not been studied in the context of bipartite graphs — to which it obviously applies.

* * * * * *

A different type of questions and results arises if we inquire about Hamiltonicity of some restricted families of configurations. For example, if we consider astral 3-configurations, one may inquire about Hamiltonian multilaterals that have the same symmetries as the configuration; we shall call them **symmetric Hamiltonian multilaterals**. In Figure 5.2.11 we show an example of a symmetric Hamiltonian multilateral in the astral (10_3) configuration. Note that both parts show the same symmetric multilateral — multilaterals are concerned with lines, not segments.

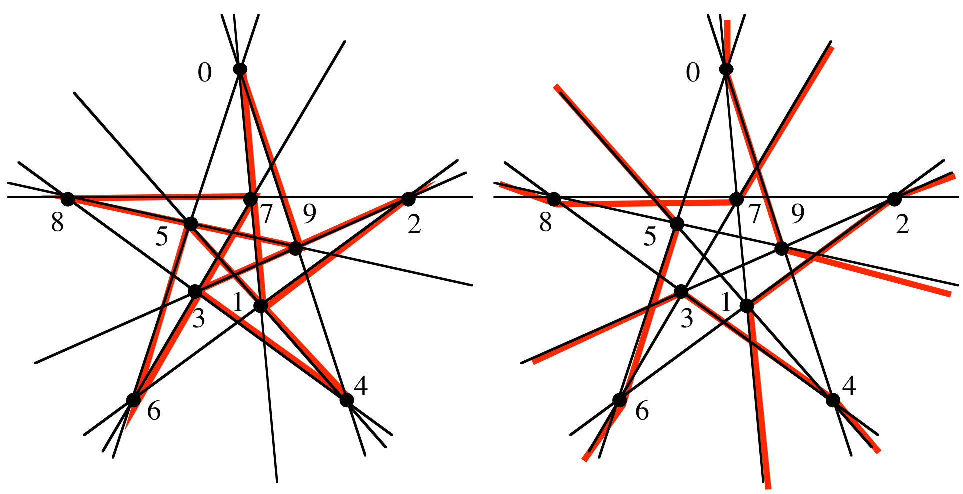

Figure 5.2.11. A symmetric Hamiltonian multilateral in the astral configurations (10_3). Both parts represent the same multilateral.

In Figure 5.2.12 we show four different symmetric Hamiltonian multilaterals on the astral (10_3) configuration. Using the notation for astral 3-configurations we introduced in Section 2.7, and which is illustrated in Figure 5.2.13, we can assert:

Theorem 5.2.4. Cyclic astral configuration m#(b, c; d) may have four types of symmetric Hamiltonian circuits:

$B_0 \rightarrow C_0 \rightarrow B_d \rightarrow \ldots$

$B_0 \rightarrow C_0 \rightarrow B_{d-c} \rightarrow \ldots$

$B_0 \rightarrow C_{-b} \rightarrow B_{d-b} \rightarrow \ldots$

$B_0 \rightarrow C_{-b} \rightarrow B_{d-b-c} \rightarrow \ldots$

A symmetric Hamiltonian circuit of one of these types exists if and only if m is relatively prime to d, d–c, d–b, or d–b–c, respectively.

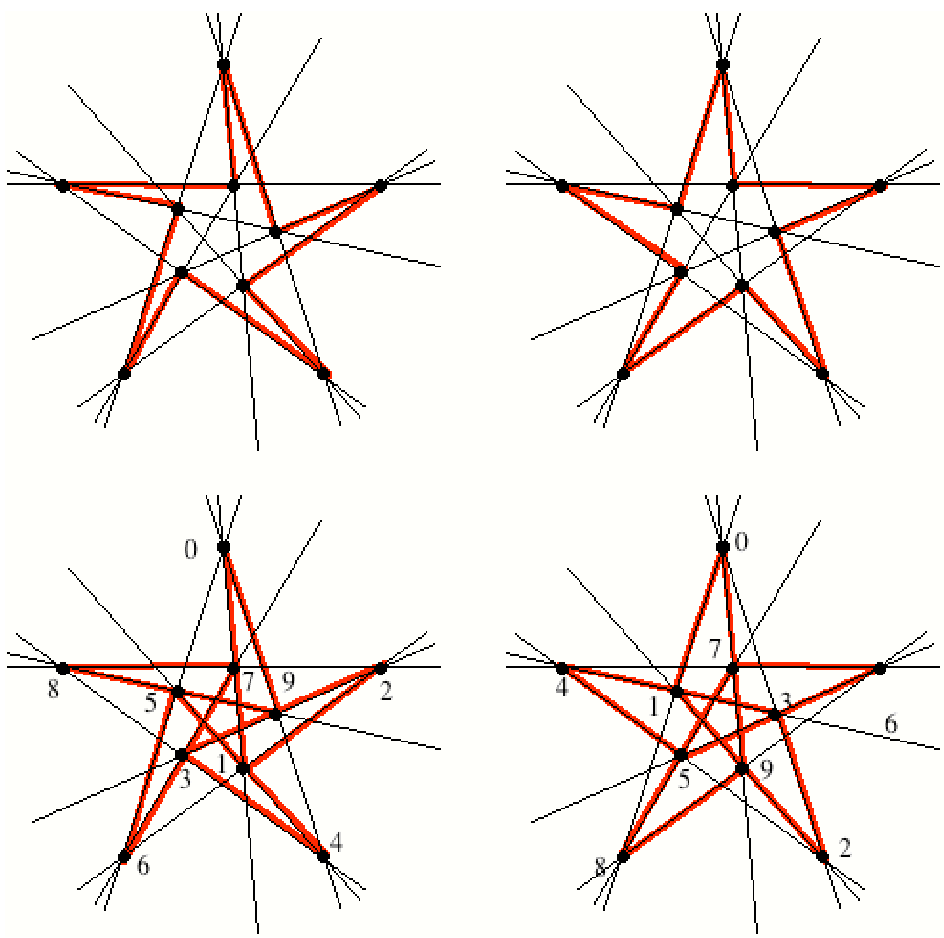

Figure 5.2.12. Four different symmetric Hamiltonian multilaterals in the astral configuration (10_3).

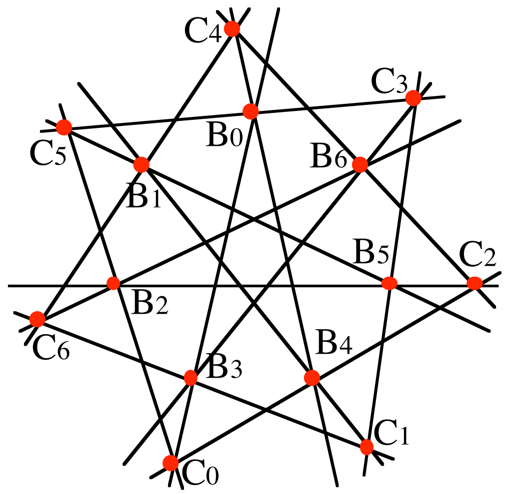

Figure 5.2.13. A reminder of the notation for astral 3-configurations, illustrated for m#(b,c;d) = 7#(3,2;4)

A related result of Hladnik *et al.* [H5], based in part on work of Alspach and Zhang [A1], should be mentioned here: Every connected cyclic 3-configuration (combinatorial or geometric) is Hamiltonian. Unfortunately, it is not clear to me exactly what is here meant by "cyclic 3-configuration".

Exercises and problems 5.2.

1. Decide the validity of the following open conjecture: Every astral 3-configurations admits a Hamiltonian multilateral.

2. Find four symmetric Hamiltonian multilaterals in the (14_3) astral configuration 7#(3,2;1).

3. Prove Theorem 5.2.4. Apply it to the configuration 8#(3,2;1).

4. The two configurations in Figure 5.2.14 do not have any symmetric Hamiltonian multilateral. If the result of [H5] mentioned above relates to them, they have Hamilto-nian multilaterals. In any case, either find a Hamiltonian multilateral, or else show that there is none such.

5. Determine whether the three 3-astral configurations (9_3) in Figure 1.1.6 admit symmetric (or any) Hamiltonian multilaterals.

6. In configurations with dihedral symmetry group one can not expect any Hamiltonian multilateral to have the same symmetry group. At most, one may look for cyclically symmetric Hamiltonian multilaterals. In Figure 5.2.15 we show three examples of this situation. Determine whether the six astral 4-configurations (36_4) shown in Figure 3.6.3 admit cyclically symmetric Hamiltonian multilaterals.

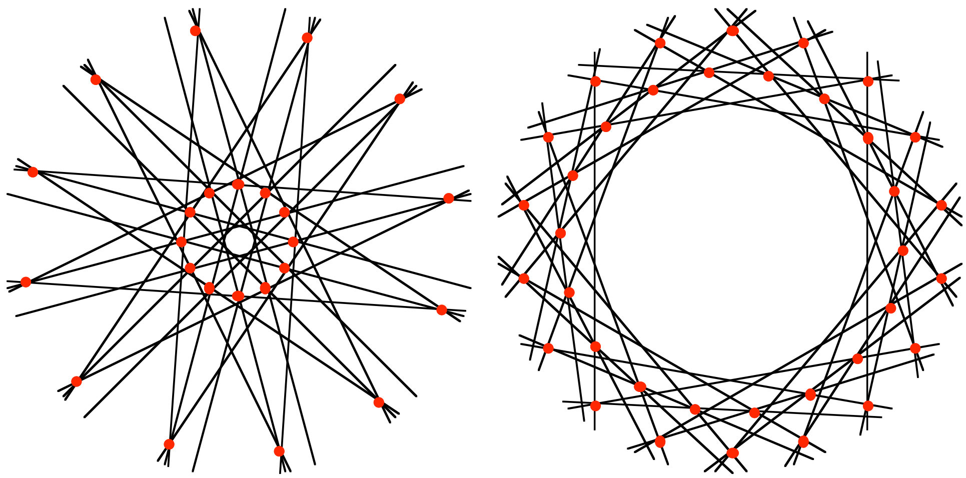

Figure 5.2.14. Selfpolar astral configurations 12#(5, 5; 2) and 18#(5, 1; 3) have no symmetric Hamiltonians. Do they have any Hamiltonian circuits at all?

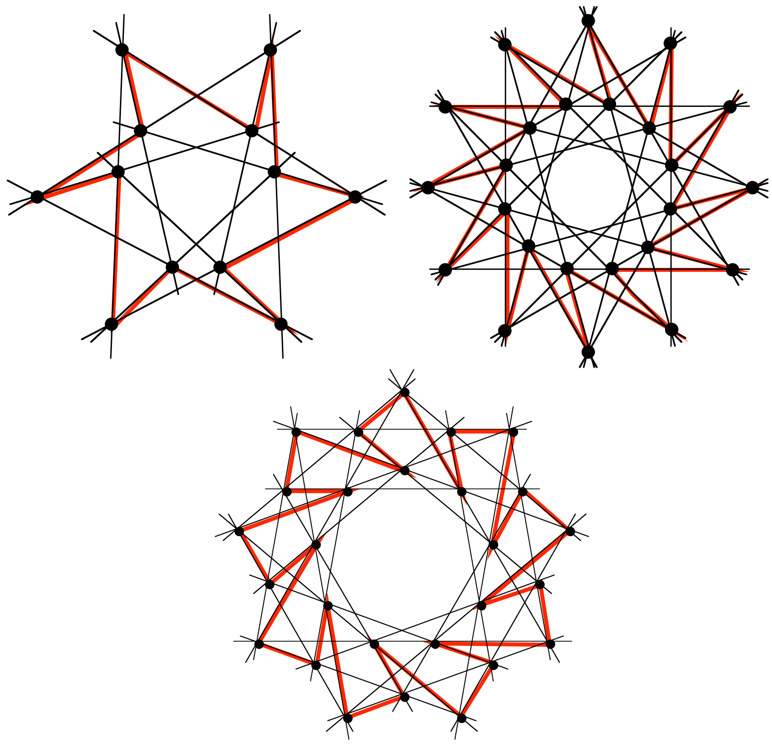

Figure 5.2.15. Examples of cyclically symmetric Hamiltonian multilaterals in three configurations with dihedral symmetry.

7. Following [D7] we say that set of points of a configuration C is a **blocking set** it if contains a point of every line of C but not all points of any of the lines. Show that the (22_3) configurations shown in Figure 5.2.2 contains no blocking set. (This example disproves two conjectures in [D7].) For more information about blocking sets and blocking set-free configurations see [G11], [G24].

5.3 MULTILATERAL DECOMPOSITIONS

In 1828 Moebius [M20] pointed out that it is obvious that two trilaterals cannot be mutually inscribed/circumscribed, and proved the impossibility of two quadrilaterals be in such mutual relationship; he dealt here with the real Euclidean plane. (This seems to be the first paper dealing with this topic.) Moebius concludes his paper by saying: "I have not extended this investigation to multilaterals with more sides." [My translation] Therefore the statement in the Wikipedia [W4] that "Möbius (1828) asked whether there exists a pair of polygons with p sides each, having the property that the vertices of one polygon lie on the lines through the edges of the other polygon, and vice versa" has to be taken with a grain of salt. In fact, the answer to the question is affirmative, even if the author is lost in history. The first mention of three mutually inscribed/circumscribed trilaterals seems to be in Graves [G6*], where the Pappus configuration (9_3) is shown to have that property. Moreover, Graves shows that the Desargues configuration (10_3) can be presented as a pair of mutually inscribed/circumscribed pentalaterals. He illustrated this in [G6*] by a diagram (reproduced here as Figure 5.3.1) in which one of the pentalaterals in rendered in color (this was in 1839!). Without diagrams, Cayley [C2*] describes this and several other examples of mutually inscribed/circumscribed families of multilaterals.

For any multilateral decomposition of a 3-configuration by a family F of p-laterals P_i, $1 \leq i \leq r$, we shall say that it is an **inscribed/circumscribed family** (or decomposition)

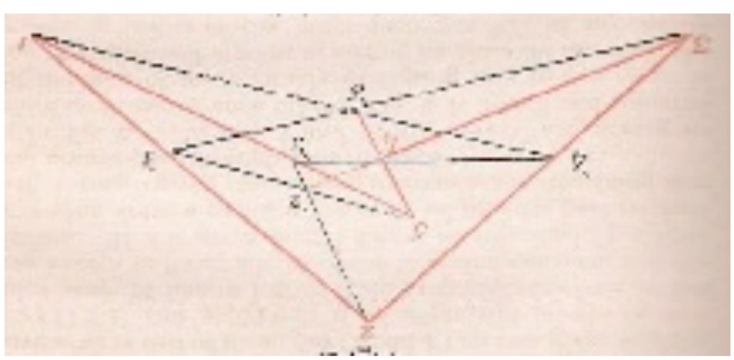

Figure 5.3.1. The Desargues configurations (10_3) presented as a pair (black, and color) of mutually inscribed/circumscribed pentalaterals. From Graves 1839 paper [G2*].

provided every line of P_i contain a vertex of P_{i+1}, for all i (subscripts taken mod r). This is illustrated (for r = 2) by the two examples in Figure 5.3.2. (The first is clearly the same as the Graves example in Figure 5.3.1.) As we discussed previously, Hamiltonian multilaterals of 3-configurations fit this description for r = 1. The astral 3-configurations considered in Section 2.7 show that for r = 2 there exist inscribed/circumscribed families of n-laterals for all $n \geq 5$. The case r = 2, n = 5 is illustrated in Figure 5.3.2(b). The k-astral 3-configurations discussed in Section 2.10 show that for every r, there exist inscribed/circumscribed families of n-laterals for all $n \geq 3$. However, in different forms, these results go much farther back.

The Desargues configuration (which we denoted $(10_3)_1$ in Section 2.2) can also illustrate a refinement of the definition. We say that a family F is an **orderly** inscribed/circumscribed family if consecutive vertices of P_{i+1} belong to consecutive lines of P_i. Although the example in Figure 5.3.2(a) shows a pair of inscribed/circumscribed pentalaterals, this family is not orderly — in contrast to the example in Figure 5.3.2(b). In fact, it can be proved that the Desargues configuration does not admit any orderly pair of pentalaterals. It is worth stressing (as Graves [G2*] did long ago) that the two pentalaterals in the Desargues configuration are combinatorially in a very symmetric reciprocal relationship although this finds no reflection in the geometric rendition.

Among other early publications are the papers [S1] and [S2] by Schoenflies. He was led to this topic by his investigation of the density of trilaterals which we shall discuss in Section 5.5. In these papers Schoenflies formally introduced the families of mutually inscribed/circumscribed multilaterals, and provided examples. (Minor errors of [S2] are corrected in [S3]. More serious shortcomings are pointed out by Steinitz in [S19, p. 488], [S20, p. 307].) Additional related investigations by Schoenflies are reported in [S3] and [S5]. Brunel [B30] considers the topic as well.

Other examples of orderly inscribed/circumscribed families are provided in Figure 5.3.3. A variety of examples is shown in [D10]. These can be generalized to all n-laterals with $n \geq 3$, and all $r \geq 3$.

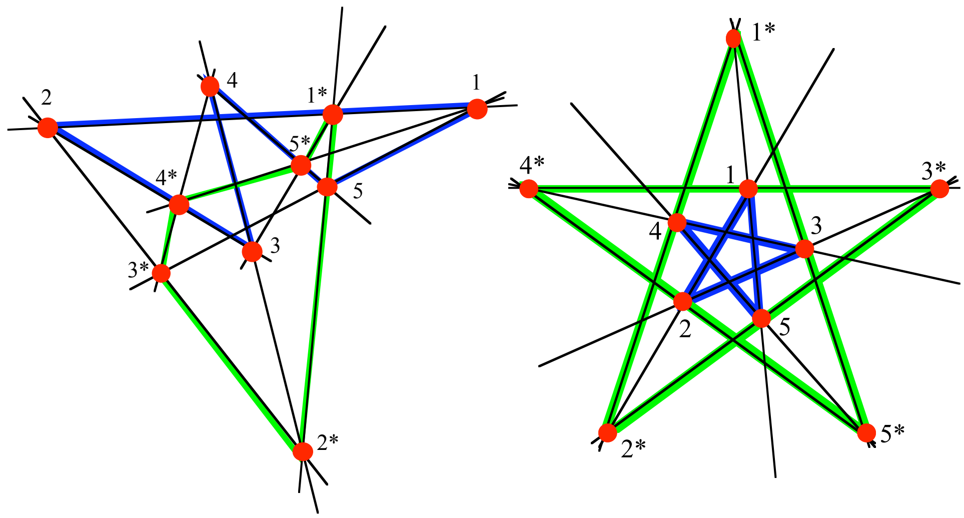

(a) (b)

Figure 5.3.2. The configurations $(10_3)_1$ (in the labeling of Section 2.2, shown in (a)) and $(10_3)_{10}$ can both be interpreted as pairs of inscribed/circumscribed pentalaterals. However, the one in (b) has an orderly pair or inscribed/circumscribed pentalaterals: The line determined by the points i and $i+1$ of the red pentalateral contains the point $i+1$ of the green one. The Desargues configuration $(10_3)_1$ does not have such an orderly pair.

Like many other aspect of the theory of configurations, families of inscribed/circumscribed multilaterals have found a home of sorts in the theory of set configurations and more general combinatorial incidence systems. Recent publications one may wish to consult for these developments include [P2], [P9], [L6], and especially [V2]; additional references may be obtained through these, as well as from other publications of the authors. However, despite the language used in the publications of this trend (including words such as points, lines, polygons, collinearity, Pappus and Desargues configurations, and others), in most cases the meaning is completely divorced from the accepted geometric interpretation of the terms used. In some of the publications there are diagrams, but they are only schematic tools, not configurations in the geometric (or even topological) sense.

As far as I am aware, there has been no consideration given to any concepts analogous to inscribed/circumscribed families of multilaterals or multilateral decompositions in k-configurations, for k ≥ 4. In fact, it is easy to come up with several meaningful interpretations. In Figure 5.3.4 we show the possibly simplest of these. A family of multilaterals in a 4-configuration is an inscribed/circumscribed family if each line of a multilateral is incident with two vertices of another multilateral in a cyclical arrangement of the multilaterals. This is illustrated in Figure 5.3.4 in case of a 3-astral configuration (21_4); in both versions the red heptalateral is inscribed in the blue one, which is inscribed in the green one, which is inscribed in the original red heptalateral.

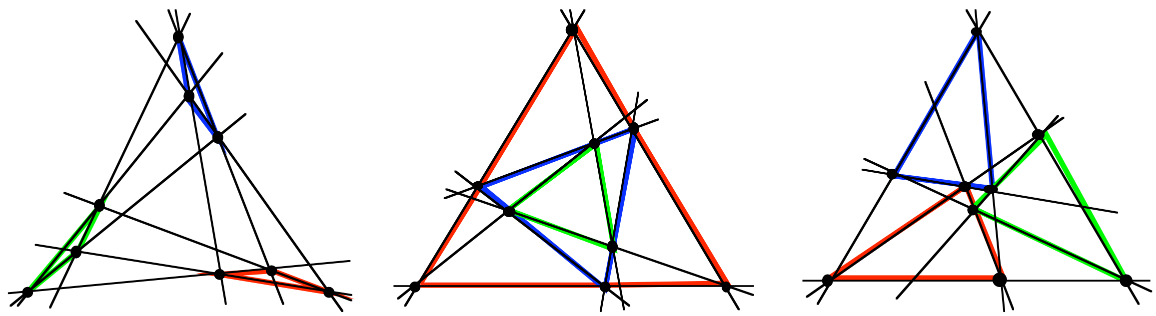

Figure 5.3.3. Examples of orderly inscribed/circumscribed families with r = 3 in rotationally symmetric realizations of the three configurations (9_3).

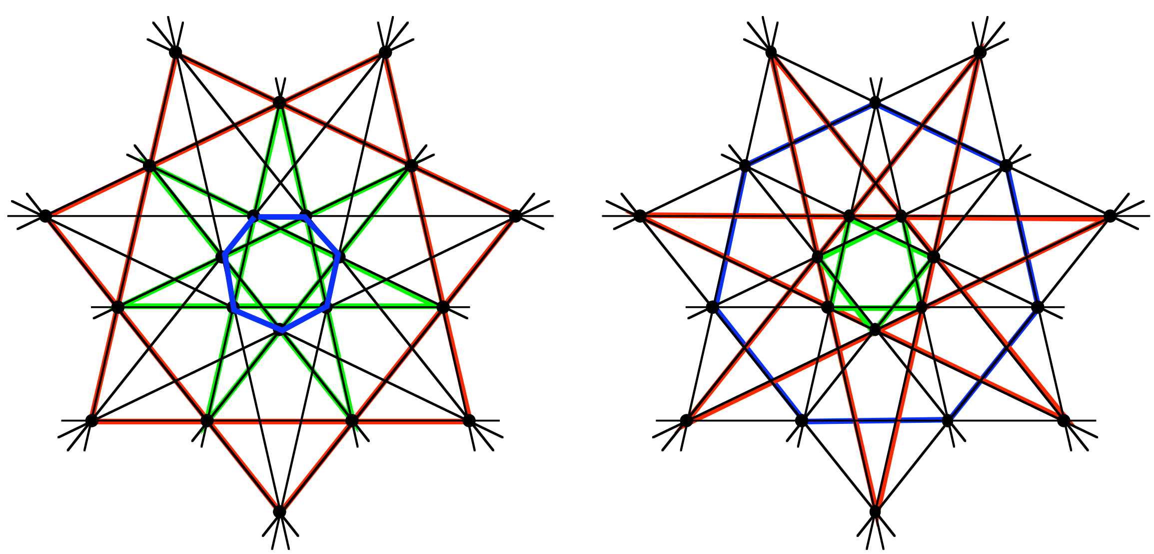

Figure 5.3.4. Two families of three mutually cyclically inscribed heptalaterals, that form a multilateral decomposition of the 3-astral configuration (21_4).

A different interpretation is illustrated in Figure 5.3.5. The multilateral decomposition of the astral configuration (24_4) consists of eight mutually inscribed/circumscribed trilaterals in a more complicated way. Each line contains points of three distinct trilaterals, and each point in incident with lines of three distinct trilaterals.

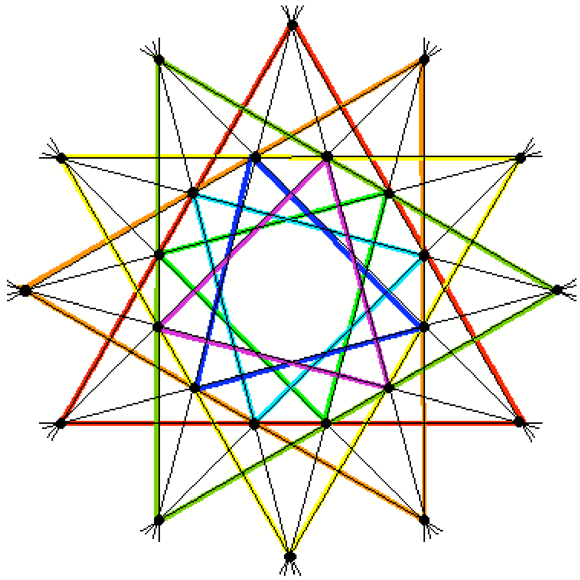

Figure 5.3.5. An illustration of the alternative interpretation of inscribed/circumscribed trilaterals in the astral configuration (21_4).

Exercises and problems 5.3

1. Prove that there is no *orderly* pair of pentalaterals in the Desargues configuration $(10_3)_1$.

2. Show that the cyclic configuration $\mathscr{C}_3(n)$ (see Section 2.1) contains an orderly family of three inscribed/circumscribed m-laterals whenever $n = 3m$. Does it contain a family of m trilaterals?

3. Investigate the general cyclic configurations $\mathscr{C}_3(n,1,k)$ (see Exercise 2 of Section 2.1) for the presence of orderly families of inscribed/circumscribed multilaterals.

4. Prove the result of Schoenflies [S5]: None of the three (9_3) configurations can be obtained by starting with nine points in general position in Euclidean 3-space, generating some of the lines and planes they determine, and intersecting these by a plane.

5. Can each of the (10_3) configurations be presented as an inscribed/circumscribed family of two pentalaterals?

6. Consider the astral configuration (60_4) shown in Figure 5.3.6. Find inscribed/circumscribed multilateral decomposition of this configuration into (i) twelve pentalaterals; (ii) four 15-laterals.

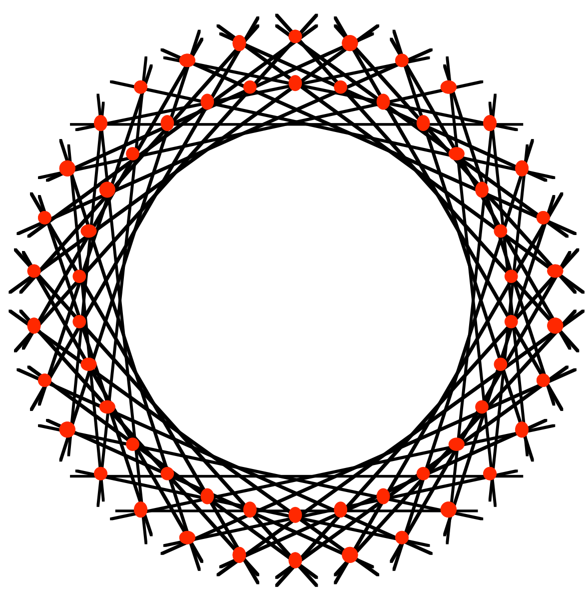

Figure 5.3.6. The astral configuration (60_4) used in Exercise 6.

5.4 MULTILATERAL-FREE CONFIGURATIONS

We turn now to one of questions concerning trilaterals (and multilaterals) in configurations, that go back to the classical period of configurations in the last quarter of the 19th century. It has seen new life in the recent decades, mostly without any acknowledged relation to the earlier results.

The first question that will occupy us asks for configurations that contain no trilaterals. Here is what is known.

Theorem 5.4.1. For every $k \geq 2$ there exist geometric k-configurations that are trilateral-free.

The proof is immediate on recalling the configurations LC(k) described in Section 1.1 as well as in [P5], and utilized in Section 5.1. The only drawback of this answer is the rather large size of these configurations. The resulting trilateral-free geometric configurations are (n_k) with $n = k^k$. ♦

We shall see below how smaller trilateral-free geometric configurations can be found in some cases. For some general estimates see Lazebnik *et al.* [L2].

Another general result gives a lower bound on the size of trilateral-free configurations.

Theorem 5.4.2. If an (n_k) configuration with $k \geq 2$ is trilateral-free then $n \geq k(k-1)^2 + k$.

The proof is straightforward on considering the situation schematically presented in Figure 5.4.1, assuming $k = 4$. Any one line (represented by the horizontal one) carries k points; through each of the points go $k-1$ other lines of the configuration, each carrying $k-1$ additional points. The only remark that needs to be made is that these points must all be distinct, since otherwise there would be a trilateral present in the configuration. This argumentation (or something similar) was shown to me by J. Bokowski. Notice that the argument does not use any geometry, and hence the result holds for combinatorial configurations as well. ♦

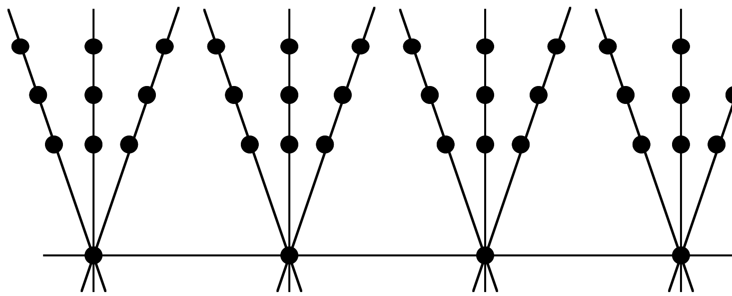

Figure 5.4.1. Schematic representation of the proof of Theorem 5.4.2.

For k = 3 the result was known to Martinetti [M1] in 1886.

The cubic bound in Theorem 5.4.2 is in contrast to the exponentially large examples in Theorem 5.4.1. We shall next show that we can do much better than the exponential example for k = 3, and slightly better for k = 4.

As a consequence of Theorem 5.4.2 we see that for k = 3 any trilateral-free k-configuration must have at least $n \geq 15$ points. Martinetti [M1] seems to be the first to have raised in 1886 the question of trilateral-free 3-configurations. He proved that such configurations have at least 15 points, and provided a combinatorial description of the unique (15_3) that is trilateral free. It needs to be stressed that, from all that we can read in his publications, Martinetti thought at that time (as well as later) that combinatorial 3-configurations are all geometrically realizable. In fact, Martinetti's trilateral-free (15_3) configuration is, indeed, geometrically realizable, see Figure 5.4.2. Moreover, in the pre-history of configurations, traces of this (15_3) geometric configuration can be found in considerations of families of straight lines on cubic surfaces, by Schläfli in 1858 and Cremona in 1868. The configuration itself is frequently called the Cremona-Richmond configuration; see [C6], [W2]. More detailed historical explanations and references can be found in [B19].

The Cremona-Richmond configuration is shown in Figure 5.4.2, and a Levi graph (see [W7]) based on a Hamiltonian multilateral, is shown in Figure 5.4.3. Since the configuration is trilateral-free, its Levi graph has no circuits of size smaller than 8; in other words, its *girth* is 8. In fact, it is the smallest 3-valent graph of girth 8, and it is famous as

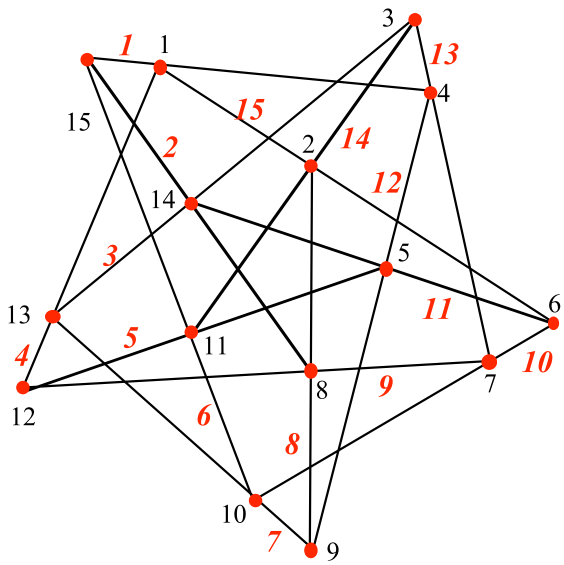

Figure 5.4.2. The Cremona-Richmond trilateral-free configuration (15_3). Point labels are in plain font, line labels are in bold italics. Same digits establish a duality correspondence between points and lines.

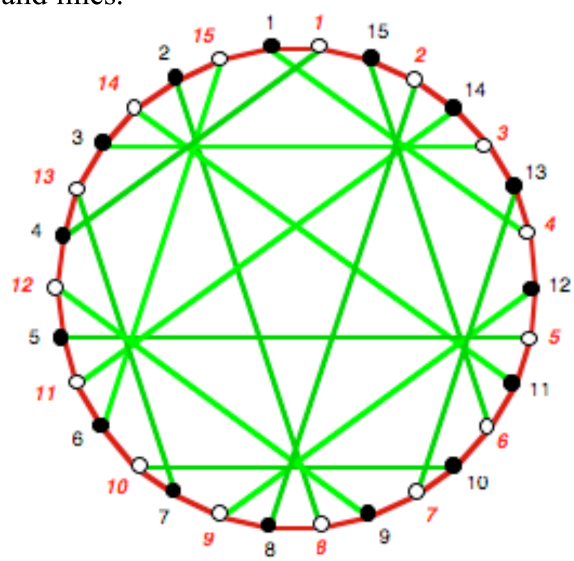

Figure 5.4.3. A Levi graph of the Cremona-Richmond configuration. It is the "Tutte 8-cage", the smallest 3-valent graph with girth 8. Similar presentations appear in [C6] and many other places.

Tutte's (3,8)-cage, or more simply, *Tutte's 8-cage.* Coxeter [C6] provides an ingenious labeling of its vertices, and calls it "the most regular of all graphs". Figure 5.4.3 also shows that this graph has a color-reversing symmetry, hence the Cremona-Richmond configuration is selfdual; this result can also be deduced from the fact that there is only one type of trilateral-free (15_3) configuration. On the other hand, it should be noted that there are infinitely many *projectively* inequivalent geometric realizations of this configuration. This is most easily seen by manipulations in some software such as Geometer's Sketchpad™.

Before continuing our description of the other results about trilateral-free configurations, we need to present some of the more recent definitions and results that deal with the same topic in a different language.

A **(k,g)-cage** is a graph with all vertices of **valence** k and of **girth** g, having the smallest possible number of vertices. For this definition, and most of the known results concerning cages, see [G19], [W7] and the references given there. For attractive illustrations of some of the cages see [P7].

The Levi graph of a (combinatorial or geometric) (n_k) configuration has, as we mentioned in Section 1.5, girth $g \geq 6$; since, as we have seen in Section 2.1, the Fano configuration (7_3) has the smallest number of vertices, its Levi graph with 14 vertices is a (3,6)-cage — in fact, the only (3,6)-cage.

Trilateral-free 3-configurations have girth at least 8; hence the Levi graph of the smallest such configuration — the Cremona-Richmond (15_3) — is the (3,8)-cage, with 30 vertices. Since the Cremona-Richmond (15_3) is the unique trilateral-free (15_3) configuration, this cage is also unique: it is the Tutte (3,8)-cage, mentioned earlier.

Another related concept is that of "generalized quadrangles". A **generalized quadrangle** is an incidence structure in which each pair of distinct points determines at most one line, and for each non-incident pair consisting of a point P and a line L, there is precisely one line L* that is incident with P and with a point P* of L. A (finite) generalized quadrangle is of **order** (s, t) if every line contains precisely s+1 points and every point is incident with precisely t+1 lines. The terminology is often justified by the fact that an ordinary quadrangle can be interpreted as a generalized quadrangle of order (1,1). Obviously, each generalized quadrangle of order (2,2) is a combinatorial 3-configuration.

The smallest generalized quadrangle of order (2,2) has 15 points; hence it is a (15_3) configuration, for which the definition of generalized quadrangles implies that it is trilateral-free. It follows that it is isomorphic with the Cremona-Richmond configuration. Polster [P7] shows several diagrams of this generalized quadrangle; two are particularly interesting. The first, which he attributes to Stanley Paine, is shown in Figure 5.4.4; the labels establish its isomorphism with the configuration in Figure 5.4.2.

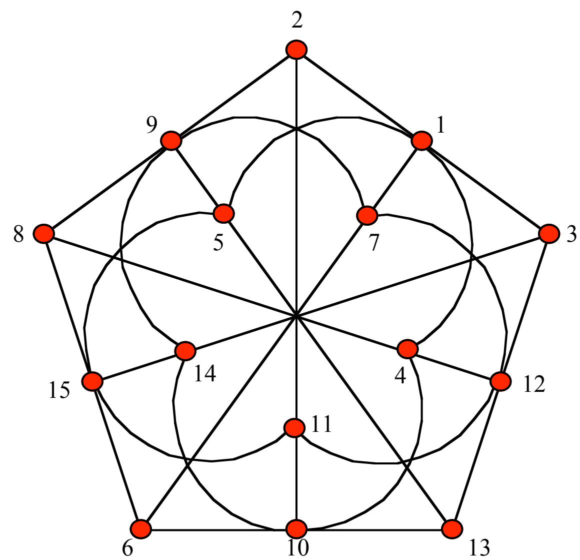

Figure 5.4.4. The "doily" of S. Payne: a geometric model of the 15-point generalized quadrangle of order (2,2) — also known as the Cremona-Richmond configuration.

The second interesting model shown by Polster [P7] is by lines (actually, line segments) in 3-dimensional space; see Figure 5.4.5. The model is best understood as being spanned by a regular tetrahedron; the tetrahedron's edges are indicated by the dashed lines and are not part of the configuration. Naturally, any appropriate projection of this model into the plane provides a planar realization of the Cremona-Richmond configuration. A figure resembling such a projection illustrates the Cremona-Richmond configuration in Wells' "Dictionary" [W2, p. 40].

Returning now to the configuration language, here are some of the additional results on trilateral-free 3-configurations, all established by Martinetti [M1]:

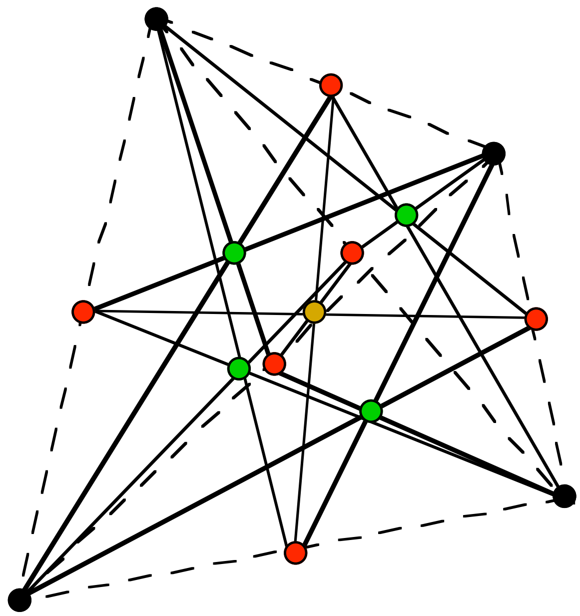

Figure 5.4.5. A realization of the 15-points generalized quadrangle of order (2,2), alias Cremona-Richmond configuration, supported in 3-space by a regular tetrahedron. (Adapted from [P7].)

- There are no trilateral-free configurations (16_3). This is not hard to show, starting with the arrangement shown in Figure 5.4.1, and noting that for a sixteenth point there are only relatively few possibilities of collinearities with the other points — none leading to a configuration, even in the combinatorial sense.
- There is a single trilateral-free configuration (17_3); again, the uniqueness implies that it is selfdual. It is interesting because of its very low symmetry. Under its group of automorphisms it has four point orbits: two of size 6 each, one of size 3, and one of size 2. It is geometrically realizable, but with no symmetry. Details (such as configuration table, geometric realization, Levi graph, automorphism group, orbits) can be found in [B19].
- There are precisely four trilateral-free configurations (18_3). Two are dual to each other, and each of the other two is self-dual. Data on all four, with geometric realizations, are given in [B19]. One of the selfdual configurations (denoted 18-D in [M1] and [B19]) is interesting because of its symmetry; it admits a selfpolar realization as an astral configuration 9#(4,2;3) in the notation of Section 2.7, and is shown in Figure 5.4.6.

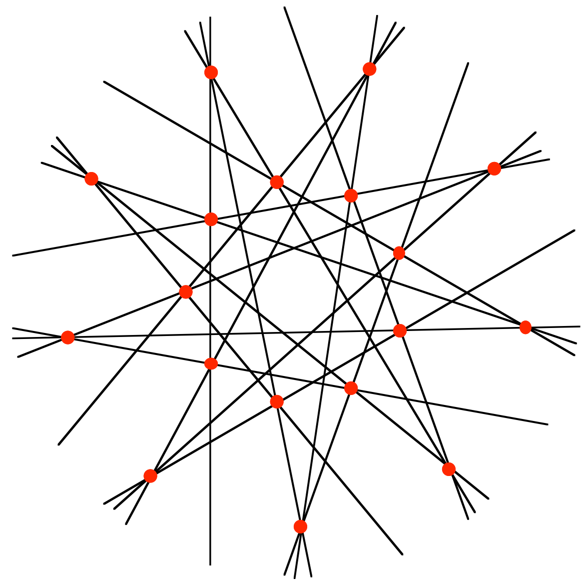

Figure 5.4.6. A realization of the trilateral-free selfpolar configuration (18_3) denoted 18-D in [B19]; it is astral with symbol 9#(4,2;3), and is the first of an infinite series of trilateral-free selfpolar configurations.

In considering these results of Martinetti [M1], one should bear in mind that although he uses geometrical language there is no diagram presenting these configurations, nor is there any hint how the corresponding geometric configurations should be constructed. The first geometric realizations seem to be the ones in [B19].

According to the data in [B14] (reproduced in [B19]) there are 19 combinatorial trilateral free configurations (19_3), 162 such configurations (20_3), and 4713 (21_3). It is not known how many are geometrically realizable.

On the other hand, we have the following:

Theorem 5.4.3. For every $n \geq 15$ except $n = 16$ and possibly $n = 23$ and 27, there are trilateral-free geometric configurations (n_3).

Proof. For n = 15, 17, 18, 19, 20, 21 trilateral-free geometric configurations are shown in [B19]. It is easy to verify that all astral configurations m#(4,2;3) for $m \geq 9$ and $m \neq 12$ are trilateral free; this shows that for all even $n \geq 18$, $n \neq 24$, there are trilateral-free configurations (n_3). The (18_3) and (20_3) configurations mentioned above are of

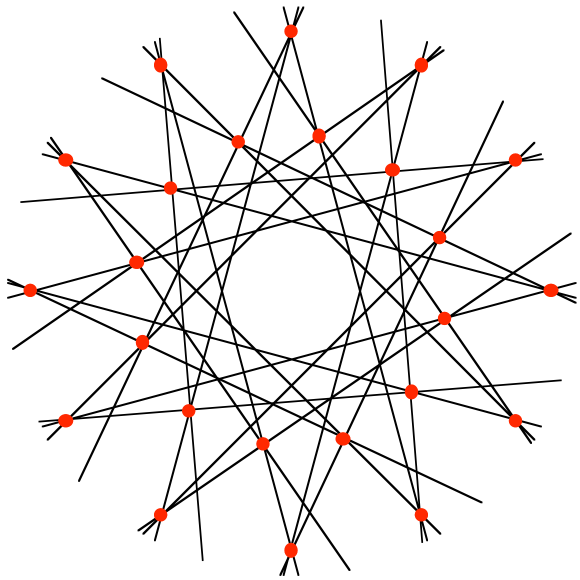

Figure 5.4.7. A trilateral-free configuration (24_3); it is astral with symbol 12#(5,3;4).

this type. For the exceptional value n = 24 a trilateral-free geometric configuration is shown in Figure 5.4.7.

The construction of the appropriate configurations for odd n is slightly more complicated. In almost all cases, the following construction works. Starting with trilateral-free geometric configurations (p_3) and (q_3), we delete one line in each and connect the three pairs of orphan points with an additional, new point. (The required alignment can always be obtained through suitable projective transformations.) This yields a trilateral-free geometric configuration (n_3) with $n = p + q + 1$. Starting from the trilateral-free configurations we already constructed, this yields the required geometric configurations for all odd $n \geq 31 = 15 + 15 + 1$. An alternative construction works for all $n \geq 29$: In analogy to the "deleted union" construction (DU-1) described in Section 3.3, we delete a line from a trilateral-free geometric configuration (p_3) and delete a point from a trilateral-free geometric configuration (q_3); by placing appropriate copies of the two configurations so that the lines of the latter (which are missing a point) pass through the points of the former (that are missing a line), we obtain a trilateral-free geometric configuration of $n = p + q - 1$ points. For $p = q = 15$ this yields $n = 29$.

The case (25_3) is particularly interesting. Visconti [V4] gives configuration tables for two distinct trilateral-free combinatorial configurations (25_3), each consisting of a family of five mutually inscribed/circumscribed pentalaterals. These are reproduced, in Visconti's notation, in Tables 5.4.1 an 5.4.2. In the somewhat analogous case of trilateral-free configuration (20_3) consisting of four mutually inscribed/circumscribed pentalaterals, Visconti provides a graphical representation, that seems to be the first *symmetric* rendition of any multiastral configuration. However, contrasting this is the fact that there is no indication in [V4] whether the (25_3) configurations described are geometrically realizable. We have verified that at least one of these can be drawn, but not in a polycyclic manner; see Figure 5.4.8. Just as in the case of the (17_3) and (19_3) configurations investigated in [B19], the configuration is asymmetric, and was constructed by successive approximations. It is very likely that the same situation exists for Visconti's other (25_3). ♦

Visconti [V4] and Martinetti [M3] provide additional examples of trilateral-free combinatorial 3-configurations consisting of mutually inscribed/circumscribed pentalaterals, and some other multilaterals as well. It may be conjectured that these are geometrically realizable as well.

It is worth noting that most astral configurations m#(b,c;d) are trilateral-free for sufficiently large m. Exceptions (such as the n = 24 case mentioned above) are usually easy to spot, but there seem to be some subtler issues that have not been tackled so far. An example of such a situation is given in Figure 5.4.9.

We are turning now to quadrilateral-free configurations; this term is somewhat of a misnomer — at least in the sense we shall use it. By **quadrilateral-free** we shall refer to configurations that have neither a trilateral nor a quadrilateral. We have no example of a configuration that has no quadrilateral but does have trilaterals; it appears to be an open question whether such configurations exist. This leads to our terminology that simplifies the locutions.

In discussing quadrilateral-free configurations, we consider only 3-configurations, since nothing on the topic of quadrilateral-free k-configurations seems to be known for $k \geq 4$.

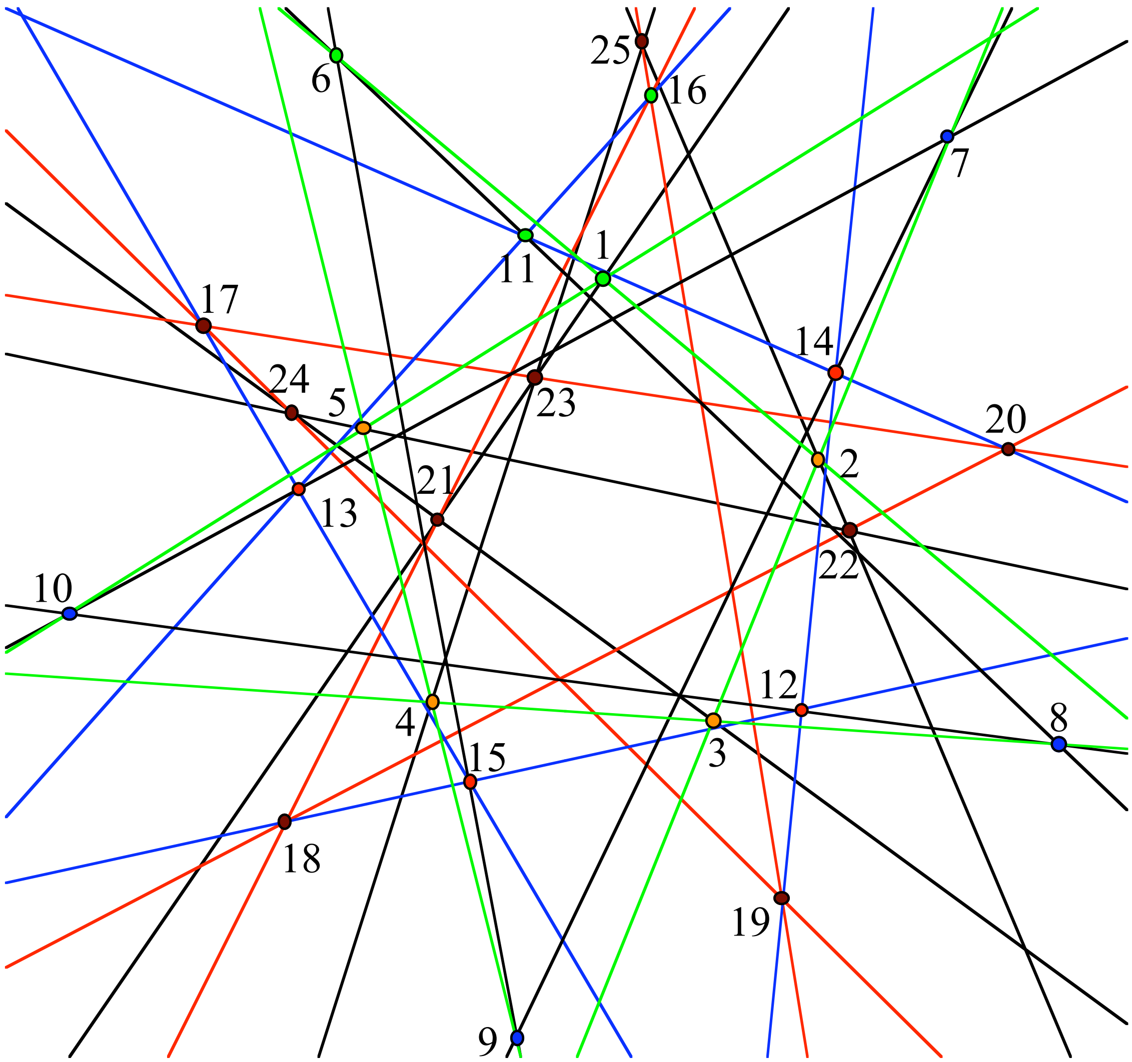

Figure 5.4.8. A geometric realization of one of the trilateral-free configurations (25_3) given by configuration tables in [V4] and Table 5.4.2 below.

1	2	3	4	5	6	7	8	9	10	11	12	13	14	15	16	17	18	19	20	21	22	23	24	25
2	3	4	5	1	8	9	10	6	7	13	14	15	11	12	18	19	20	16	17	23	24	25	21	22
6	7	8	9	10	11	14	12	15	13	16	19	17	20	18	21	24	22	25	23	1	2	3	4	5

Table 5.4.1. The configuration table of one of the trilateral-free configurations (25_3) found by Visconti [V4].

1	2	3	4	5	6	7	8	9	10	11	12	13	14	15	16	17	18	19	20	21	22	23	24	25
2	3	4	5	1	8	9	10	6	7	13	14	15	11	12	18	19	20	16	17	23	24	25	21	22
6	7	8	9	10	11	14	12	15	13	16	19	17	20	18	21	24	22	25	23	1	5	4	3	2

Table 5.4.2. The configuration table of the other trilateral-free configuration (25_3) found by Visconti [V4]. A geometric realization of this configuration is given in Figure 5.4.8.

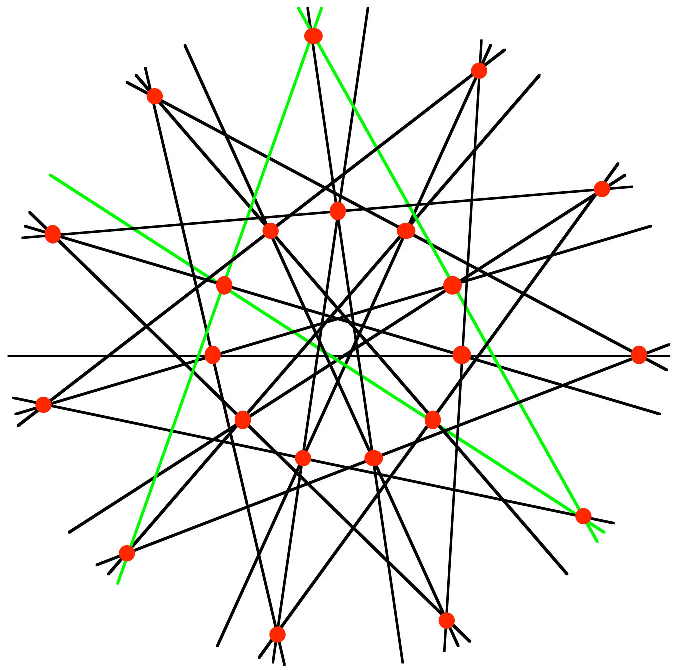

Figure 5.4.9. The astral configuration 11#(5,4;2) is not trilateral-free; one trilateral is shown by green lines. For m such that $13 \le m \ne 15$, the configuration m#(5,4;2) is trilateral-free.

The only published work I am aware of that deals with quadrilateral-free geometric 3-configurations is [P6]; the configurations are studied using their Levi graphs.

Through the Levi graphs, the question of quadrilateral-free configurations is related to 3-valent bipartite graphs of girth at least 10. Such graphs have been extensively investigated; a large quantity of relevant literature can be found in [W6] and [W7].

The result of these graph-theoretic studies that is most relevant to our topic is that there exist exactly three 10-cages (also called (3,10)-cages), that is, 3-valent graphs of girth 10 with the smallest number of vertices, namely 70; all three are bipartite. The first one was found by Balaban [B1], the other two by O'Keefe and Wong [O2]; Wong [W6] proved that these three are the only ones. Balaban's 10-cage has a color-interchange automorphism, the other two do not have any such automorphism.

In [P6], Pisanski *et al.* describe in detail these three 10-cages, and the resulting five quadrilateral-free configurations (35_3). Since Balaban's 10-cage has a color-reversing symmetry, the corresponding configuration is selfdual. The other two 10-cages yield a pair of dual configurations each. It is clear that the three 10-cages can be interpreted as Levi graphs of quadrilateral-free *combinatorial* 3-configuration (35_3); however, Pisanski *et al.* prove that they admit *geometric* realizations, and provide in [P6] diagrams for three of the five. These three admit polycyclic representations which the last two do not have; for them there is in [P6] a description of the method of proof (following [B25]), and a reference to the full set of coordinates listed at a website. In [P6] there is also described a construction of quadrilateral-free geometric configurations (n_3) for an infinite sequence of values of n.

An improvement of this last result is the following:

Theorem 5.4.4. For every $n = 4m \geq 40$, there exists a quadrilateral-free geometric configuration (n_3). There exists an n_0 such that for every $n \geq n_0$ there is a quadrilateral-free geometric configuration (n_3). The available estimate is $n_0 \leq 320$.

Proof. It is easily verified that for $m \geq 10$ the astral configuration (2m)#(m-1,1;4) is quadrilateral-free. I am indebted to T. Pisanski for showing me one of the two smallest of these configurations, 20#(9,1;4), see Figure 5.4.10(a). The next members of the sequence, the pair of dual 22#(10,1;4) are shown in Figure 5.4.11. The proof of the fact that the (2m)#(m-1,1;4) configurations are quadrilateral-free is easy by generalizing the argument indicated by the coloring of the points in Figures 5.4.10 and 5.4.11. Since the configuration is astral, and any quadrilateral would have to contain a point of the outer ring, it is enough to show that the point marked by the large black dot is not part of any quadrilateral. The only six points at (graph-)distance 1 are the six red points, and those at distance 2 are the 24 green ones. The presence of any quadrilateral would imply that two of the green points coincide — which does not happen since this would imply that there are at most 23 green points.

In order to prove the existence of n_0 we may use the same construction as in the proof of theorem 5.4.3 for odd n. We take two quadrilateral-free configurations (p_3) and (q_3), and using convenient representatives delete one line from each; an additional point and three lines through it and the points on the two deleted lines form a quadrilateral-free configuration (n_3) with $n = p + q + 1$. Repeating the construction r times leads to configurations with r points more than the sum of the numbers of points of the configurations used. This yields the bound $n_0 \le 320$. ♦

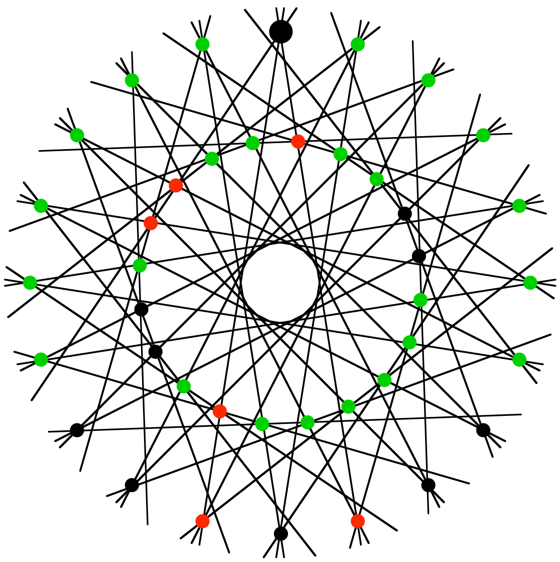

(a) (b)

Figure 5.4.10. The two dual astral configurations 20#(9,1;4). Both (40_3) configurations are quadrilateral-free.

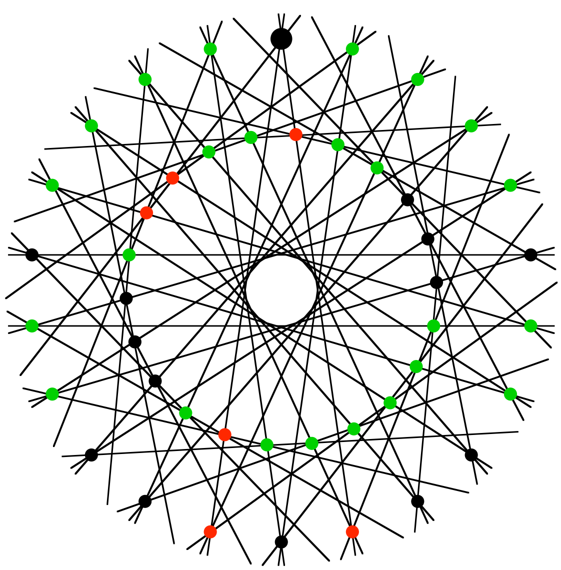

Figure 5.4.11. A dual pair of astral, quadrilateral-free (44_3) configurations 22#(10,1;4).

In analogy to our convention concerning quadrilaterals, we say that a configuration is **pentalateral-free** if it contains no t-laterals for t = 3, 4, 5. The information available is exceedingly meager. A (3,12)-cage has 126 points and happens to be bipartite; hence it can be interpreted as the Levi graph of a pair of dual (63_3) *combinatorial* configurations. Schroth [S9] found graphic representations of these two configurations, which we reproduce in Figures 5.4.12 and 5.4.13. (The title of Schroth's paper refers to the "generalized hexagons" of order (2,2); the uniqueness of the dual pair was established in [C3].)

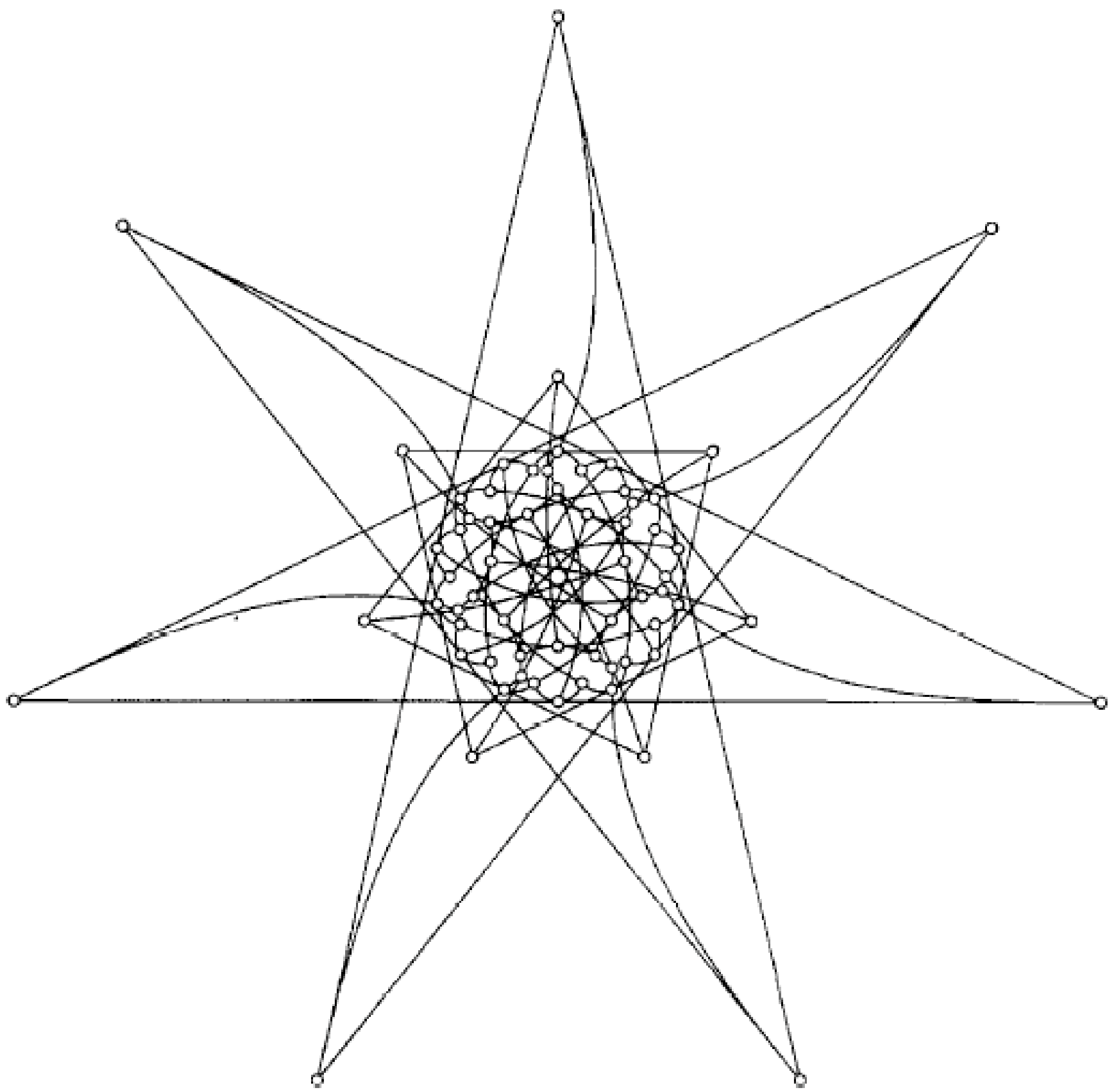

Figure 5.4.12. One of the "generalized hexagons of order (2,2)" shown by Schroth [S9]. Its points and arcs are a graphic rendition of a (63_3) configuration.

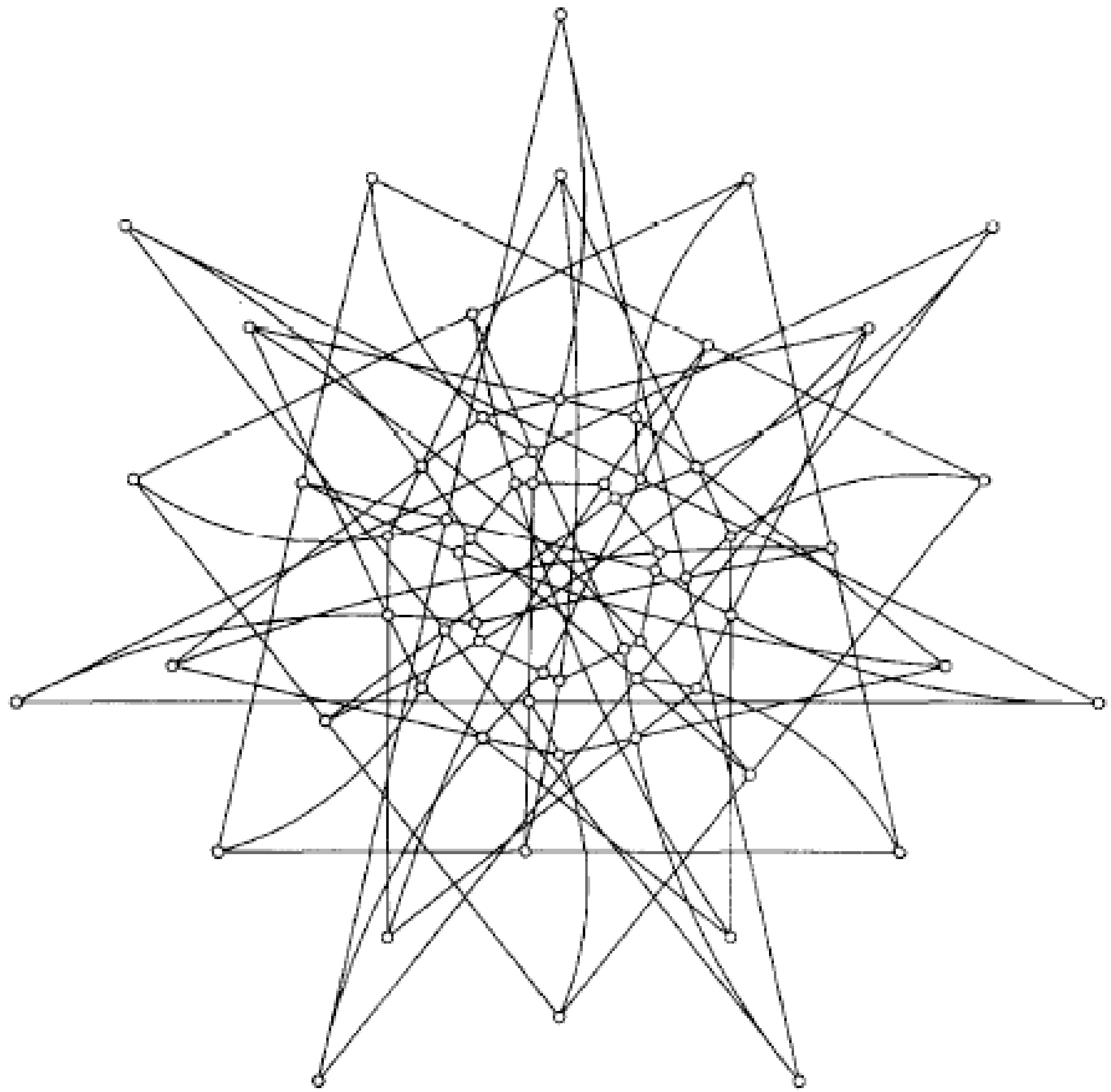

Figure 5.4.13. The other (63_3) configuration from Schroth [S9].

The diagrams in these two figures naturally lead to the question whether the two pentalateral-free configurations are geometrically realizable. The affirmative answer was provided by M. Boben and T. Pisanski, soon after the publication of [S9], but never published. With their permission, one of the two geometric pentalateral-free configurations (63_4) is reproduced in Figure 5.4.14, by a diagram they supplied. In Figure 5.4.15 we show the reduced Levi diagram of this configuration, as kindly provided by Boben and Pisanski.

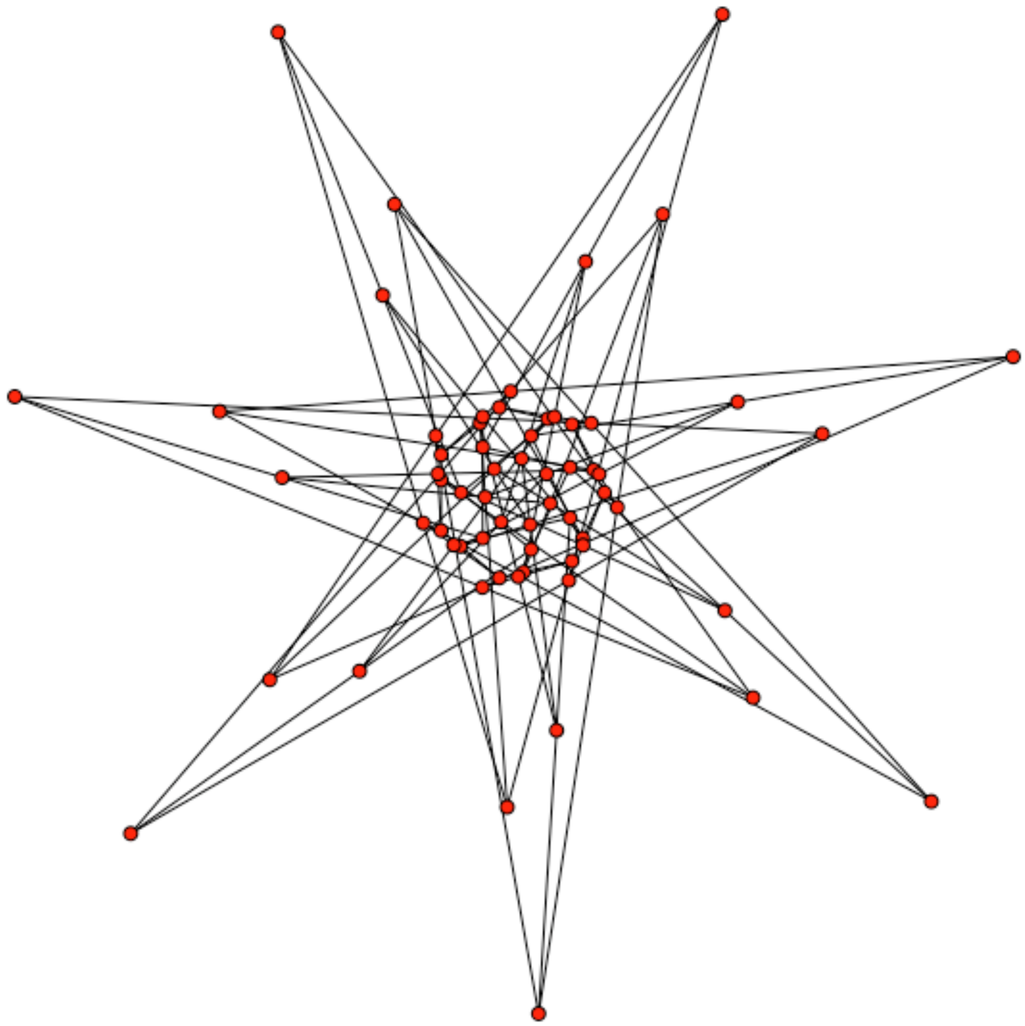

Figure 5.4.14. A geometric realization of a pentalateral-free configuration (63_3). (Courtesy of M. Boben and T. Pisanski, from unpublished work.)

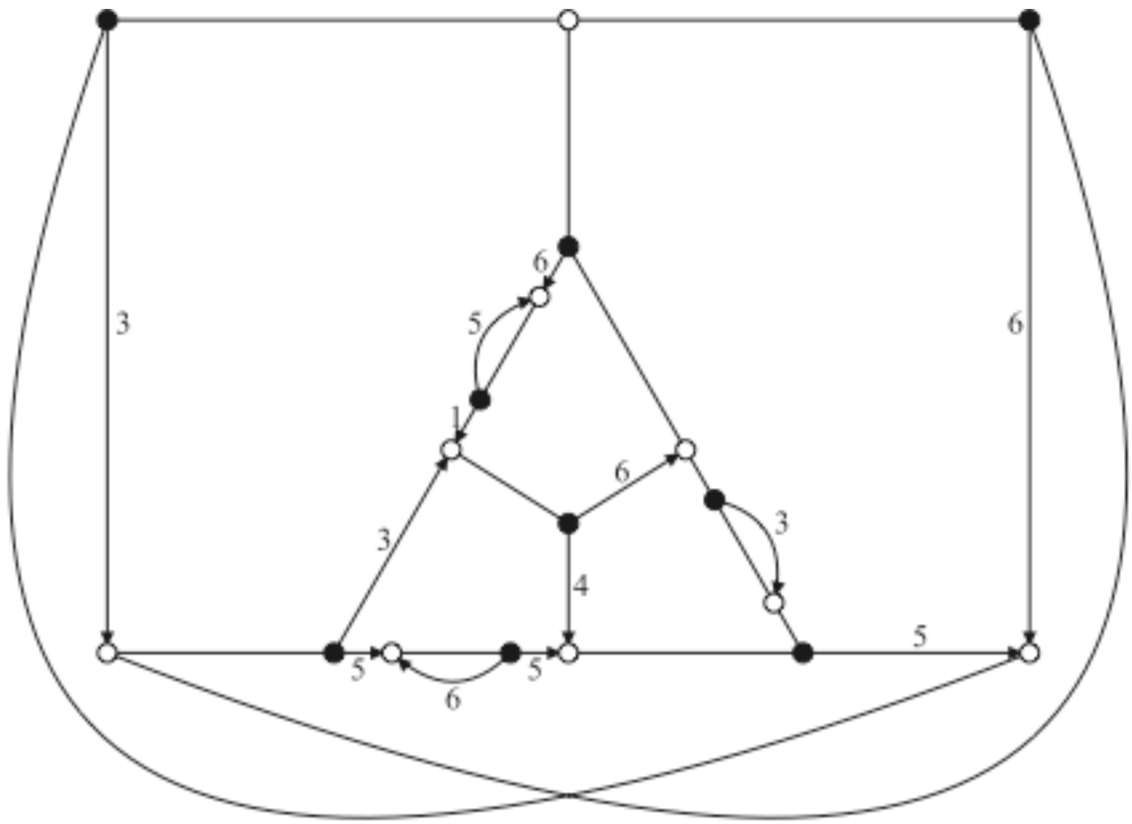

Figure 5.4.15. The reduced Levi graph (in their notation) of the pentalateral-free configuration in Figure 5.4.14. (Courtesy of M. Boben and T. Pisanski, from unpublished work.)

The Boben and Pisanski construction of the pentalateral-free (63_3) configuration is a piece of supporting evidence for Conjecture 2.6.1, according to which all 3-connected combinatorial 3-configurations can be realized by points and (straight) lines. (The 3-connectedness of the 12-cage can be directly established, but it also follows from the more general result of Fu *et al.* [F3] that all (3,g)-cages are 3-connected, or the more general result of Daven and Rodger [D4] that for $k \geq 3$ all (k,g)-cages are 3-connected; there is a conjecture in [F3] that all (k,g)-cages are k-connected.)

* * * * * *

Turning next to the case of trilateral-free 4-configurations, there is much less information available. A trilateral-free *combinatorial* configuration (40_4) was found recently by Hendrik van Maldeghem. Van Maldeghem's example attains the bound of Theorem 5.4.2 for $k = 4$; hence it corresponds to a (4,6)-cage. The construction of this example is described by Bokowski in [B21, pp. 263–265], where an incidence matrix is also shown (in two forms). However, no information seems available concerning the possibility of realizing this configuration geometrically, or even just topologically.

As already mentioned, the configuration LC(4) provides an example of a trilateral-free geometric configuration (n_4) with $n = 4^4 = 256$. Smaller trilateral-free configurations (120_4) are the astral configurations 60#(22,21,2,9) and 60#(27,26,3,14) shown in Figures 5.4.16 and 5.4.17, and their duals. By using the (3m+) and (DU-1) constructions described in Section 3.3, from the (120_4) configurations we can construct infinite families of geometric trilateral-free configurations.

However, much a better example of a trilateral-free 4-configuration is a (60_4) found very recently by M. Boben. It and its polar are shown in Figure 5.4.18.

The procedures analogous to the one describe earlier, applied to the configurations LC(k) for $k \geq 5$, show that in all these cases there are infinite families of trilateral-free geometric configurations. Unfortunately, they are all far too large for intelligible graphics ...

It is not known whether for $k \geq 5$ there exist trilateral-free *combinatorial* configurations (n_k) with $n = k(k-1)^2 + k$.

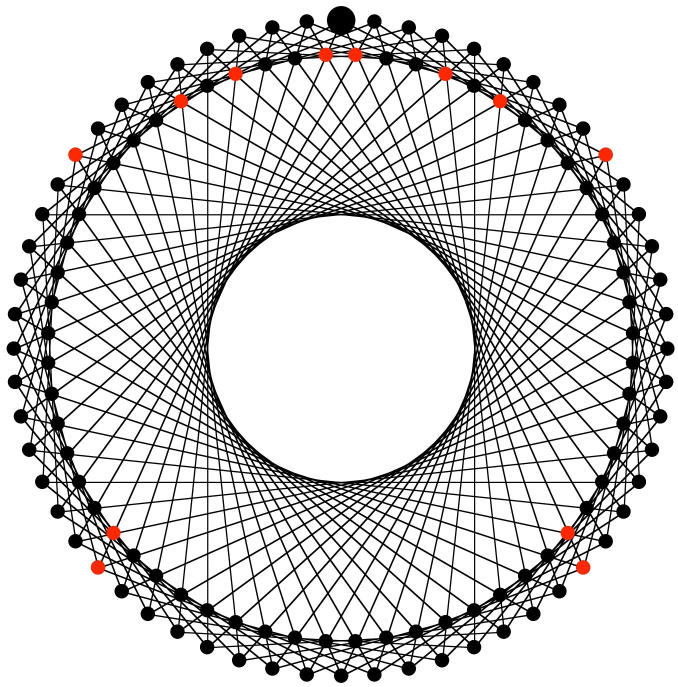

Figure 5.4.16. A trilateral-free geometric configuration (120_4). It is a sporadic astral configuration, with symbol 60#(22,21,2,9).

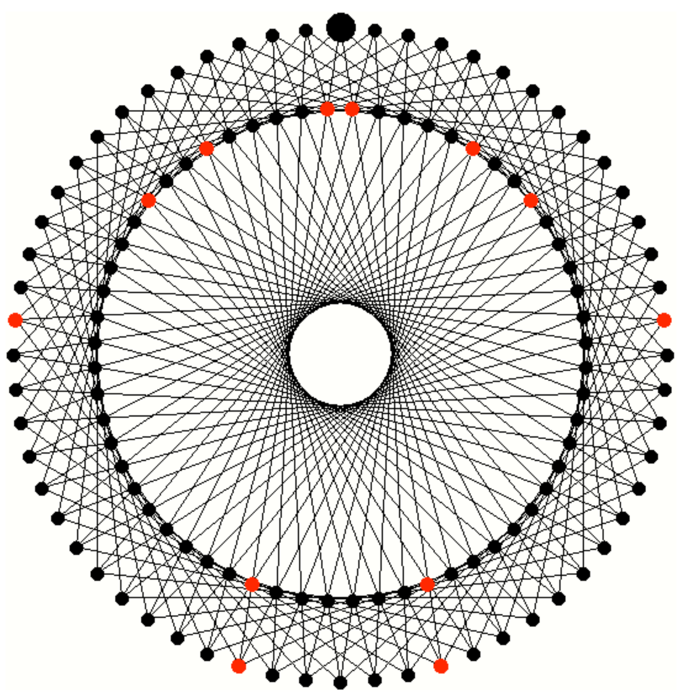

Figure 5.4.17. 60#(27,26,3,14)

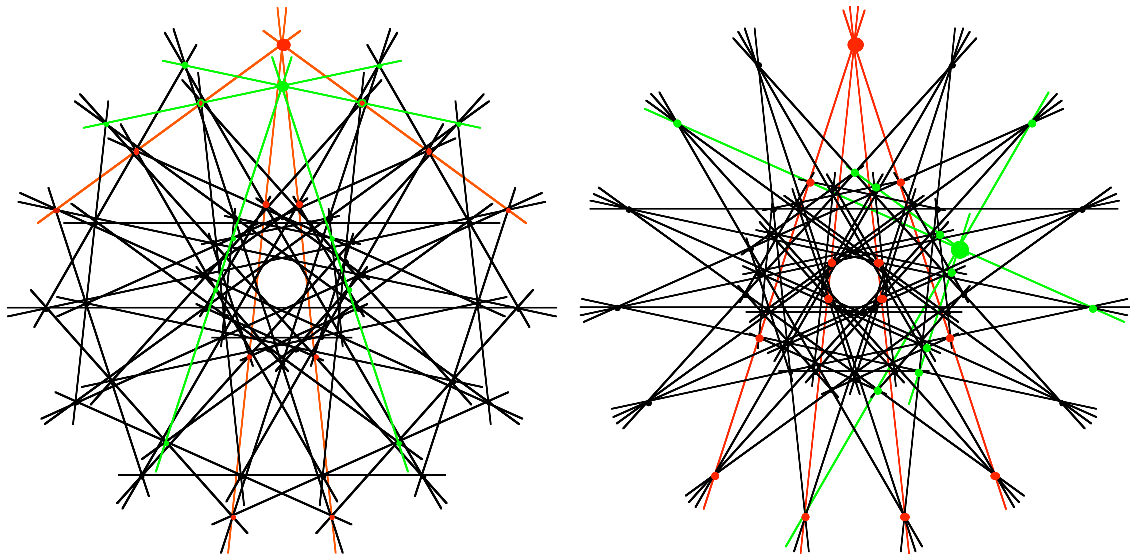

Figure 5.4.18. The trilateral-free (60_4) 4-astral configuration 15#(1,3;7,6;4,3;2,6) found by M. Boben, and its polar. (Courtesy of M. Boben.)

Exercises and problems 5.4

1. Find other astral families of quadrilateral-free 3-configurations.

2. Is there a quadrilateral-free configuration (n_3) for every $n \geq 35$? Or for all but a very small number of values of n?

3. Decide whether it is possible for a 3-configuration to have no quadrilaterals but contain some trilaterals.

5.5 "DENSITY" OF TRILATERALS IN CONFIGURATIONS

Another classical question is the following: Consider (combinatorial or geometric) 3-configurations for which the group of automorphisms acts transitively on the points and on the lines; for the purposes of this section (and only here) we shall follow the early writers and call such configurations **regular.** For a regular configuration we shall denote by $t = t(C)$ the number of trilaterals that meet one (hence every) point of a regular configuration C. The question of possible values of the "density" t is a topic raised by Schoenflies in [S1] and [S2], where he provided a partial answer. We shall present his results soon, but first a word of warning. These papers, like many in that period, are far from clear regarding exactly what are the configurations under discussion; quite a few of the assertions show a degree of naïveté that one does not expect from serious mathematicians. For example, Schoenflies states in [S1] that every regular configuration is self-dual; he repeats the assertion in [S2]. This error was noticed by Steinitz [S20]; he mentions that the smallest counterexample is a geometric (18_3) configuration; its underlying combinatorial version is denoted 18.7 in [B14, p. 337]. Also, although Schoenflies *seems to think* that he deals with geometric configurations (in the complex plane !) and therefore does not notice the Fano plane (7_3), Schoenflies does not address the question whether his configurations can actually be *geometrically* realized — even in the complex plane.

Acknowledging the work of Martinetti [M1] on configurations with no trilaterals (though giving an incorrect reference for it), Schoenflies asserts in [S1] that t must have one of the values 9, 6, 4, 3, or 2. (Note that the Fano plane has $t = 12$.) However, as noticed by Steinitz [S20], $t = 1$ is possible as well. The first result in [S1] is that $t(C) = 9$ happens if and only if $C = (8_3)$, the Mobius-Kantor configuration. (Unless one considers this as a combinatorial configuration, it can be "realized" only in the complex plane.) But Schoenflies here clearly missed the restriction to connected configurations — if C consists of several disconnected copies of (8_3) then $t(C) = 9$ as well; he corrected this error in [S2], as well as providing there a correct reference for [M1]. Similar shortcomings afflict some of his other assertions. For example, another statement is that there are three possibilities for $t = 6$: (i) The Pappus configuration (9_3); (ii) The Desargues configuration (10_3); and (iii) The cyclic configurations $\mathscr{C}_3(n)$ for $n \geq 9$, with lines $(j, j+1, j+3)$, (which we consider in Section 2.1 and 5.6). But as noted by Steinitz [S19, p. 488], t = 8 for the cyclic (9_3). The possibilities for t = 2, 3, or 4 are also discussed in detail in [S1] and in particular in [S2]; they consist of various families of mutually inscribed/circumscribed multilaterals. Steinitz [S19] also corrected Schoenflies' erroneous assertion that t(C) = 1 is not possible.

Steinitz [S20] and [S19, p. 489] also notes that all points of a 3-configuration may be in one orbit under automorphisms of the configuration, without the lines necessarily being in one orbit. Also, even if both points and lines are in single orbits, the configurations needs not be self-dual. On the other hand, all examples of this type are not relevant to cyclic configurations and their properties.

There is little motivation to discuss in more details of the results of Schoenflies and others and their proofs. However, several open questions deserve mention.

- Are there are any 3-configurations that are not regular but for which there exists a "density" of trilaterals — in other words, every point is incident with as many trilaterals as every other point.

Possibly some of the astral 3-configuration may provide examples, but the question seems not to have been investigated.

- Is there a reasonable classification of "regular" 4-configurations that have a "density" of trilaterals?

For example, the astral (24_4) configuration shown in Figure 3.6.2 has 16 trilaterals incident with every point.

- What about "densities" of quadrilaterals in "regular" 3- or 4-configurations? The same question may be asked for other multilaterals, including Hamiltonian multilaterals.

Questions in the same spirit have often been asked and investigated for graphs, and in some cases for combinatorial configurations or more general incidence structures. As this material has little connection to geometric configurations, we do not consider it here.

Exercises and problems 5.5

1. Verify the claim that the configuration in Figure 3.6.2 has 16 trilaterals incident with each point.

2. Find the number of trilaterals incident with each point of the 3-astral configuration (21_4) in Figure 3.7.1. How many quadrilaterals are incident with every point?

3. Are all points of the 2-astral configuration (48_4) shown in Figure 3.6.1 incident with the same number of trilaterals?

4. Investigate the astral 3-configurations (n_3) with $10 \le n \le 14$ concerning the numbers of trilaterals incident with each point. Quadrilateral? Any general hypotheses?

5.6 THE DIMENSION OF A CONFIGURATION

In Section 1.3 we introduced the concept of "dimension of a configuration". For convenience, we repeat it here. If C is a configuration we say that C has dimension d if this is the largest integer for which G admits a geometric representation (by points and straight lines) in some Euclidean space, such that the affine hull of the imbedding has dimension d.

Among meaningful questions that one can ask is the determination of the dimension of a given configuration, the possible dimensions of k-configurations for a given k, what criteria can we find to determine whether a given configuration (or class of configurations) has this or that dimension, and so on. The material presented in this section has not been published before; it was developed in an ongoing collaboration with Tomaz Pisanski.

Here are some examples to help develop an understanding of the issues.

First, we consider the three smallest 3-configurations, the (9_3) configurations shown in Figure 5.6.1 (which we have seen earlier, as Figure 2.2.1). Each is (obviously) drawn in the plane — but could we somehow imbed it in 3-space so that it not be contained in a plane? The negative answer is easily established: Regardless of the dimension of the space, the plane determined by points 1, 5, 7 of $(9_3)_1$ necessarily contains also the points 3, 4, 8 and hence also 2, 6, 9, and thus the whole configuration. Similarly, the plane containing the points 1, 5, 7 of $(9_3)_2$ contains 2, 3, 8, hence 4, 6, 9; the plane containing 1, 5, 8 of $(9_3)_3$ contains also 2, 6, 9, and then 3, 4, 7 — in both cases the whole configuration.

A different situation prevails with respect to the Desargues configuration which we have denoted $(10_3)_1$; see Figure 5.6.2. Consider the four points 0, 1, 2, 3 imbedded in any Euclidean space of dimension at least 3, in such a way that no plane contains all four; this we occasionally call "general position". Then the points 4, 5, 6 determine another plane; we choose them so that the plane is not parallel to the plane of 1, 2, 3, and does not contain any of the four earlier points. These two planes determine (as their intersection) a line, which contains the points 7, 8, 9 determined, respectively, on that line by the planes of 1,3,6,4, 1, 2, 4, 5, and 2, 3, 6, 5. Hence all points (and all lines) of the configuration are in the 3-dimensional space affinely spanned by 0, 1, 2, 3. It follows that the dimension of the configuration $(10_3)_1$ is 3.

However, it would be wrong to conclude that an increase in the number of points implies an increase in the dimension. For example, the configuration $(10_3)_2$ shown in Figure 5.6.3 is 2-dimensional. Indeed, the plane containing points 1, 3, 5 contains also 2, 4, 9, hence 6, 7, 8, and 0, and thus the whole configuration.

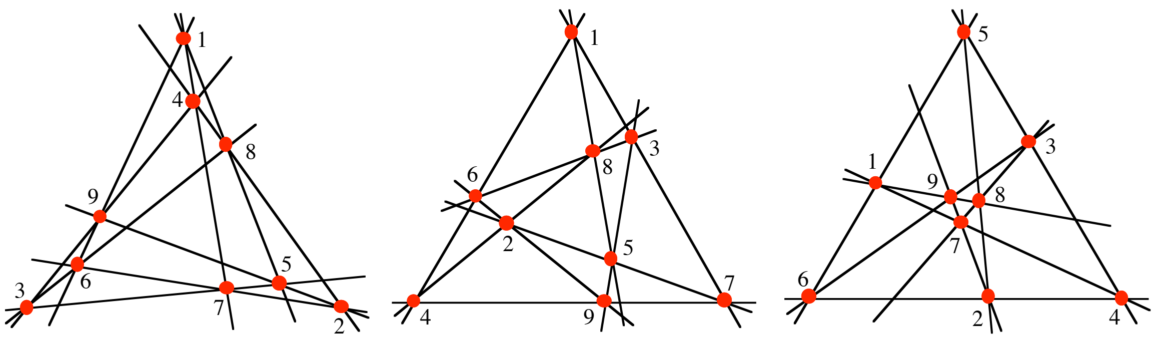

$(9_3)_1$ $(9_3)_2$ $(9_3)_3$

Figure 5.6.1. The three configurations (9_3).

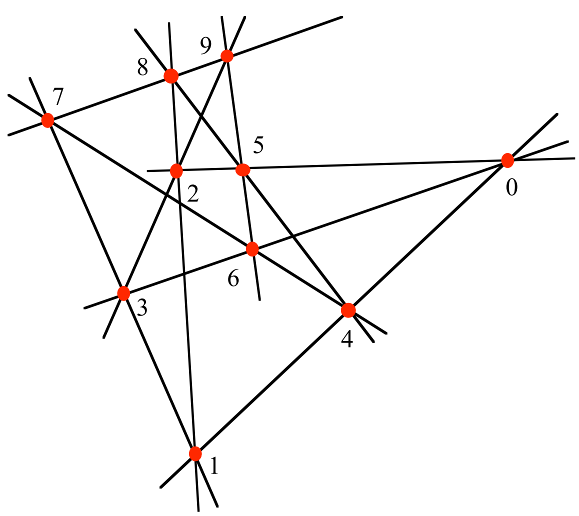

Figure 5.6.2. The configuration $(10_3)_1$ – the Desargues configuration — has dimension d = 3.

Theorem 5.6.1. There exist 3-configurations with arbitrarily large dimensions.

Proof. Start with any 3-configuration in the plane. Take three copies vertically above each other in 3-space, delete copies of the same line from each, and insert three vertical lines through the points on these lines. This raised the dimension by 1 (at least). Repeating the same procedure with three copies of this configuration, placed in suitable positions in parallel 3-spaces within a 4-dimensional space, deleting copies on one line from each and adding three transversals, raises the dimension of the resulting configuration to 4 (at least). Obviously we can continue indefinitely by the same method. ◊

The configurations constructed in the proof of Theorem 5.6.1 are quite large. It may be of interest to find smaller examples, at least for small dimensions d. We have already seen such configurations for d = 2 and 3. For d = 4 we can use the Cremona-Richmond configuration shown in Figure 5.6.4; we encountered this configuration earlier, in Sections 1.1 and 5.4. Indeed, consider the 15 points in the 4-dimensional Euclidean space E^4, listed in Table 5.6.1 by their labels in Figure 5.6.4. Then it is easily checked that all 15 triplets that are supposed to be collinear indeed are, while it is obvious that the affine hull of the set is 4-dimensional.

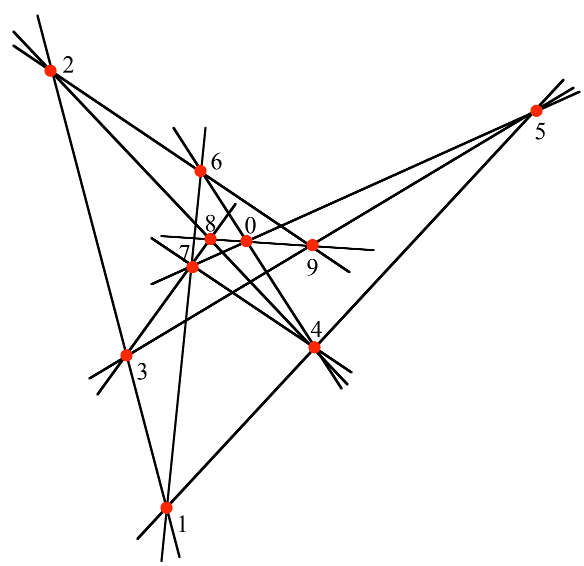

Figure 5.6.3. The configuration $(10_3)_2$ has dimension d = 2.

As reported in Section 2.3, there is no information available on the family of geometric configurations (n_3) for n = 13 or 14 (beyond some examples). Hence it is not possible to definitely assert that the Cremona-Richmond configuration is the smallest 3-configuration of dimension d = 4. We venture:

Conjecture 5.6.1. All configurations (n_3) with $n \leq 14$ have dimensions 2 or 3.

A question that arises quite naturally is whether dual configurations have the same dimension. A negative answer is obvious from the example in Figure 5.6.5: The configuration (6_2, 4_3) is clearly contained in the plane determined by any two of its lines, while the dual configuration (4_3, 6_2) spans the 3-dimensional space if the four points are chosen in affinely independent positions. While it is possible to generalize this example, the situation concerning connected but not 2-connected configurations discussed in Section 5.1 makes it plausible that balanced configurations may behave differently from unbalanced ones.

Conjecture 5.6.2. If C is a balanced configuration then the dimensions of C and its dual C* are the same.

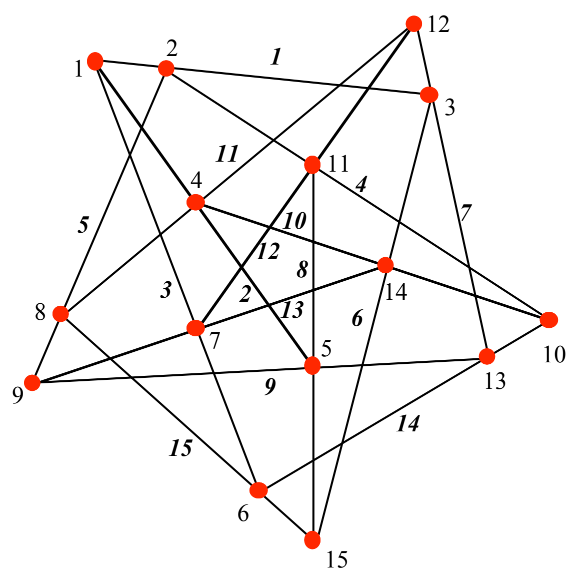

Figure 5.6.4. The Cremona-Richmond configuration (15_3) is 4-dimensional.

1 = (0,0,0,0), 2 = (1,0,0,0), 3 = (-1,0,0,0), 4 = (0,1,0,0), 5 = (0,-1,0,0),
6 = (0,0,1,0), 7 = (0,0,-1,0), 8 = (0,0,0,1), 9 = (2,0,0,2), 10 = (1,1,1,1),
11 = (0,2,2,2), 12 = (0,2,0,2), 13 = (2,2,0,2), 14 = (2,0,2,2), 15 = (0,0,2,2).

Table 5.6.1. Coordinates for the points of a realization of the Cremona-Richmond configuration (15_3) in the 4-dimensional Euclidean space. The names of the points refer to the labels in Figure 5.6.4.

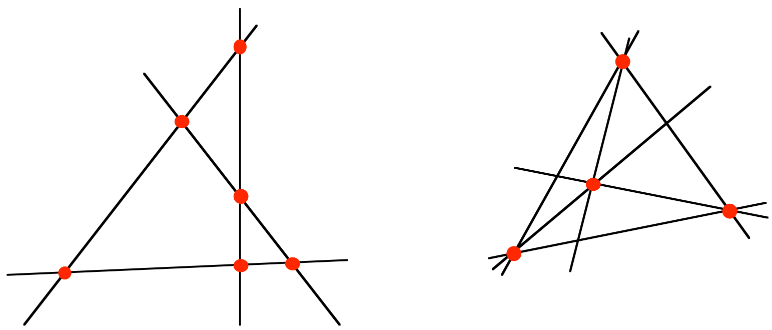

(a) (b)

Figure 5.6.5. (a) The configuration $(6_2, 4_3)$ known as the *complete quadrilateral* is 2-dimensional. (b) Its dual $(4_3, 6_2)$, the *complete quadrangle*, is 3-dimensional.

It is easy to show that the cyclic configuration $\mathscr{C}_3(n)$ is 2-dimensional in all cases in which it is realizable by a geometric configuration, namely $n \geq 9$. Indeed, consider the typical Levi diagram of $\mathscr{C}_3(n)$, shown in Figure 5.6.6. The plane that contains the points P_0, P_1, P_2 contains the lines L_0, L_1, and hence the points P_3, P_4; then the lines L_2 and L_3 are in this plane, therefore the points P_5 and P_6 as well. Since this pattern continues indefinitely, the whole configuration is in one plane.

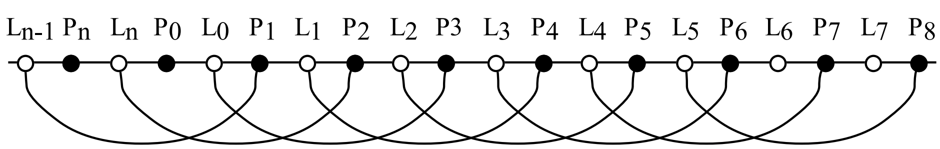

Figure 5.6.6. A stretch of the Levi graph of the cyclic configuration $\mathscr{C}_3(n)$ used to show that that the configuration is 2-dimensional for all $n \geq 9$.

So far we have dealt mainly with the dimension of 3-configurations. What is known about 4-configurations? Very little seems to be known at present. It is easy to verify that the astral configuration (24_4) shown in Figure 3.6.5 is 2-dimensional, as is the 3-astral configuration (21_4) shown in Figure 3.7.1. In case of the six astral configurations (36_4) shown in Figure 3.6.6 the proof that all are 2-dimensional is only slightly more involved. Experimental evidence on k-astral configurations has not turned up any that are demonstrably d-dimensional with $d \geq 3$. However, it is well possible that for reasonably large n some k-astral (n_4) configurations are not 2-dimensional; it would be interesting to decide this question at least for astral 4-configurations, or for 3-astral ones.

On the other hand, the (41_4) configuration in Figure 3.3.16 is easily seen to be 3-dimensional. The two parts that are joined at the four collinear points by the four concurrent lines show how to "bend" the configuration into 3-dimensional space.

A challenging task — that may be impossible to fulfill — is finding combinatorial criteria for the dimension of a configuration.

Exercises and problems 5.6

1. Determine the dimensions of the remaining seven configurations (10_3), shown in Figures 2.2.3 and 2.2.5.

2. Does the analogy with the results of Section 5.1 for unbalanced configurations extend to the dimensions? Specifically, do there exist [q,k]-configurations (with $3 \leq q \neq k \geq 3$) such that the dimensions of C and its dual C* are different?

3. How large can be the difference between the dimensions of a dual pair of configurations is Exercise 2 ?

4. Recall from Section 2.1 that a *general cyclic configuration* $\mathcal{C}_3(n,a,b)$ consists of triples $\{j, a+j, b+j\}$, for given a, b with $0 < a < b < n$ and for $1 \leq j \leq n$, all entries taken mod n. Determine the dimension of the various configurations $\mathcal{C}_3(n,1,b)$, and possibly of the general $\mathcal{C}_3(n,a,b)$.

5.7 MOVABLE CONFIGURATIONS

In this section we shall investigate to possibilities of changes of shape among configurations of a fixed isomorphism type. Applying any affine or projective transformation is most likely to produce a different configuration – but we shall consider such differences trivial and endeavor to find and describe more substantial modifications. In other words, we are considering equivalence classes of configuration, where members of each class are projectively equivalent to each other.

For example, all geometric realizations of (3_2) configurations are in one equivalence class, as are those of (4_2). On the other hand, configurations (5_2) have infinitely many projectively distinct forms; in fact, since any four points in general position can be projectively mapped on any other such quadruple of points, the projective equivalence class is determined by any fifth point. It follows that the (5_2) configurations form a variety of dimension 2.

We shall say that a configuration is **rigid** if its geometric realizations form a single class under projective transformations. Both the theorem of Steinitz (as presented in Section 2.6) and practical experience suggest:

Conjecture 5.7.1. There are no rigid 3-configurations.

In view of the more stringent constraints that k-configurations with $k \geq 4$ have to satisfy, it may be tempting to believe that at least some of them are rigid. This may well be the case — however, none has been found that is demonstrably rigid. Hence we venture:

Conjecture 5.7.2. There are no rigid k-configurations for any $k \geq 3$.

A configuration that is not rigid shall be called **movable**. The motion itself can happen in a variety of ways. For example, with 3-configurations, in all cases that have been investigated, after having fixed a sufficient number of points and lines to eliminate projective maps it is at least possible to move either a point arbitrarily on a line, or pivot a line about a point (or both). This is illustrated by four of the (10_3) configurations illustrated in Figure 2.2.5; after arbitrarily choosing four points, the only remaining choice is that of a point on one of the already determined lines. In many 3-configurations (such as the ones illustrated in Figure 5.7.1) it is easy to see that they are movable even if keeping considerable parts of the configuration unchanged. However, there are analogous 3-configurations, such as the one in Figure 5.7.2, in which some of the parts have to be modified ; similar examples can easily be multiplied. There are other examples in which the connecting lines between parts are neither parallel nor concurrent, and others in which the connection between parts are through points rather than lines.

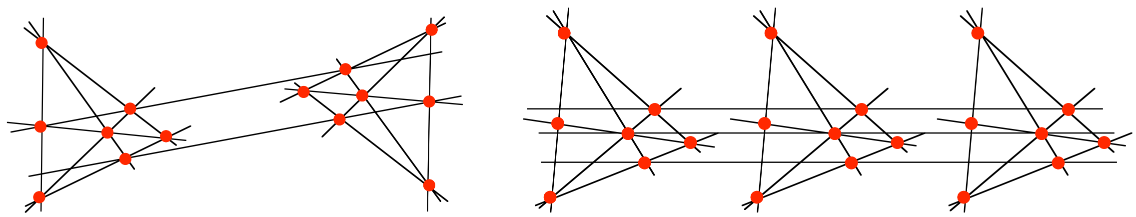

(a) (b)

Figure 5.7.1. Two 3-configurations in which solid parts may be simply pulled apart. (a) A 2-connected (14_3). (b) A 3-connected (21_3).

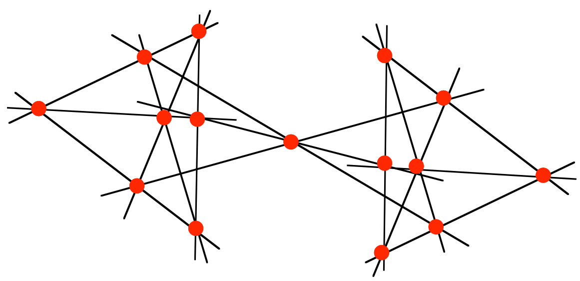

Figure 5.7.2. A 3-connected configuration (14_3) with a half-turn symmetry, in which solid parts may be separated by a greater or smaller distance.

In all the movable situations described so far there is essentially no symmetry except possibly by reflection in a mirror or by a halfturn, and in some special positions. Much more interesting are movable configurations in which the configuration retains some non-trivial cyclic or dihedral symmetry throughout the motion. We have encountered such configurations in Section 2.9, when discussing dihedral astral 3-configurations.

However, it seemed rather unlikely that analogous movable k-configurations, with considerable symmetry, can exist for $k \geq 4$. But exactly this type of configurations was discovered by L. Berman in the summer of 2006, and was first published in [B7]. We mention in passing that another kind of movable 4-configurations are the "floral configuration", the first of which was found by J. Bokowski somewhat later in 2006. We presented the relevant results in Section 4.7, and shall not dwell upon them here.

The simplest of Berman's methods of generating such configurations can be described as follows.

Starting with two 4-configurations, in one of them we omit one half of the lines of one orbit, and in the other one half of the points in one orbit. If the configurations and the orbits have been chosen appropriately, it is possible to locate the deficient configurations in such a way that the points that were incident with the deleted lines slide on the lines from which a point was deleted, thus supplying the correct numbers of incidences. The new configuration has four fewer points and lines than the original ones had jointly. Naturally, the choices of the points and lines to be omitted have to be made carefully, subject to some very stringent conditions. These restrictions are made explicit in [B7], and the complete characterization and proofs are given there. They are far too detailed and delicate to be included here, and the interested reader is advised to consult the original paper (which is easily accessible). A glimpse of the result of Berman's construction can be seen in Figure 5.7.3, which shows the smallest movable configuration obtainable by this method. Berman's paper [B7] contains some additional constructions and developments as well.

A new paper by Berman [B10] (private communication) presents additional constructions of movable configurations that retain cyclic symmetry during motion. It is more parsimonious, but the construction steps depend on the parity of the starting regular polygon. All configurations in this class have five point orbits of equal size. The smallest movable configuration that can be obtained is a (30_4). Several positions of this configuration are shown in Figure 5.7.4, adapted from [B10].

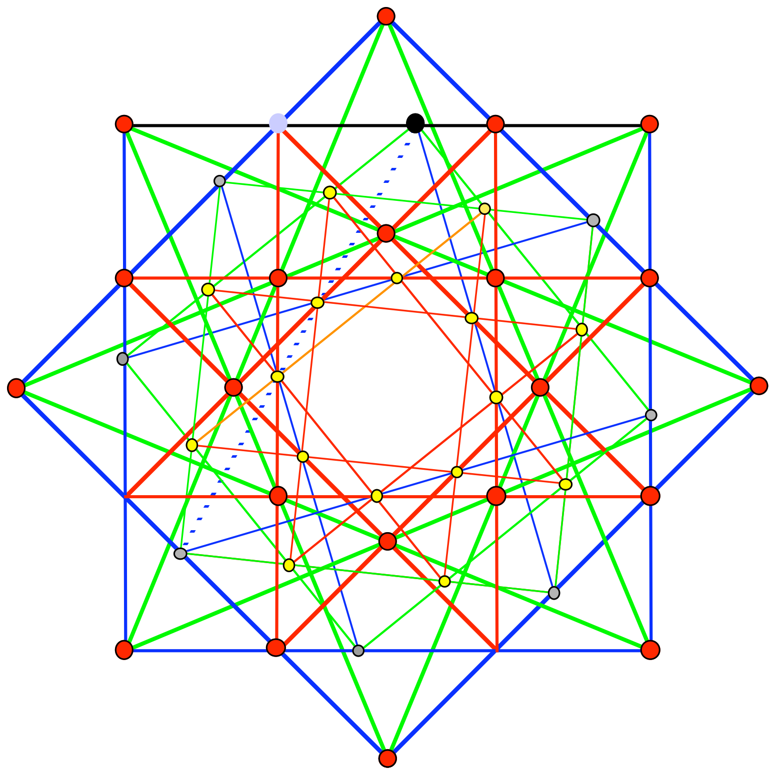

Figure 5.7.3. A movable (44_4) configuration, adapted from [B7], Figure 7. It is constructed from two copies of the 3-cyclic configuration (24_4) with symbol 8#(2,1;3,2;1,3]; one is shown in heavy lines and large red dots, the other with thin lines and smaller yellow dots. From the former the grey dot and the three analogous points (not shown) have been omitted, while from the latter the dotted line and its three analogs are deleted. The missing incidences are replaced by placing the black dot on the black line, and the corresponding points of its orbit on the corresponding lines; because of the choice of the parameters and orbits, the black point is freely movable on the black line, provided the sizes of the configurations are adjusted appropriately.

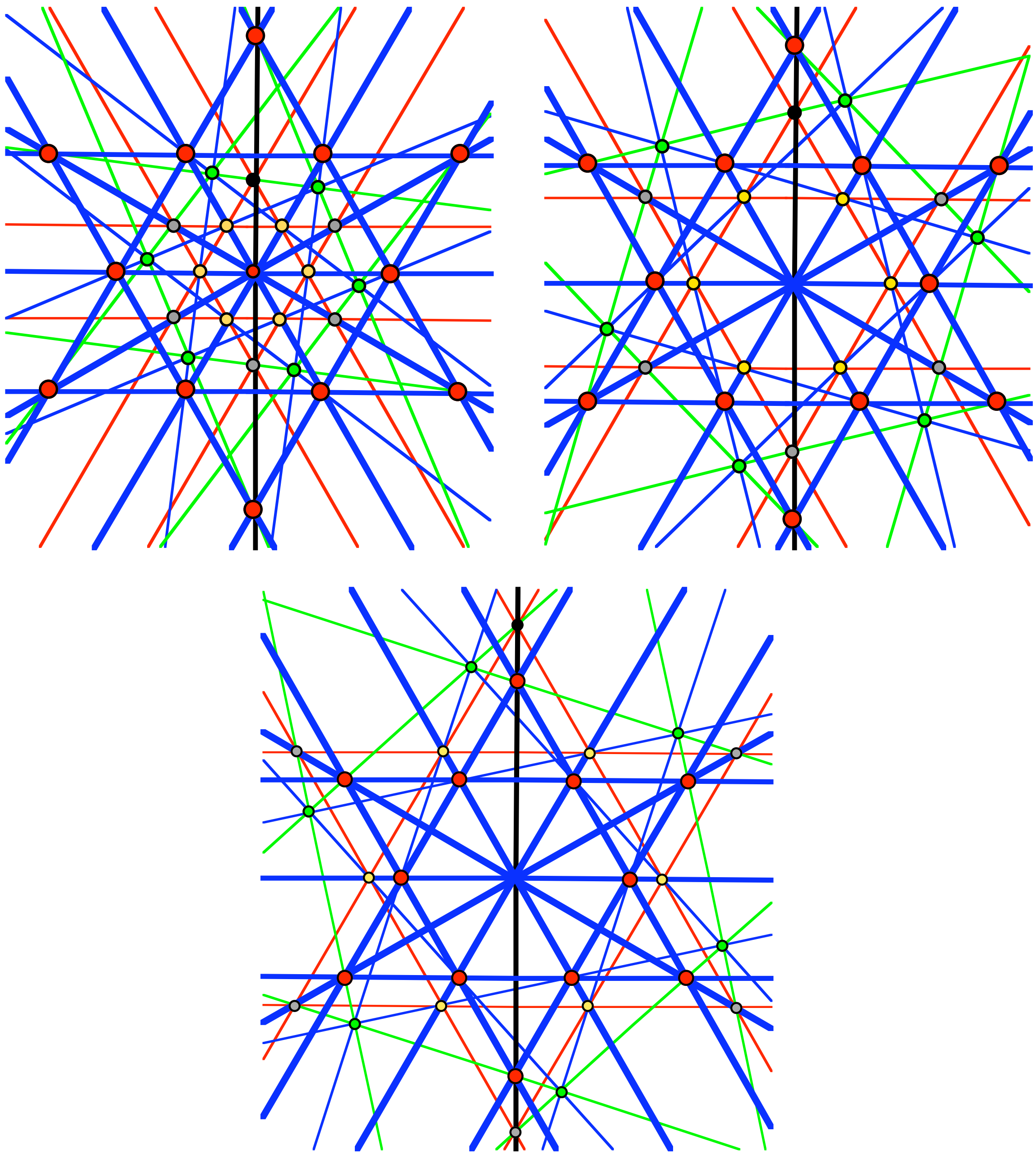

Figure 5.7.4. The smallest movable configuration from Berman's [B10]. It is a 5-orbits configuration (30_4). The black point can move freely on the black line as illustrated in the three parts.

Berman's construction in [B10] is considerably simpler than the ones in [B7], since it does not require deletion and pasting. However, it seems that the construction we shall consider next has certain advantages; it is presented here for the first time. It has been discovered a very short time before this book was going to print, and I have not had the time to figure out all conditions for the applicability of the method.

Consider the following example, which is the smallest to which the construction is applicable but is typical in all other respects. We start with the tricyclic configuration 10#(2,1;4,2;1,4); it has symmetry group d_{10}. However, we wish to consider it with only one of its d_5 subgroups. The situation is illustrated in Figure 5.7.5. Without the constraints imposed by the deleted mirrors and the accompanying rotations, the configuration is movable! In Figure 5.7.6 are shown several stages of the motion. The images were created with the Geometer's Sketchpad® software, the top green point being freely movable on the blue line with positive slope incident with it. An interesting and useful observation is that the points on the disregarded mirrors remain collinear throughout the motion.

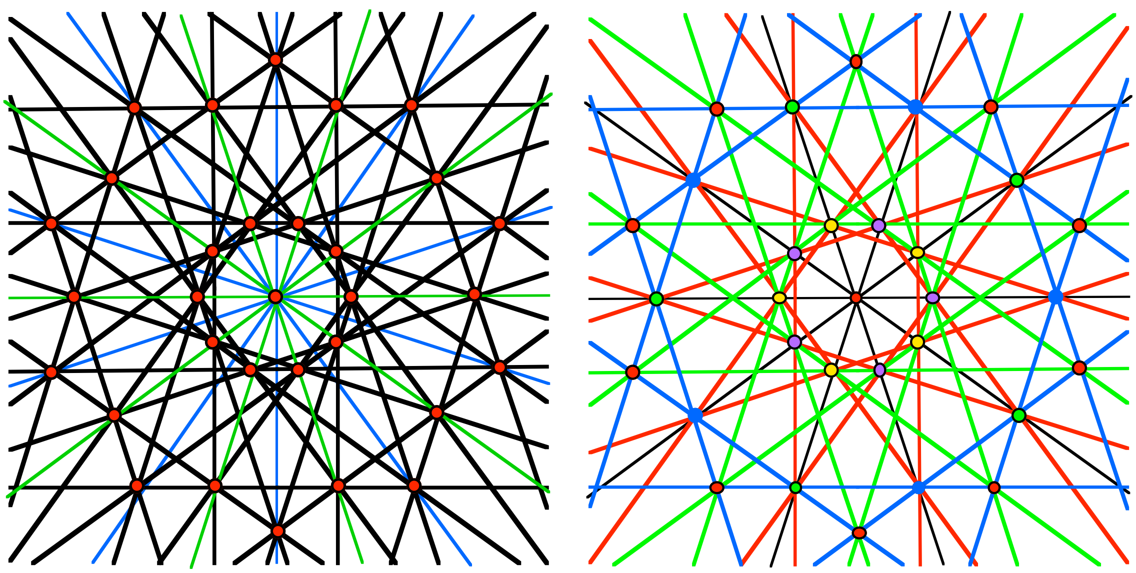

(a) (b)

Figure 5.7.5. (a) The tricyclic configuration (30_4) with symbol 10#(2,1;4,2;1,4), shown with its ten mirrors; its symmetry group is d_{10}. (b) The same configuration, but equipped with only five of the mirrors. The three orbits of lines and the five orbits of points under the symmetry group d_5 are distinguished by their colors.

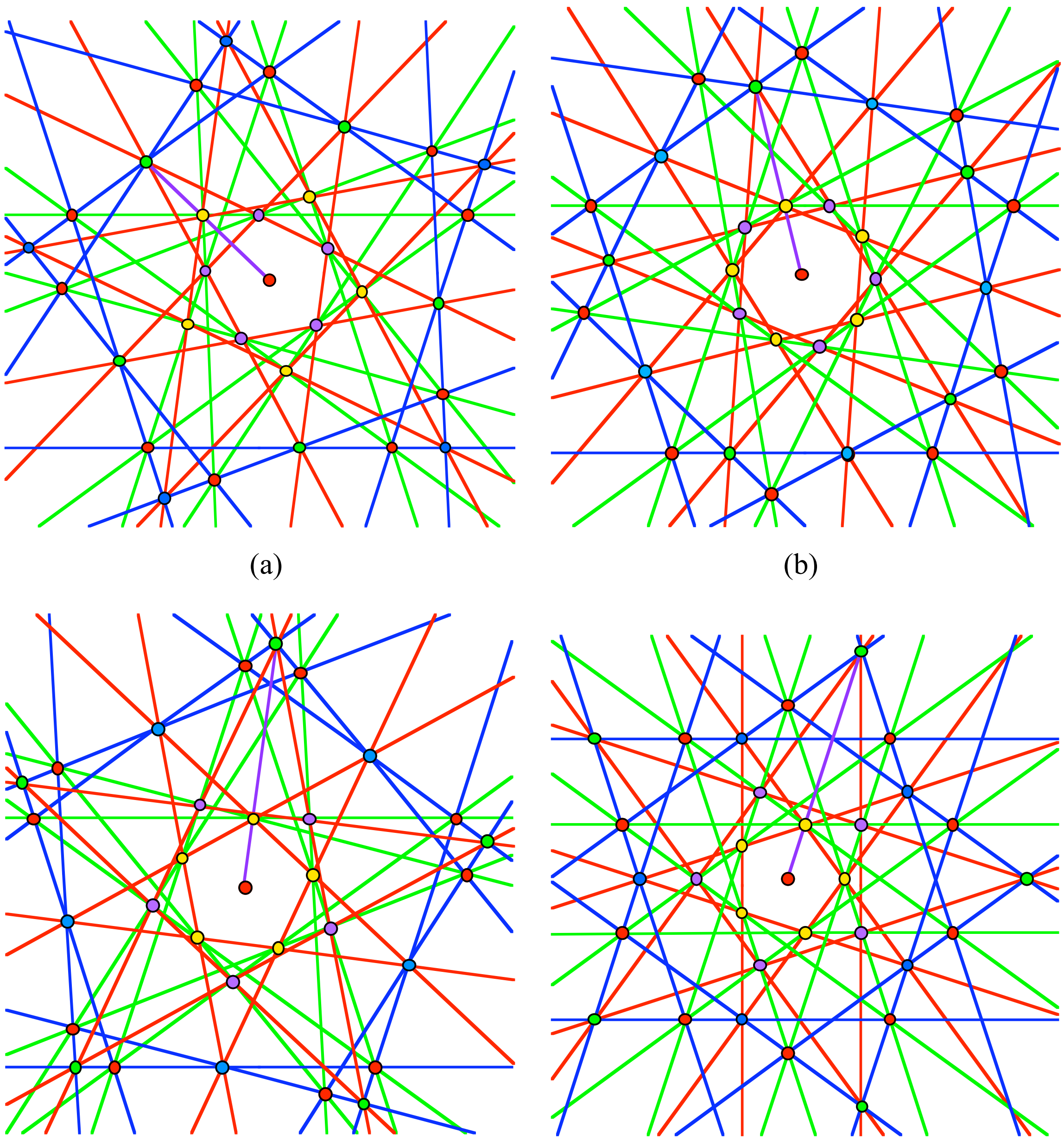

(a) (b)

(c) (d)

Figure 5.7.6. Four snapshots of different stages in the motion of the (30_4) configuration from Figure 5.7.5(b). The purple segment indicates one of the mirrors.

This circumstance can be used to construct another family of movable configurations, using the (5/6m) construction from Section 3.3. Applied to the (30_4) configuration in Figure 5.7.5(b) it yields the smallest known movable 4-configuration, a (25_4), illustrated with several snapshots of its motion in Figure 5.7.7.

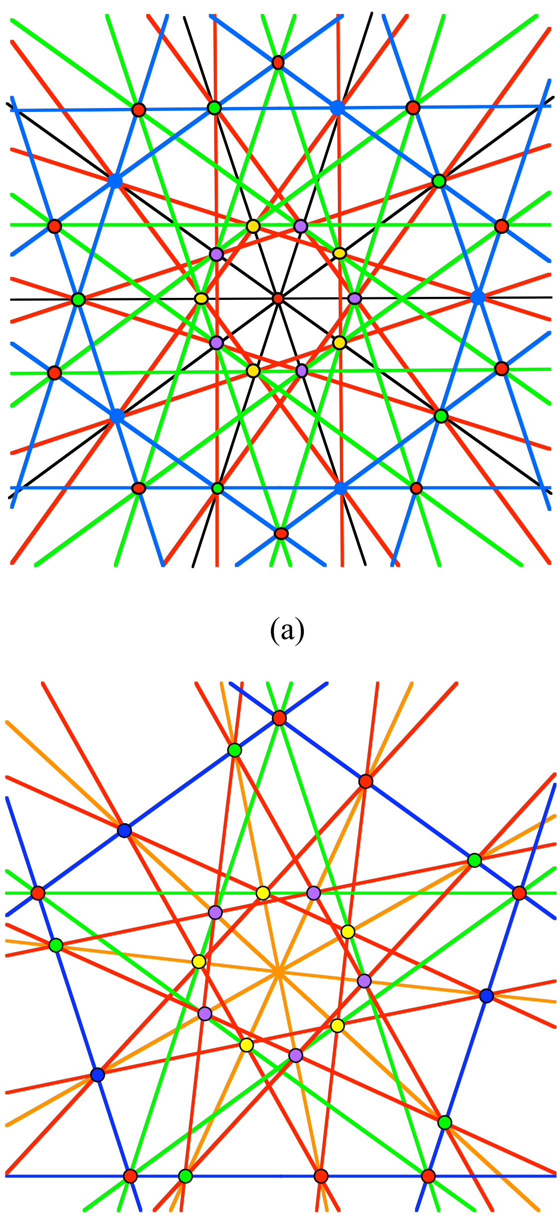

(a) (b)

(c) (d)

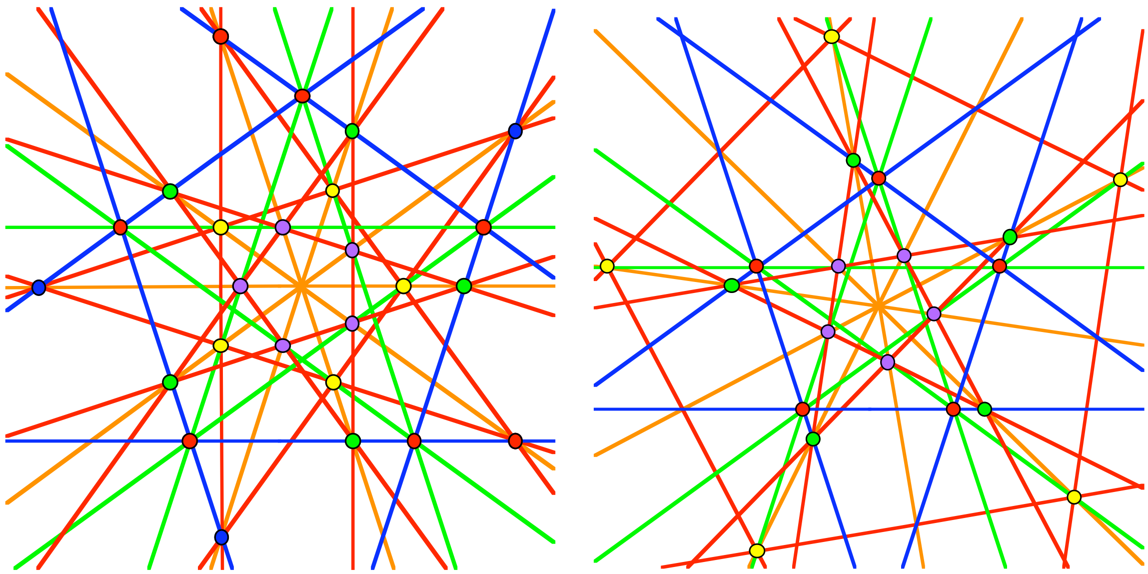

(e) (f)

Figure 5.7.7. (a) The (30_4) configuration with symmetry group d_5, from Figure 5.7.5(b). (b) A (25_4) configuration obtained from the configuration in (a) by omitting the points in the orbit of the lowest red point, and the lines incident with these points, and by adding the orange diametral lines (that go along the mirrors of the starting (30_4) configuration). This is the construction we introduced in Section 3.3 under the designation (5/6m); this particular instance is the same as the first part of Figure 3.3.13. (c) to (f) Four snapshots of different stages in the motion of the (25_4) configuration from part (b).

Exercises and problems 5.7

1. Investigate the possible motions of the astral configurations such as (10_3), allowing for departure from astrality.

2. Describe movable examples of 4-configurations that can be obtained by using copies of [3,4]-configurations. What are the smallest configurations of this kind? Apply the same construction to the superfiguration (9_3) shown in Figure 1.3.4.

3. Investigate to which configurations are the methods we used in Figures 4.7.6 and 5.7.7 applicable.

5.8 AUTOMORPHISMS AND DUALITY

In Section 1.5 we introduced the combinatorial concepts of automorphism and duality in a superficial way. In Section 2.10 we presented some results on the duality of 3-configurations, in particular, the astral ones. Here we will discuss such topics in more detail, with particular attention to the various ways in which such combinatorial properties and relations interact with geometric symmetries. The main reason for doing so is the absence of a coherent account of such interdependence of combinatorics and geometry; the examples we shall present are only brief glimpses of these relations. They lead to a large number of essentially unexplored questions.

We recall that an incidence-preserving map between the elements (points and lines) of two configurations is an **isomorphism** if points are mapped to points and lines to lines, and it is a **duality** if points are mapped to lines and vice versa. An isomorphism of a configuration with itself is an **automorphism**, while a duality of a configuration with itself is a **selfduality**. An automorphism of a configuration that is induced by an isometry of the plane is a **symmetry** of the configurations, while a selfduality that is induced by reciprocation in a suitable circle is a **selfpolarity**. Similarly, a pair of dual configurations may be **polar** to each other; this means that when situated appropriately, the reciprocation in a circle maps one onto the other. On the other hand, as we shall discuss later, the situation may be much more complicated.

We shall first illustrate the possibilities of the duality relations on a variety of examples, introducing additional classes and concepts as we are led by these experiences. In Figure 5.8.1 we show a pair of dual configurations (18_3). It is an easy exercise to find a duality mapping between the two configurations. There is no polarity between the two realizations of the dual pair. In contrast, in Figures 5.8.2, 5.8.3, and 5.8.4 we show the (24_4) configuration 12#(5,4;1,4) with three distinct labelings of its points and edges. The first shows that this configuration is selfdual, under the mapping that interchanges the green and blue labels. Since the configuration is very symmetric, it is reasonable to inquire about polarity. The correspondence between the labels actually establishes a more particular kind of selfduality. Although the polar of the configuration does not coincide with the configuration itself, it coincides with a copy reflected in a suitable mirror. In such a situation we shall say that the configuration is **oppositely selfpolar**. The necessity of using

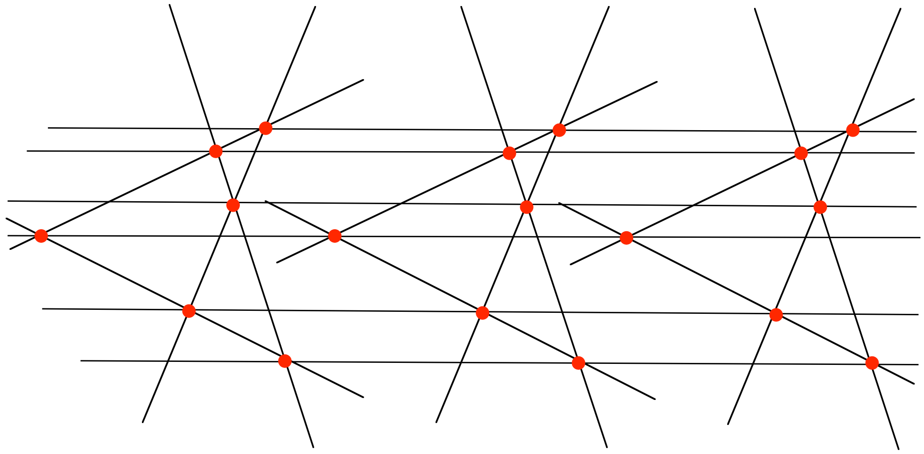

(a)

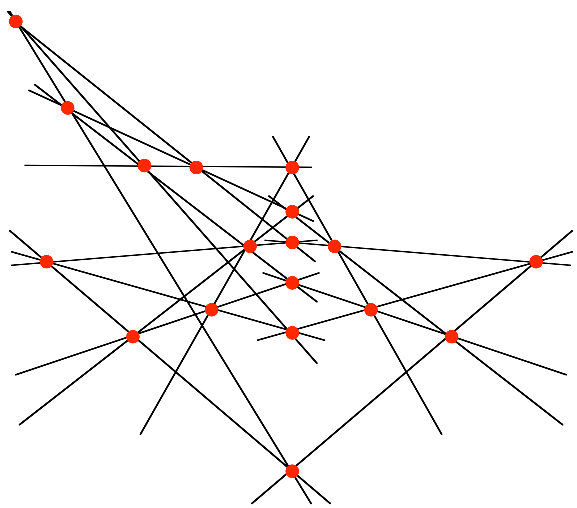

(b)

Figure 5.8.1. A pair of dual configurations (18_3). The configuration in (a) consists of three (6_2, 4_3) subconfigurations (also known as "complete quadrilaterals") connected by six "parallel" lines. The dual configuration in (b) consists of three (4_3, 6_2) subconfigurations (known as "complete quadrangles") and six points at which the three subconfigurations are joined.

a mirror is obvious from the opposite orientations of the red and blue labels. The impossibility of finding a different selfduality that would not require a mirror follows from the observation that the outer ring of points gets mapped into the inner family of lines – but these are not aligned in the required way. Similar arguments will be applicable in several cases to be mentioned later.

The same configuration (24_4) exhibits **orbit transitivity** (or "ring transitivity"). This means that there is an automorphism that interchanges the (geometric) symmetry orbits. For a proof of this assertion it is enough to consider Figure 5.8.3, in which the labels indicate an isomorphism with Figure 5.8.2.

We shall see similar behavior with other configurations. However, the (24_4) configuration exhibits a more rare kind of symmetry: It is not just point-transitive and line-transitive under automorphisms, but it is **flag-transitive.** (By this is meant that all **flags**, each consisting of an incident pair point-line, are equivalent under automorphisms of the configuration.) This is made visible by considering another labeling of the configuration, shown in Figure 5.8.4. With this labeling (and the geometric symmetries of the configuration) it is easy to show that all flags for a single orbit under automorphisms. Obviously, this implies point-transitivity and line-transitivity.

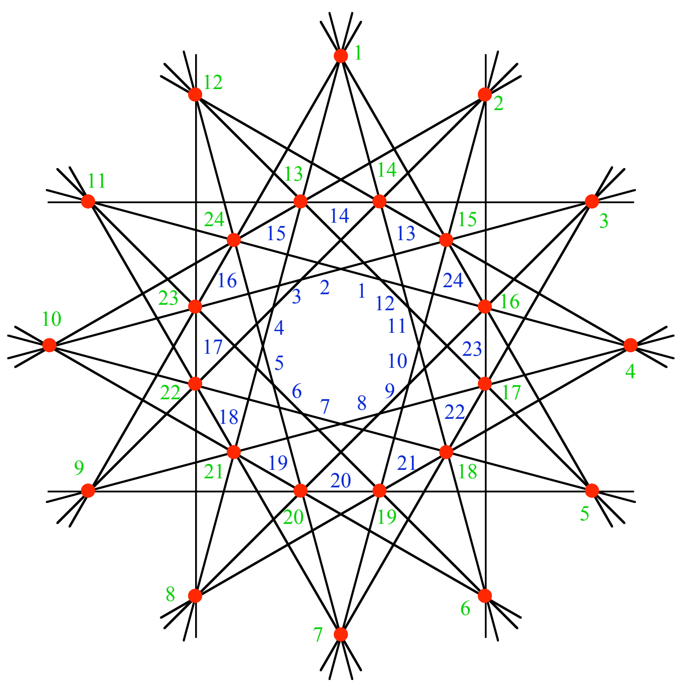

Figure 5.8.2. The (24_4) astral configuration 12#(5,4;1,4) is oppositely selfpolar; its polar needs to be reflected in order to coincide with the original.

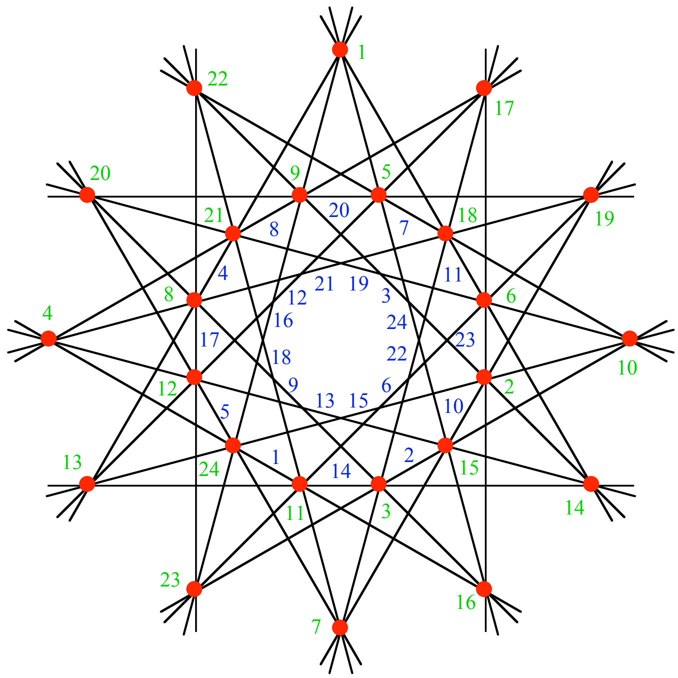

Figure 5.8.3. A different labeling of the (24_4) configuration from Figure 5.8.2. The identity map of the labels establishes that there is an automorphism of the configuration that maps the inner orbit of points onto the outer one, and similarly for lines.

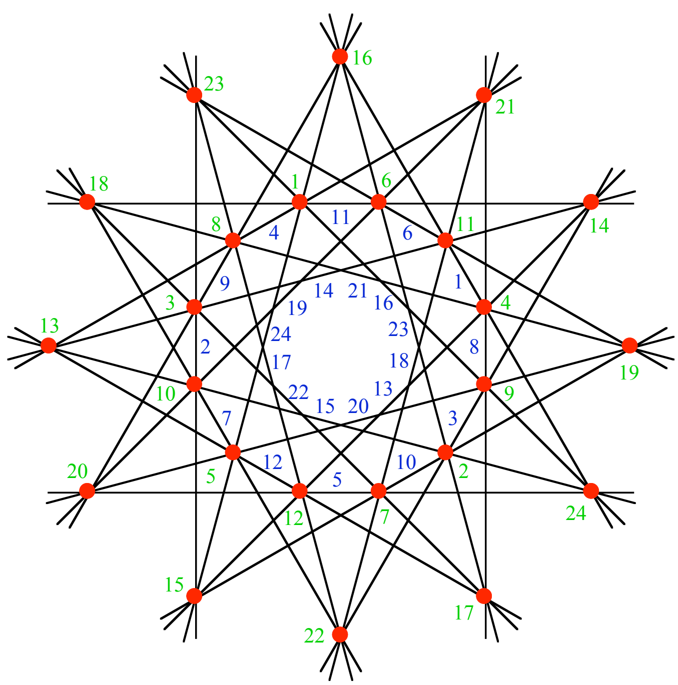

Figure 5.8.4. A labeling of the (24_4) configuration that can be used to establish the flag-transitivity of the configuration.

In Section 3.6 we mentioned that there are six different astral configurations (36_4), and we presented them in Figure 3.6.3. The labels on three of these show how they are isomorphic. Each can be shown to be polar to the one near it, hence these are all isomorphic as well. In contrast to the configuration (24_4), none of these six configurations is selfpolar. Moreover, there are two orbits of points, and two of lines, in each of these configurations; hence there is no transitivity of anything.

As mentioned in Section 3.6, the astral configurations (48_4) belong to four cohorts: 24#{{11,1},{10,8}}, 24#{{9,3},{8,6}}, 24#{{8,2},{7,5}}, 24#{{10,2},{8,8}}. This gives rise to seven distinct configurations, with symbols 24#(8,7;2,5), 24#(8,5;2,7), 24#(11,10;1,8), 24#(11,8;1,10), 24#(9,8;3,6), 24#(9,6;3,8), and 24#(10,8;2,8). By the general results from Section 3.5, the last one is disconnected and consists of two copies of 12#(5,4;1,4); hence we shall not be concerned with it here. Each of the other six is selfdual, but this does not translate into any geometric selfpolarity. In fact, the polars of 24#(8,7;2,5), 24#(11,10;1,8), 24#(9,8;3,6) are 24#(8,5;2,7), 24#(11,8;1,10), and 24#(9,6;3,8), , respectively. Moreover, 24#(8,7;2,5), 24#(8,5;2,7), 24#(11,10;1,8), 24#(11,8;1,10), are all isomorphic, and 24#(9,8;3,6) and 24#(9,6;3,8) are isomorphic. These combinatorial symmetries are far from obvious. In Figure 5.8.5 and 5.8.5 we show the first two of these configurations, with labels that indicate the selfduality of each as well as the polarity between them. By switching the label colors, it also indicates isomorphism. In Figure 5.8.7 we show the configuration 24#(11,10;1,8), with only the points labeled to show its isomorphism with the other two. (See exercise 5.) In Figure 5.8.8 and 5.8.9 we show the configurations 24#(9,8;3,6) and 24#(9,6;3,8), labeled to show their selfpolarity and the polarity and isomorphism between them.

There is no additional information available at present concerning the combinatorial properties of other 2-astral 4-configurations. The large number of such configurations — already for (60_4) there are 15 configurations — make "experimental" progress unlikely without some new theoretical insights.

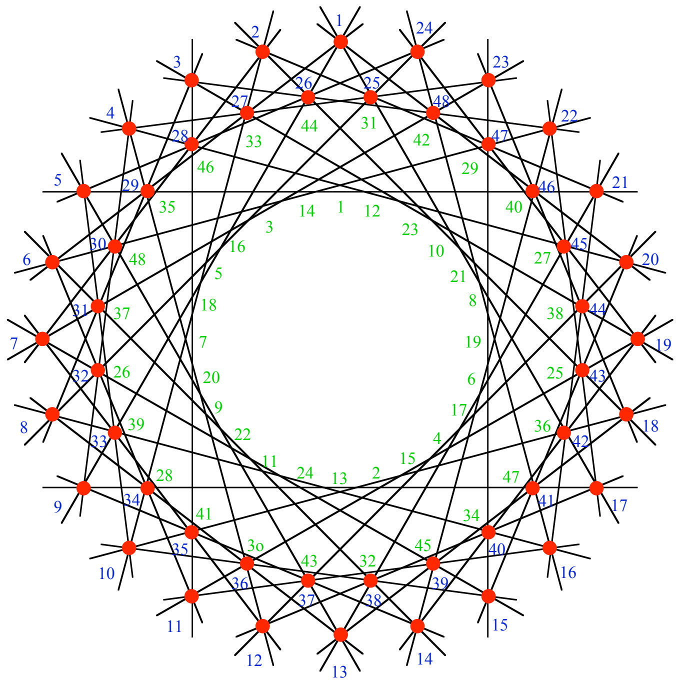

Figure 5.8.5. The configuration 24#(8,7;2,5) labeled to show its selfduality.

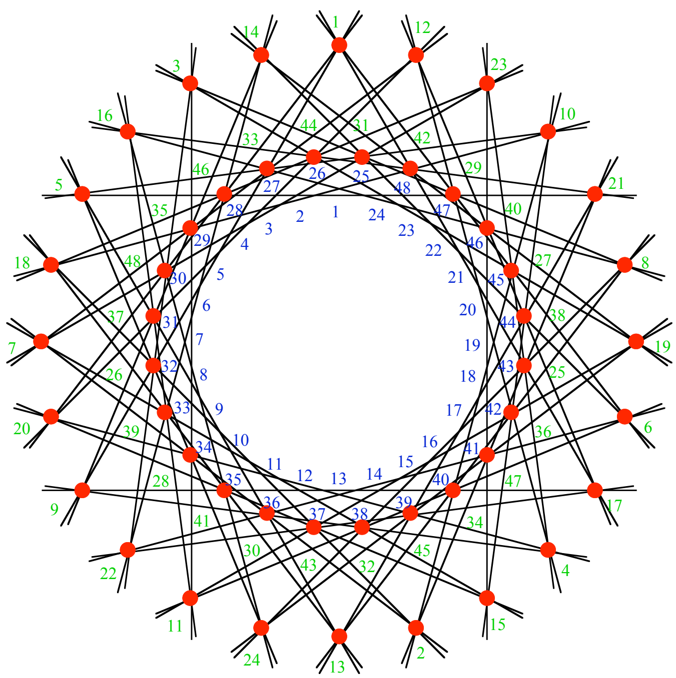

Figure 5.8.6. The configuration 24#(8,5;2,7) labeled to show its selfduality, and its polarity and isomorphism with 24#(8,7;2,5), the last by switching colors on labels.

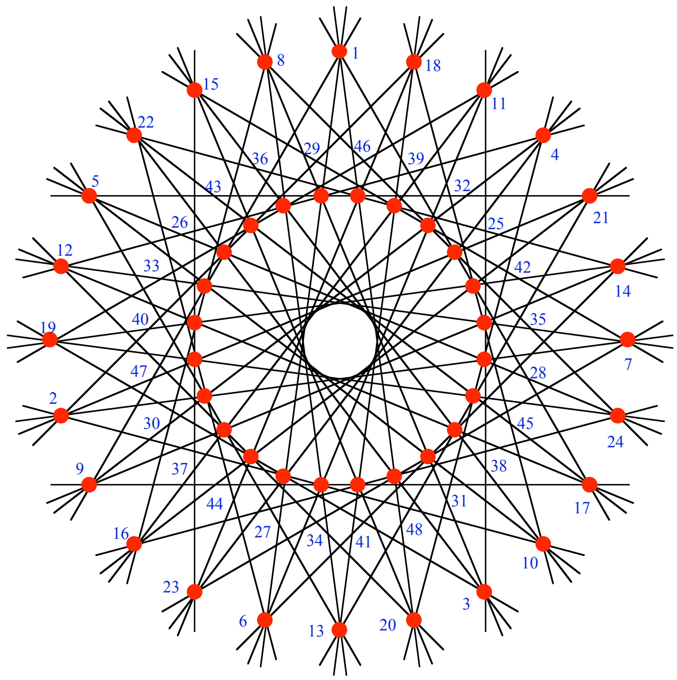

Figure 5.8.7. Configuration 24#(11,10;1,8) with points labeled to show isomorphism with 24#(8,7;2,5), and hence with 24#(8,5;2,7).

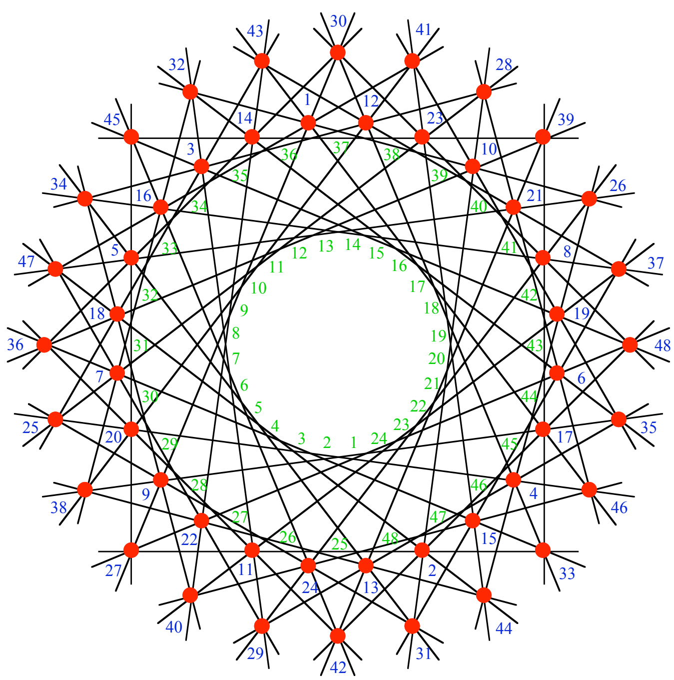

Figure 5.8.8. The configuration 24#(9,8;3,6) with labels that show the selfduality.

On the other hand, there is some knowledge of the situation concerning 3-astral 4-configurations. To begin with, by the general results of Sections 3.5, and 3.7, all such configurations are selfdual. Already in [G50] it was noted that the smallest 3-astral configuration (21_4) (shown in Figure 3.7.1, as well as in Figure 5.8.10) is selfpolar, orbit-transitive, and flag-transitive. We show these relations in the two parts of Figure 5.8.10.

This highly symmetric behavior does not extend to the next larger 3-astral configuration. In Figure 5.8.11 we show the (24_4) configuration 8#(3,2;1,3;2,1), with labels that show it is selfpolar. However, a count of symmetric trilaterals shows that there are three distinct orbits of points, hence also of lines.

The 3-astral configurations (27_4) show an interesting variety. There are six such configurations. Three of the trivial ones are isomorphic, as shown in Figure 5.8.12; one of these is selfpolar, while the other two are selfpolar*. We use the term **selfpolar*** to indicate that the polar configuration needs to be reflected in the origin (that is, turned 180°) in order to coincide with the original configurations. In each there are three orbits of points

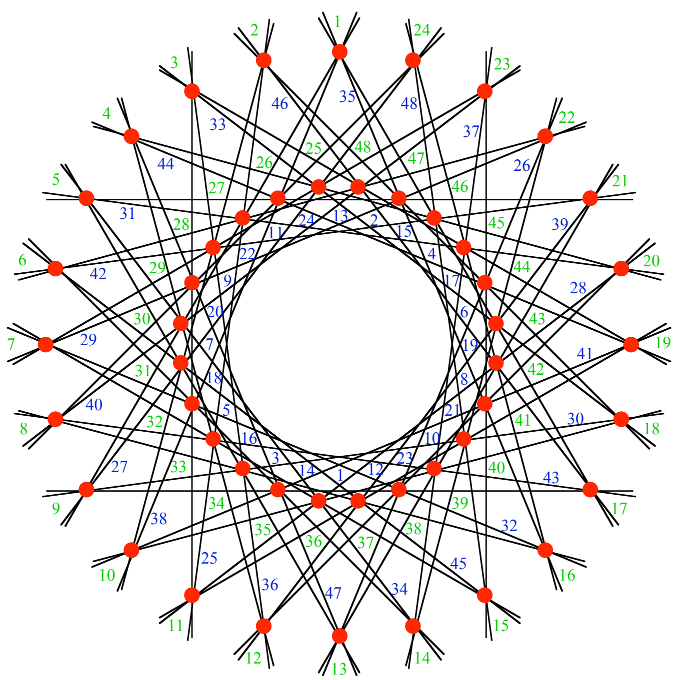

Figure 5.8.9. The configuration 24#(9,6;3,8) with labels that show its selfduality, and its polarity with 24#(9,8;3,6), as well as it isomorphism with that configuration (on interchanging the colors of the labels.

and three orbits of lines. There is one other trivial configuration, 9#(4,2;1,4;2,1), which is also selfpolar* but is not isomorphic to any of the other (27_4) 3-astral configurations. It is

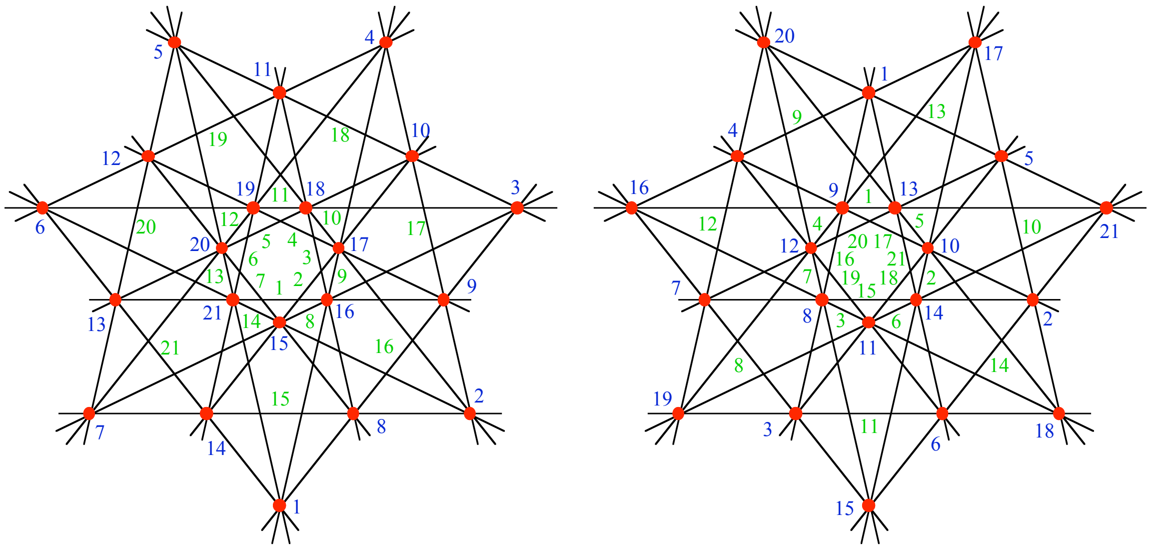

(a) (b)

Figure 5.8.9. The 3-astral (21_4) configuration 7(3,2;1,3;2,1). (a) The labels indicate a selfpolarity. (b) Together with part (a), the labels indicate orbit-transitivity as well as flag-transitivity. (A more elegant labeling to exhibit these relations is used in [G50].)

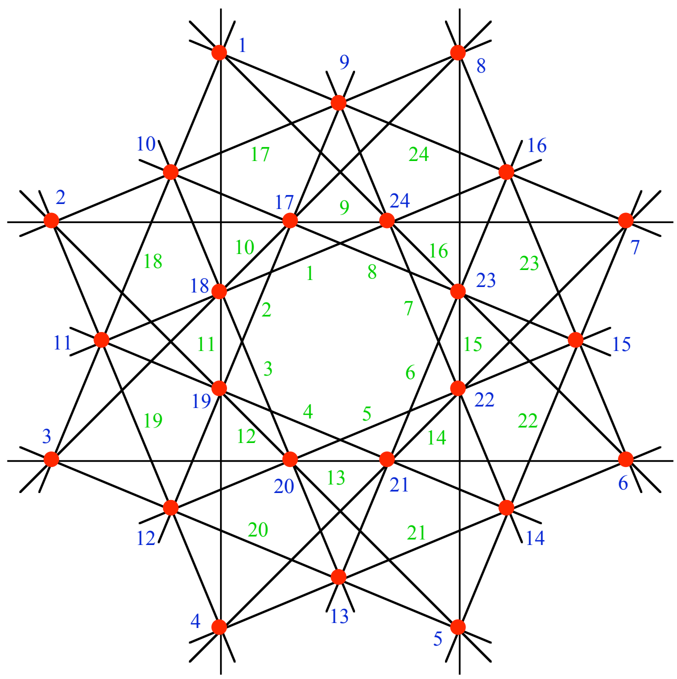

Figure 5.8.11. The 3-astral configuration (24_4), with symbol 8#(3,2;1,3;2,1) is selfpolar, but has three orbits of points and three of lines.

shown in Figure 5.8.13, with labeling that enables a check of the orbit-transitivity of the configuration. The last two configurations of this family, 9#(4,3;2,3;1,3) and 9#(4,3;1,3;2,3), are the first non-trivial 3-astral 4-configurations we encountered so far. In

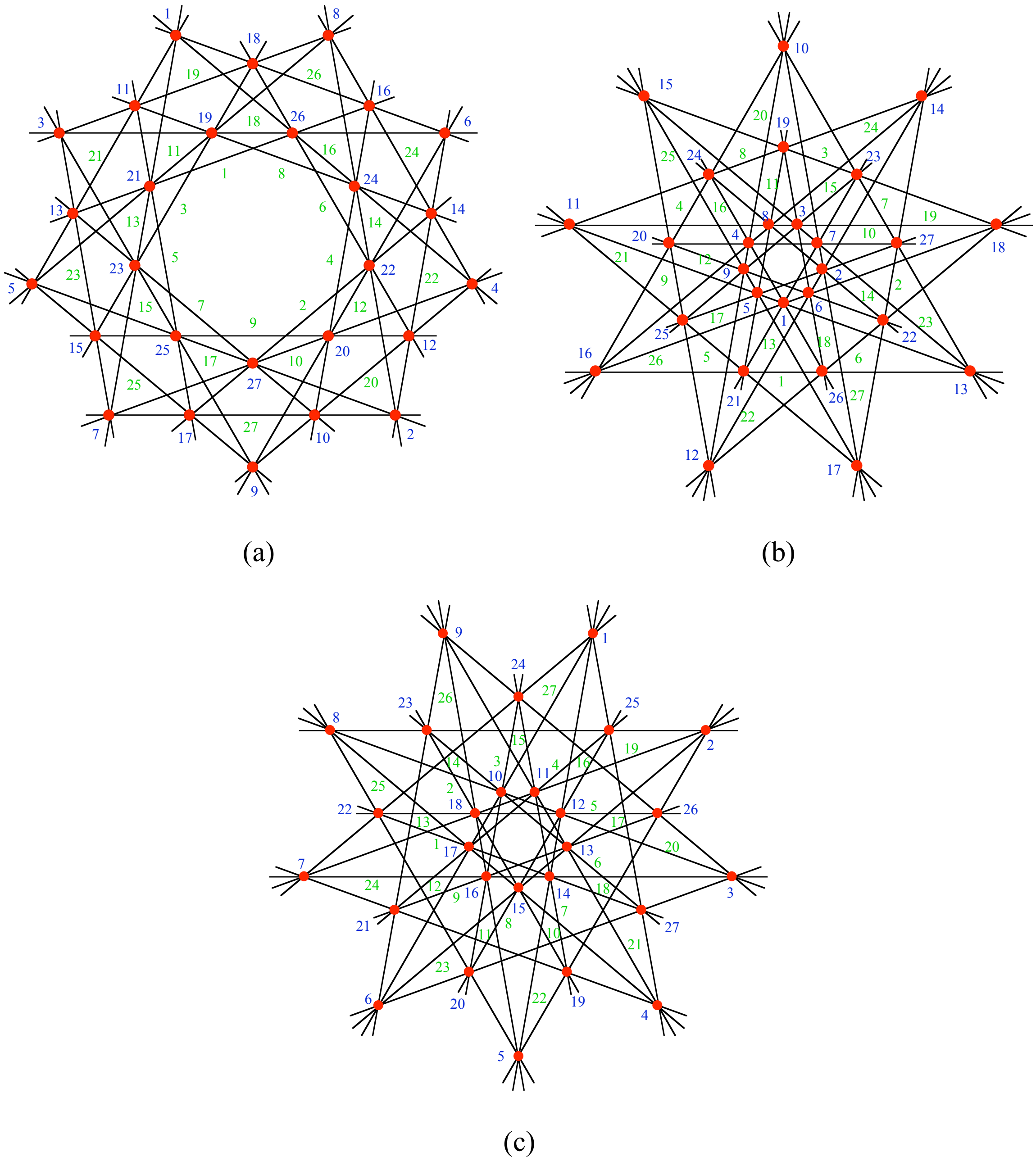

(a) (b) (c)

Figure 5.8.12. Three 3-astral configurations (27_4) that are isomorphic, with appropriate labels. (a) 9#(3,2;1,3;2,1) and (b) 9#(4,3;1,4;3,1) are selfpolar, while (c) 9#(4,3;2,4;3,2) is selfpolar*.

the terminology we used in Section 3.7, they belong to the family (2) with m divisible by 3. The two configurations are polars of each other, and are point- and line-transitive.

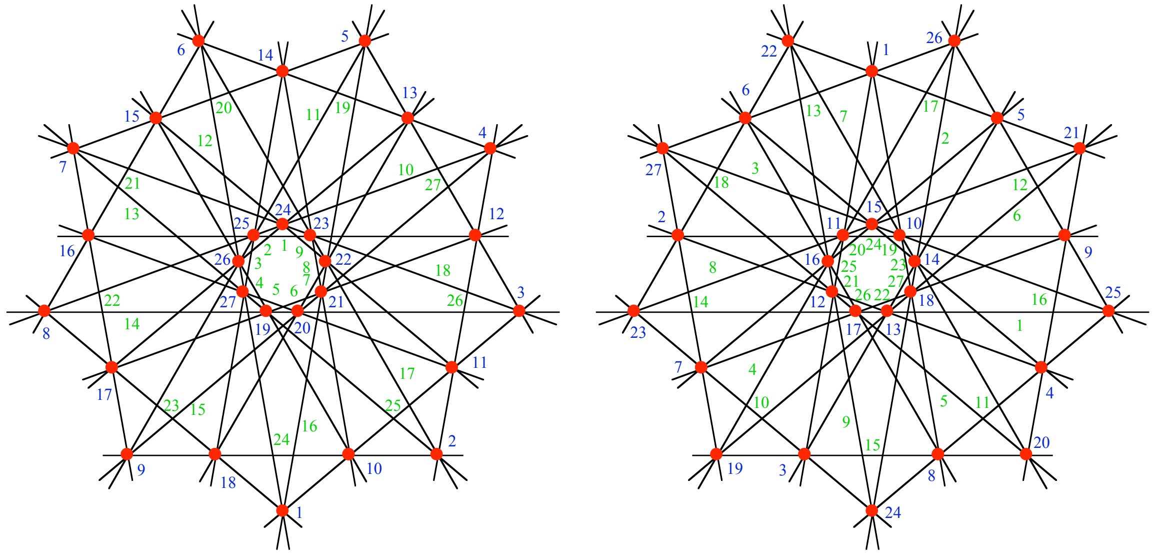

(a) (b)

Figure 5.8.13. (a) The 3-astral (27_4) configuration 9#(4,2;1,4;2,1) is selfpolar*, as shown by the labels. (b) Comparison with (a) shows that the three point-orbits are equivalent, hence there is point-transitivity and line-transitivity.

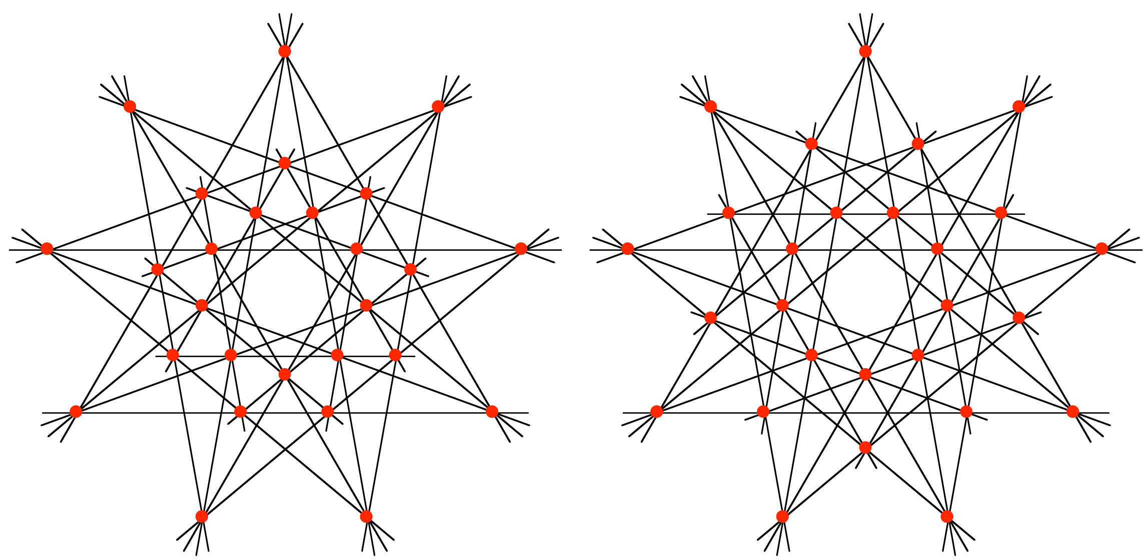

(a) (b)

Figure 5.8.14. The last two 3-astral configuration (27_4); they are polar to each other, but there are no transitivity properties beyond that. (a) 9#(4,3;2,3;1,3). (b) 9#(4,3;1,3;2,3).

There are seven 3-astral configurations (30_4). Four are trivial, and three are systematic. Among the trivial ones, 10#(3,2;1,3;2,1) and 10#(4,3;1,4;3,1) are selfpolar, the other two are oppositely selfpolar. In the notation of Section 3.7 the nontrivial configurations are in the cohort of the family (1) with q = 5, p = 1, and r = 2. The configuration 10#(4,3;1,2;1,3) is selfpolar, the other two in this cohort are polars of each other. The details of their isomorphisms and transitivities have not been investigated, nor is any non-obvious information available concerning the ten 3-astral configurations (33_4) or any (n_4) with n > 11.

D. Marusic and T. Pisanski [M3*] investigated configurations in which the group of automorphisms does not act transitively on flags, but automorphisms together with dualities do act transitively on flags. They call such configurations **weakly flag-transitive**, and prove that there are no weakly flag-transitive k-configurations for k = 2 and any odd k. To complement this they construct several weakly flag-transitive 4-configurations; they show the smallest known such configuration, a (27_4). In retrospect, it is easy to check that this is a 3-astral configuration from the trivial family, namely 9#(2,1;4,2;1,4). Similarly, their smallest known with an even number of vertices is the 3-astral configuration (42_4), namely 14#(3,1;5,3;1,5). Their final example is a trilateral-free 4-configuration (68_4), the sporadic 17#(3,1;6,2;5,4;7,8).

There is also a complete absence of information concerning the isomorphism and duality properties of k-astral configurations with k ≥ 4. There is a whole family of unexplored problems, waiting for new initiatives and insights.

* * * * * *

Returning now to the more complicated situations possible for more general configurations, we first note that is a configuration C is selfdual under a selfduality δ, then obviously the inverse map δ^{-1} is also a selfduality. In most situations it is also true that the automorphism δ∘δ is the identity map ι on C. However, this does not happen in all cases, a larger number of repetitions of the map δ needs to be applied to reach the identity automorphism ι. We call the smallest such number the **rank** r = r(δ) of δ. In Figure

5.8.15 we show a (5_2) configuration, with two selfdualities; one has rank 2, the other rank 10. The minimum of the ranks of all selfdualities of a selfdual configuration C is called the rank r(C). Obviously, the rank of the configuration in Figure 5.8.14 is 2. In contrast, the rank of the selfduality τ of the octalateral (8_2) in Figure 5.8.15 is 16; however, although there are several other selfdualities of this configuration, they all have rank 16, hence this is the rank of the configuration.

Several facts concerning rank can be established easily. First, the rank of any configuration C is a power of 2, that is, $r(C) = 2^k$ for some $k \geq 1$. It is also obvious that the case of the configuration in Figure 5.8.16 illustrates the general fact that the rank of any (2^k)-lateral is 2^{k+1}. Finally, if $r(C) = 2$, then one may use the same labels for the points and the lines of C. Conversely it is obvious that a selfduality that preserves the labels is of rank 2.

Regarding configurations (n_3) it is known (and easily verified) that for $n \leq 10$ all are selfdual of rank 2. According to Betten *et al.* [B14] among the 31 configurations (11_3) there are 25 selfdual ones of rank 2, and three pairs of mutually dual configurations — however, there is no identification of the dual pairs. In the same paper it is stated that among the 229 configurations (12_3) there are 95 that are selfdual of rank 2, the other forming dual pairs. Among the 2036 configurations (13_3) there are reported to be 366 selfdual ones, all but one of which have rank 2. There is no indication in [B14] what is the rank of that configuration, but it is possible to determine that the rank is 4. The authors also report in [B14] that among the 21399 configurations (14_3) there is one selfdual of rank greater than 2, and among the 245342 configurations (15_3) there are three of rank greater than 2. For neither of these is the rank indicated, but their configuration tables are given; this makes it possible to find out their rank, if enough effort is put into it. One may conjecture that they all have rank 4.

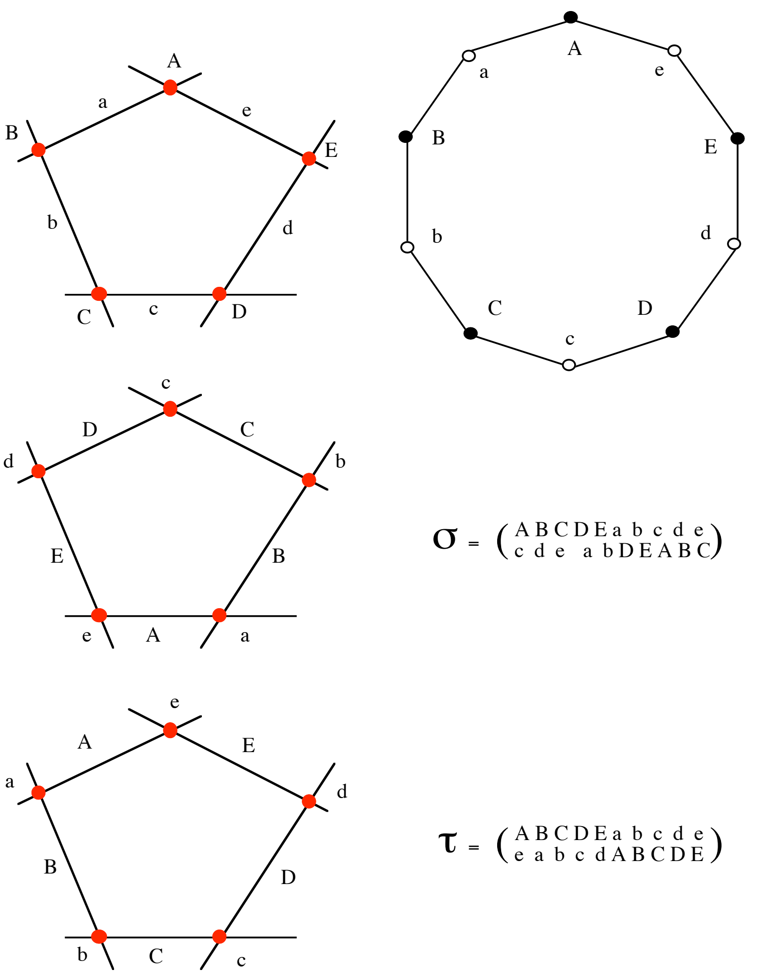

$$\sigma = \begin{pmatrix} A & B & C & D & E & a & b & c & d & e \\ c & d & e & a & b & D & E & A & B & C \end{pmatrix}$$

$$\tau = \begin{pmatrix} A & B & C & D & E & a & b & c & d & e \\ e & a & b & c & d & A & B & C & D & E \end{pmatrix}$$

Figure 5.8.14. A configuration (5_2) (that is, a pentalateral) and two of its selfdualities. Either from the permutation representation, or by using the Levi graph shown, it is easy to verify that the rank of the selfduality σ is 2, and the rank of τ is 10.

In another direction of investigation of configurations, in [A3] Ashley *et al.* constructed for ever k, selfdual configurations (n_3) with rank 2^k. Moreover, one can find such configurations with $n \leq 2^{k+5}$. The construction is quite complicated, and we shall not reproduce it here.

There seems to be no information available concerning the rank of 4-configurations. However, we venture:

Conjecture 5.8.1. Every selfdual geometric configuration of rank 2 has a realization such that the polar (in a suitable circle) is congruent to the original configuration.

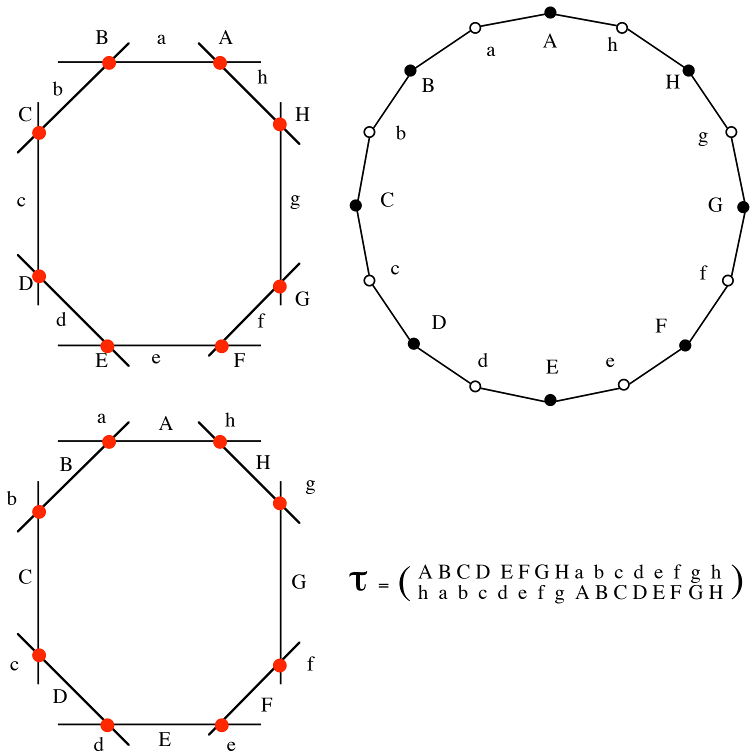

$$\tau = \begin{pmatrix} A\,B\,C\,D\,E\,F\,G\,H\,a\,b\,c\,d\,e\,f\,g\,h \\ h\,a\,b\,c\,d\,e\,f\,g\,A\,B\,C\,D\,E\,F\,G\,H \end{pmatrix}$$

Figure 5.8.15. An octalateral (8_2) and one of its selfdualities. This selfduality, as well as all other selfdualities of the octalateral, have rank 16; this is therefore the rank of the octalateral as well.

Conjecture 5.8.2. For every $q \geq 1$ and every $k \geq 1$ there exist selfdual geometric q-configurations of rank 2^k.

Exercises and problems 5.8.

1. Show that the astral topological configuration 11#(5,4;1,4) shown in Figure 5.8.3 is selfpolar*. Investigate its transitivity properties (that is, orbit-, point-, line-, flag-transitivity).

2. Prove the assertions made above concerning the astral configurations (36_4).

3. The connectedness of a configuration has nothing to do with such properties as selfduality. Prove that the configuration 24#(10,8;2,8) is selfpolar and flag transitive.

4. Provide arguments that prove that the configuration 24#(8,7;2,5) is not selfpolar in any sense.

5. Draw the configuration 24#(11,8;1,10) and show its isomorphism with 24#(11,10;1,8).

6. Verify the claim that the 3-astral configuration (24_4), with symbol 8#(3,2;1,3;2,1) has three orbits of points.

7. Find a selfduality of rank 2 of the topological configuration $(10_3)_4$.

5.9 OPEN PROBLEMS

1. Is there a relationship between the maximal size of an independent family, and the maximal sizes of independent families consisting of points only, or of lines only? Notice that in the examples in Figures 5.1.8 and 5.1.9 the first is strictly greater than the latter two.

2. If C is a 4-configuration and H a Hamiltonian multilateral in C, then each line is determined by two vertices of H and passes through two other vertices of C. Is it possible to obtain a new Hamiltonian multilateral H* of C by using such pairs of points of C as vertices of a multilateral? If so, can this happen in a k-astral 4-configuration, or even in an astral 4-configuration?

3. It is conceivable that *every* connected configuration (n_k) can be presented as a family of mutually inscribed/circumscribed multilaterals; this naturally includes Hamiltonian multilaterals. Either a counterexample, or an affirmation (at least for k = 3 or 4) would be very interesting.

4. Is there any relationship between the maximal size of an independent family in a configuration C, and the dimension of C?

5. Are all movable k-astral 4-configurations 2-dimensional?